



Cape Peninsula
University of Technology

**APPLICATION OF MASS AND ENERGY BALANCES TO DETERMINE COAL, AIR
REQUIRED AND FLUE GAS FLOW RATES IN A POWER PLANT**

by

LANDRY MBANGU KATENDE

Thesis submitted in fulfilment of the requirements for the degree

Master of Engineering: Mechanical Engineering

in the Faculty of Engineering

at the Cape Peninsula University of Technology

Supervisor: Prof Graeme John Oliver

Co-supervisor: Michael Petersen

External Supervisor: Prof Walter Schmitz (Wits)

Industrial Mentor: Prof Louis Jestin (EPPEI)

Bellville Campus

Date submitted March 2019

CPUT copyright information

The dissertation/thesis may not be published either in part (in scholarly, scientific or technical journals), or as a whole (as a monograph), unless permission has been obtained from the University

DECLARATION

I, Landry Mbangu Katende, declare that the contents of this dissertation/thesis represent my own unaided work, and that the dissertation/thesis has not previously been submitted for academic examination towards any qualification. Furthermore, it represents my own opinions and not necessarily those of the Cape Peninsula University of Technology.

Signed

Date

ABSTRACT

The primary objective of this study was to determine the heat rate of the power plant using the measurements of critical parameters and MEB calculations. An additional goal of the project was to determine the flue gas and air mass flow rates which influence the efficiency of the coal power plant.

The consumption of coal is a critical parameter affecting the efficiency of coal-fired steam boilers. From an operational perspective, the mass flow rate of pulverised coal is a major indicator of the rate of combustion and plant heat rate. However, the cost of electricity production in thermal coal power plants operated by ESKOM, is predominantly influenced by pulverized coal which represents between 60-70% of the total cost. Monitoring the consumption of coal can determine corrective actions which will ultimately improve the power plant's efficiency, reliability and associated economic benefits.

Initially, the fundamental concepts of a boiler and its auxiliaries were studied, which led to the required coal, air and flue gas systems required in a coal-fired boiler plant. From the literature review, it was established that coal consumption is a critical indicator of a plant's performance in terms of cost and efficiency. The different methods used for the flow measurements of coal, air and flue gas in a coal-fired boiler plant, such as MEB and CFD were reviewed. The-MEB method was used to determine the pulverised coal, air, and flue gas mass flow rates and the plant's heat rate. The MEB method was used to establish a coherent set of input and output data for the boiler, as well as to troubleshoot existing measurements from ESKOM's coal-fired power plant. The plant's coal consumption and heat rate results were calculated by means of a Mathcad model that was developed using BMEB methodology. Mathcad was chosen because it allows to visually check calculations. Furthermore ANSYS Fluent was used for the CFD simulation in the secondary air system.

ACKNOWLEDGEMENTS

First of all, my sincere thanks to EPPEI for the bursary funds provided to me in order to complete this Master's project.

I would like to direct my sincere gratitude and appreciation to my supervisors at CPUT, Prof Graeme Oliver, and Michael Petersen for their continuous support, encouragement, and guidance throughout the duration of my research.

I would like to thank my industrial mentor/supervisor Professor Louis Jestin from EPPEI and my external academic supervisor Professor Walter Schmitz from Wits for their guidance throughout the thesis.

I would like also to thank Prof Stephen Bosman for the project planning and PLMCC facility with advanced engineering software.

I would like to thank Mrs Charlene Govender as Process Manager at the coal-fired power plant who organised process engineers and technical personnel to assist me during site visits at the power station.

I would also like to thank Mr Waleed Moses at ESKOM Megawatt Park for the technical assistance, Smartplant/Bentley training and General arrangement 2D drawing of the plant.

I would also like to acknowledge Assoc Prof Wim Fuls and Prof Pieter Rousseau from UCT for the Power Plant Analysis, MEB and MathCAD course.

Lastly, I would like to thank my lovely wife Clarisse for total support and encouragement.

TABLE OF CONTENTS

DECLARATION	ii
ABSTRACT	iii
ACKNOWLEDGEMENTS	iv
TABLE OF CONTENTS	v
LIST OF FIGURES.....	vii
LIST OF TABLES	ix
GLOSSARY.....	x
CHAPTER ONE	1
THESIS OVERVIEW.....	1
1.1 Introduction	1
1.2 Background	2
1.3 Problem Statement.....	8
1.4 Objectives.....	8
1.5 Limitations of the study	8
1.6 Methodology.....	9
1.7 Chapter outline	12
CHAPTER TWO	13
LITERATURE REVIEW.....	13
2.1 Flow Measurement in a Coal-fired plant	13
2.1.1 The Measurement of the flow of coal	13
2.1.2 Air and Flue Gas Flow Measurement.....	19
2.2 MEB (Mass and energy balance).....	24
2.3 CFD Modelling.....	25
CHAPTER THREE	28
BOILER MASS AND ENERGY BALANCE METHODOLOGY	28
3.1 Boundary Selection	28
3.2 MEB Calculation	29
3.3. MEB implementation	38
CHAPTER FOUR	41
COMPUTATIONAL FLUID DYNAMICS (CFD)	41
4.1 Introduction	41

4.2 Simulation process	42
4.3 Sensitivity study on the mesh	49
CHAPTER FIVE	51
MEB CALCULATION RESULTS AND SENSITIVITY ANALYSIS	51
5.1 The boiler’s MEB Results.....	51
5.2 Sensitivity Analysis	53
CHAPTER SIX.....	61
CFD RESULTS	61
6.1 Results from the CFD model	61
6.2 Discussion.....	69
7. CONCLUSIONS, RECOMMENDATIONS AND FUTURE STUDY	71
7.1 Conclusions	71
7.2 Recommendation and future project	73
8. BIBLIOGRAPHY	74
9. APPENDIX / APPENDICES	77
APPENDIX A: MEB-MATHCAD CALCULATIONS	77
APPENDIX B: POWER STATION A-OPERATION PARAMETERS (ETAPRO CONTROL SYSTEM).....	90
APPENDIX C: POWER STATION A- OPERATION PARAMETERS DATASHEET	91
APPENDIX D: COAL ANALYSIS REPORT.....	96
APPENDIX E: ANSYS CFD SIMULATION	97
APPENDIX F: COAL-FIRED BOILER 2D PLANT LAYOUT	108
APPENDIX G: COAL-FIRED BOILER 3D PLANT LAYOUT.....	111

LIST OF FIGURES

Figure 1.1: Coal-Fired Power Station A (ESKOM, 2016)	2
Figure 1.2: Pulverised coal flow system at Power Station A (Catia 3D View).....	3
Figure 1.3: Primary air system at Power Station A (Catia 3D View).....	4
Figure 1.4: Secondary air system at Power Station A (Catia 3D view).....	5
Figure 1.5: Example of a secondary air heater (Rothamule air heater) (Jashuva et al., 2014)	5
Figure 1.6: The Flue gas system at Power Station A (Catia 3D View).....	6
Figure 1.7: Slagging on the super-heater’s tubes (Tootla, 2015).....	7
Figure 1.8: Boiler MEB calculation flow diagram	9
Figure 1.9: Operating parameters: flow and pressure for coal-fired Power Station A .	10
Figure 1.10: Operating parameters-Temperatures for coal-fired Power Station A.....	10
Figure 1.11: ANSYS simulation solver (ANSYS, 2015)	11
Figure 2.1: (Left) Coal ball mill (IHI Corporation, 2017), (Right) PF Coal Ball Mill (ESKOM, 2018)	14
Figure 2.2: Coal composition (Rousseau & Fuls, 2018).....	15
Figure 2.3: PF Flow Meter (ABB, 2018)	16
Figure 2.4: Coal Flow measurement in a PF pipe (Suresh et al., 2012).....	17
Figure 2.5: Mass flow of coal at different loads (Suresh et al., 2012)	17
Figure 2.6 : Gravimetric feeder (Ramulu, 2017).....	18
Figure 2.7: Online coal ashmeter analyser (Klein, 2013)	19
Figure 2.8: Eureka AF Series Aerofoil (EUREKA, 2018).....	20
Figure 2.9: Aerofoil description (EUREKA, 2018).....	21
Figure 2.10: Pitot tube flow measurement in air/gas ducting (Matthews, 2016).....	22
Figure 2.11: Air flow measurement in a duct with in-line calibration test ports (Sabin, 2016)	23
Figure 2.12: (Lft): Traverse sampling (ASME, 2010), (Right): Traverse ports measurement (Catia 3D View).....	23

Figure 2.13: Boiler Energy Inputs (Rousseau & Fuls, 2018).....	24
Figure 2.14: Boiler Energy Outputs (Rousseau & Fuls, 2018).....	25
Figure 2.15: Flue gas computational flow analysis (CFD) in a coal-fired boiler (Ferreira et al., 2010)	26
Figure 2.16: Tertiary Air Flow Simulation (Ferreira et al., 2010).....	26
Figure 3.1: MEB boundary for a coal-fired boiler plant at Power Station A.....	28
Figure 3.2: Simplified MEB boundary	29
Figure 4.1: Secondary Air Ducting to boiler (Catia 3D View).....	41
Figure 4.2: Air flow system's inlet boundaries	41
Figure 4.3: Air flow system's outlet boundaries.....	42
Figure 4.4: Fluid element for pressure and flow analysis (ANSYS, 2015).....	42
Figure 4.5: Fluid element mesh type (ANSYS, 2015).....	43
Figure 4.6: ANSYS Simulation Process Flow Diagram (ANSYS, 2015).....	44
Figure 4.7: Air flow system's meshing for the simulation process.....	50
Figure 5.1: Flow rates comparison between MEB results and Etapro Control System Data	52
Figure 5.2: Flow rates comparison between MEB results and plant design specifications	53
Figure 5.3: Coal mass flow rate sensitivity variation	57
Figure 5.4: Air mass flow rate sensitivity variation.....	58
Figure 5.5: Flue gas mass flow sensitivity variation	59
Figure 6.1: Air flow simulation in Main Ducting (3D View).....	61
Figure 6.2: Air flow simulation in Main and distribution Ducting (Top View).....	62
Figure 6.3: Air flow simulation in Front Main and distribution Ducting (Front View).....	63
Figure 6.4: Air flow simulation across aerofoil.....	64
Figure 6.5: Results of the analysis of the size of mesh in the air flow simulation.....	65
Figure 6.6: Iso-velocity diagram after the aerofoil in the burners' ducting	66
Figure 6.7: Iso-velocity diagram in the distribution ducting	67
Figure 6.8: Iso-velocity diagram in the main ducting	68

Figure 6.9: Measurement points for the analysis of secondary air flow	70
---	----

LIST OF TABLES

Table 3.1: Heat release from combustion reaction by coal elements (Rousseau & Fuls, 2018)	31
Table 3.2: Molar mass of elements of the coal's combustion (Rousseau & Fuls, 2018)	32
Table 3.3: Stoichiometric coefficient (Rousseau & Fuls, 2018).....	33
Table 3.4: Coefficient for calculating the enthalpy of various gases at 1 bar (Rousseau & Fuls, 2018).....	34
Table 3.5: Cp for Typical solids (Rousseau & Fuls, 2018)	35
Table 3.6: List of plant measurements used for MEB at Full Loads for Power station A	38
Table 3.7: ESKOM MEB Assumptions	40
Table 4.1: Mesh size used for the air flow simulation	50
Table 5.1: MEB calculation results	51
Table 5.2: Comparison MEB results with ETAPRO Plant operation Data.....	51
Table 5.3: Comparison between MEB results and plant design specification data....	52
Table 5.4: Input parameters at 521 MW Full load values for MEB sensitivity analysis	55
Table 5.5: Sensitivity variation of mass flow rate of coal	57
Table 5.6: Sensitivity variation of mass flow rate of air	59
Table 5.7: Sensitivity variation of mass flow rate of flue gas	60
Table 5.8: Sensitivity variation of MEB outputs.....	60

GLOSSARY

Acronyms and Abbreviations

A/H	Air heater
BMEB	Boiler mass and energy balance
CFD	Computerized Fluid Dynamics
CV	Calorific value
DP	Differential Pressure
EA	Excess air
EPPEI	Eskom Power Plant Engineering Institute
ESP	Electrostatic precipitator
FD	Forced draught
FFFR	Fossil fuel firing regulations
FG	Flue gas
GCV	Gross calorific value
HHV	Higher heating value
HP	High Pressure
ID	Induced draught
IP	Intermediate pressure
LP	Lower pressure
LPH	Lower pressure heater
MEB	Mass and energy balance
NCV	Net calorific value
NHR	Net heat rate
PA	Primary air
PF	Pulverised fuel
SA	Secondary air

List of Nomenclature

General symbols

$\%Air_{ing}$	Mass percentage of ingress air in total humid air	%
$\%b_{Ash}$	Mass percentage of bottom ash in total ash	%
$\%f_{Ash}$	Mass percentage of fly ash in total ash	%
$\%C_{fa}$	Mass percentage of carbon in fly ash	%
$\%C_{ba}$	Mass percentage of carbon in bottom ash	%
C_p	Specific heat at constant pressure	$\text{kJ/kgK} \text{ } ^\circ\text{K}$
$CV_{pf.coal}$	Calorific value of pulverised coal	kJ/kg
DAR	Dry air	$\text{kg of air/kg of coal}$
$EA_{A/H.fg.in}$	Excess air at air heater flue gas inlet	%
E_{in}	Total Power inputs	MW
E_{out}	Total Power outputs	MW
fEA	Excess Air	$\text{kg of air/kg of coal}$
FGR	Mass flow rate of flue gas per kg of coal	$\text{kg of flue gas/ kg of coal}$
G_k	Turbulence kinetic energy	kJ
$h_{air.AH.out}$	Enthalpy of air at air heater outlet	kJ/kg
$h_{air.amb}$	Enthalpy of air at ambient temperature and pressure	kJ/kg
h_{BA}	Enthalpy of bottom ash	kJ/kg
HAR	Humid air required	$\text{kg of air/kg of coal}$
h_{coal}	Enthalpy of coal	kJ/kg
$h_{fg.AH.inlet}$	Enthalpy of flue gas at air heater inlet	kJ/kg
$h_{fw.econ.in}$	Enthalpy of feedwater at economiser inlet	kJ/kg
$h_{H_2O.vap}$	Latent heat of vaporisation of water	kJ/kg
$h_{rh.in}$	Enthalpy of steam at reheater inlet	kJ/kg

$h_{rh.att}$	Enthalpy of reheater attemporator water	kJ/kg
$h_{steam.rh.out}$	Enthalpy of steam at reheater outlet	kJ/kg
$h_{steam.sh.out}$	Enthalpy of steam at superheater outlet	kJ/kg
IM	Inherent moisture	%
\dot{m}	Mass flow rate	kg/s
$\dot{m}_{air.AH.out}$	Mass flow rate of air at air heater outlet	kg/s
$\dot{m}_{air.ingress}$	Mass flow rate of ingress air	kg/s
$\dot{m}_{air.AH.total}$	Total mass flow rate of air inside control volume	kg/s
\dot{m}_{coal}	Mass flow rate of coal	kg/s
m_{fc}	Unburnt carbon per kg of coal	kg of Carbon /kg of coal
m_{fcc}	Energy of unburnt carbon per unit energy in coal	kJ of Carbon/kJ of coal
$\dot{m}_{fg.AH.in}$	Mass flow rate of flue gas at air heater inlet	kg/s
$\dot{m}_{fw.econ.in}$	Mass flow rate of feed water	kg/s
$\dot{m}_{seal.air}$	Total mass flow rate of seal air into mills	kg/s
$\dot{m}_{rh.att}$	Mass flow rate of reheater attemporator water	kg/s
$\dot{m}_{rh.in}$	Mass flow rate of reheater inlet steam	kg/s
$\dot{m}_{rh.out}$	Mass flow rate of reheater outlet steam	kg/s
$\dot{m}_{sh.att}$	Mass flow rate of superheater attemporator water	kg/s
$\dot{m}_{sh.out}$	Mass flow rate of superheater outlet steam	kg/s
P_{atm}	Atmospheric Pressure	kPa
P_{fw}	Pressure of feed water	kPa
$P_{sh.att}$	Pressure of superheater attemporator spray water	kPa
$P_{steam.drum}$	Pressure of steam/water inside drum	kPa
$P_{steam.sh.out}$	Pressure of steam at final superheater outlet	kPa
P_{mills}	Power to mills	MW
$P_{PA.fans}$	Power to PA fans	MW
Pr	Prandtl number	
P_{ratio}	Pressure ratio	

$P_{seal.fans}$	Power to mill seal air fans	MW
$P_{seal.fans}$	Power to mill seal air fans	MW
$Q_{credits}$	Power of credits	MW
Q_{loss}	Power loss	MW
Q_{out}	Power out	MW
Re	Reynolds number	
SM	Surface moisture content in coal	%
TAR	Stoichiometric air required	
$T_{air.AH.out}$	Temperature of air at air heater exit	°C
T_{amb}	Ambient temperature inside boiler house	°C
T_{atm}	Atmospheric Temperature	°C
$T_{BA.exit}$	Temperature of bottom ash leaving boiler control volume	°C
$T_{fg.AH.in}$	Temperature of flue gas at air heater inlet	°C
$T_{fg.AH.out}$	Temperature of flue gas at air heater outlet	°C
$T_{fw.econ.in}$	Temperature of feedwater at economiser inlet	°C
$T_{fw.econ.out}$	Temperature of feedwater at economiser outlet	°C
TM	Total moisture content in the coal	%
$T_{steam.sh.out}$	Temperature of steam at final superheater outlet	°C
$T_{sh.att}$	Temperature of attemporator spray water	°C
X_{Ash}	Mass percentage ash content of coal	%
X_C	Mass percentage Carbon content of coal	%
X_H	Mass percentage Hydrogen content of coal	%
X_O	Mass percentage Oxygen content of coal	%
X_N	Mass percentage Nitrogen content of coal	%
X_S	Mass percentage Sulphur content of coal	%
X_{moist}	Mass percentage moisture content of coal	%
y	Normal distance to the nearest wall	m

Greek symbols

η_{boiler}	Boiler efficiency	%
α	Inverse Prandtl number	
∇	Flow gradient	
μ	Dynamic viscosity	Pa.s
τ	Static pressure	Pa
ρ	density	Kg/m ³
v_r	Flow radial velocity	m/s
v_x	Flow axial velocity	m/s
ω	Specific humidity of ambient air	kg of water/kg of dry air

CHAPTER ONE

THESIS OVERVIEW

1.1 Introduction

Coal is the primary source of energy in a country like South Africa and contributes substantially to the economic growth. According to the National Department of Statistics, for the past decade, the electricity production from coal-fired power stations has increased coal consumption, which accounted for 60-70% (Constenla et al., 2013) of the total power energy supplied to the grid. This is due to its abundance in South Africa where the necessary quantities can be continuously supplied by mines located near the coal power stations. Coal will still be one of the most reliable source of electrical energy production in South Africa for years to come, in spite of the many challenges such as global warming and the decline in coal quality (ESKOM, 2016).

Power stations using coal-fired processes are the most important suppliers of electricity in many countries and contribute to job creation. However, the consumption of coal has a major impact on production costs for power producers like ESKOM. In a coal-fired power station, the pulverised coal-fired boiler and its auxiliary system (air, flue gas and mills) constitute the major components that produce the heat energy required to generate steam to drive the turbines. The coal-fired boiler as well as condensing system, turbines and feed heaters are the main components that influence the heat rate of the total power plant. The mass flow rate of coal is influenced by the overall combustion or process system which includes the air system, PF milling plant and burners' arrangement. Coal consumption is an indicator of power plant efficiency which eventually has a significant effect on both boiler efficiency and overall plant reliability (Constenla et al., 2013).

Traditional methods have proven that, it is difficult to measure accurately the quantity of pulverized coal fuel used in the furnace at many ESKOM plants, with equipment and instruments available on site, due to the size of ducting which requires advanced technologies. The mass flow rate of the coal can be determined indirectly using the boiler mass energy and balance (MEB) calculation method, taking into consideration flue gas and air flows that are key relative parameters influencing the total energy output. The accuracy of these MEB calculations in most cases is still dependent on the plant's input parameters, and the suitability of this method, for online monitoring, depends on the availability of measurements from the plant (ESKOM, 2016). In effect, the comparison of the mass flow rates determined with the MEB calculation and plant online ETAPRO data, is necessary in order to provide a clear analysis of the actual plant's performance as specified by its design.

1.2 Background

1.2.1 Boiler and auxiliary system at Power Station A

This section gives an overview of power station A which has been used for the implementation of this research project.

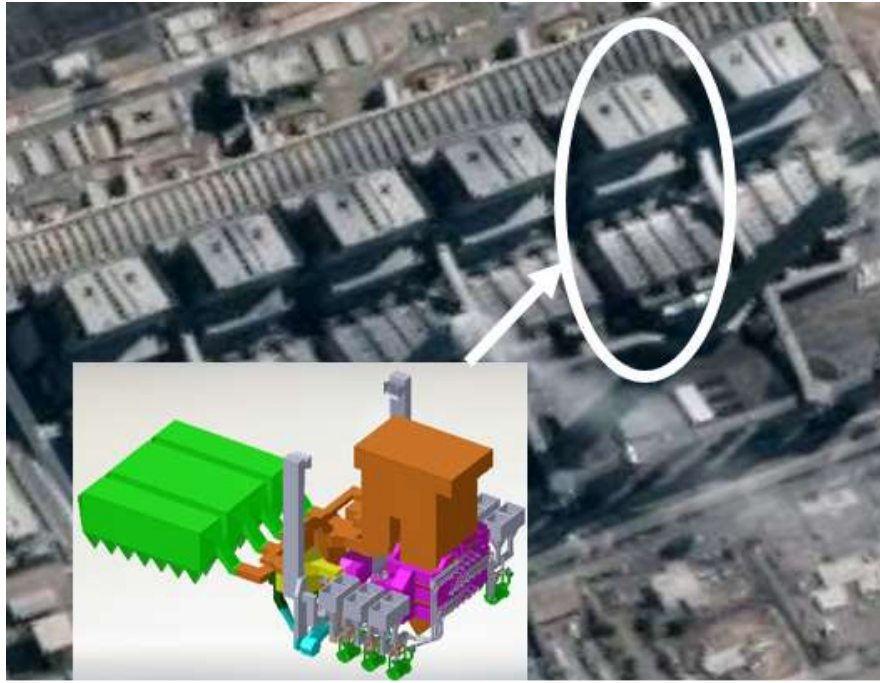


Figure 1.1: Coal-Fired Power Station A (ESKOM, 2016)

The six boiler units at the Coal-Fired Power Station A, as shown in Figure 1.1, are the size of an office building of 35 floors, and in a unique configuration when compared to other coal power stations. These boiler units have been designed to allow for the efficient use of coal energy extracted during combustion to heat up water. The pulverised coal supplied by the six horizontal ball mills is carried by the hot primary air into the boiler's furnace, where it ignites by a series of burners located on the rear and front walls. The air is extracted from the surrounding atmosphere by two FD fans and supplied to the air heater (A/H) where its temperature is increased (on average) to 250°C, as required for an efficient combustion process. The combustion of the pulverized coal is activated by the fuel oil which is injected in the furnace at high pressure, by means of a series of nozzles as mentioned above. Inside the boiler furnace the maximum temperature reached during combustion is $\pm 1400^{\circ}\text{C}$ during full load. The flue gas is extracted from the boiler by the ID fans and then exhausted into the atmosphere through smoke stacks after some pollutant substances are removed in the ESP unit (ESKOM, 2016).

a) The Coal system at Power Station A

The coal system in a boiler unit at the Coal-Fired Power Station A, as shown in Figure 1.2, comprises of 6 ball mills supplying 36 burners (18 burners in the front and back walls respectively) through high (PF) pipes carrying the pulverized fuel.

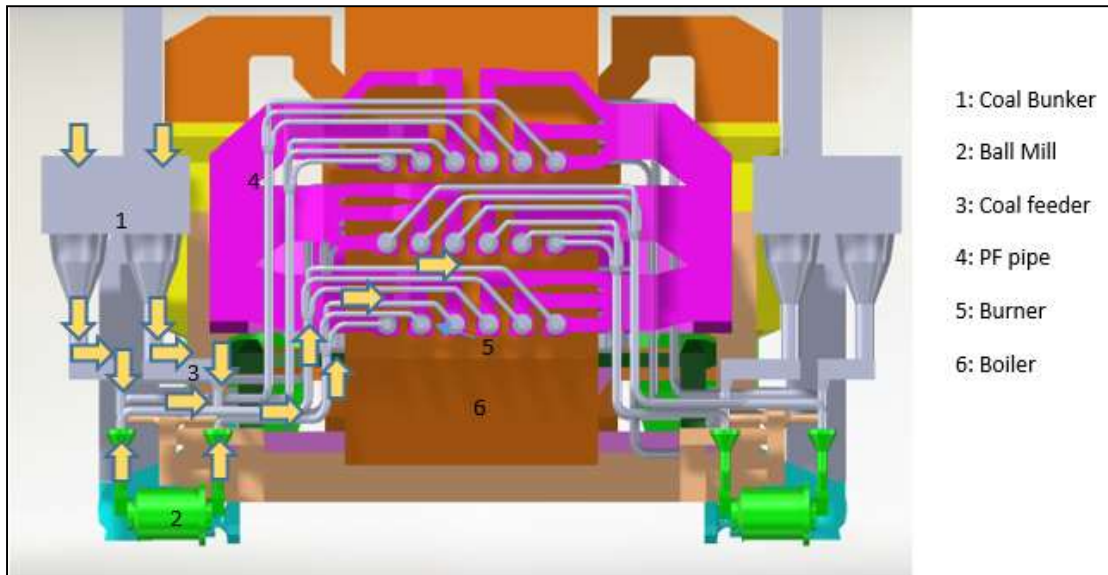


Figure 1.2: Pulverised coal flow system at Power Station A (Catia 3D View)

PF boilers are the most common type of boiler used for steam generation in coal power stations, due to the way they have been designed to burn pulverised coal, which consists of very small highly flammable particles. The raw coal is sourced from a nearby mine via a set of conveyor belt systems, to multiple bunkers which supply the mill feeders. The mill feeders adjust the rate at which the coal is fed into the ball mills, in order to be ground down to the required size. There are two coal feeders per ball mill at two inlets; the pulverised coal is supplied to the burners through two outlets. An air seal is used in the mills to prevent any PF leak and external contamination. The seal is supplied by a seal fan which is mounted on the mill (ESKOM, 2016).

b) The Air system at Power Station A

The total air supplied to the PF boiler at Power Station A is supplied by the FD fans which are installed on the left and right-side walls. The FD fans extract all the required air from the atmosphere, from the highest point on the boiler where the temperature is higher than the ambient, in order to reduce the energy required to heat it up. The mass flow rate of the air supplied is required for stoichiometric combustion of the pulverised coal, together with the excess to achieve efficient and complete combustion. The air is firstly heated up inside the heater and fed to the boiler at a temperature in the range between 250°C to 300°C.

The PA fan draws air from the FD steam to be supplied to the mills in order to pneumatically convey the PF particles to the burners. The remainder of the FD stream, the secondary air (SA), is directly supplied to the boiler to accelerate and increase the combustion process (ESKOM, 2016).

The air system at the coal-fired power station A can be further specified as follows:

PA System:

Figure 1.3 illustrates the primary air flow at the ESKOM power station A. The PA is taken from the FD ducting before the secondary air heater and is heated up by the hot flue gas in the tubular primary air heater (A/H). Then it is mixed with tempering air to avoid overheating the air supplied to the mill via the primary air ducting.

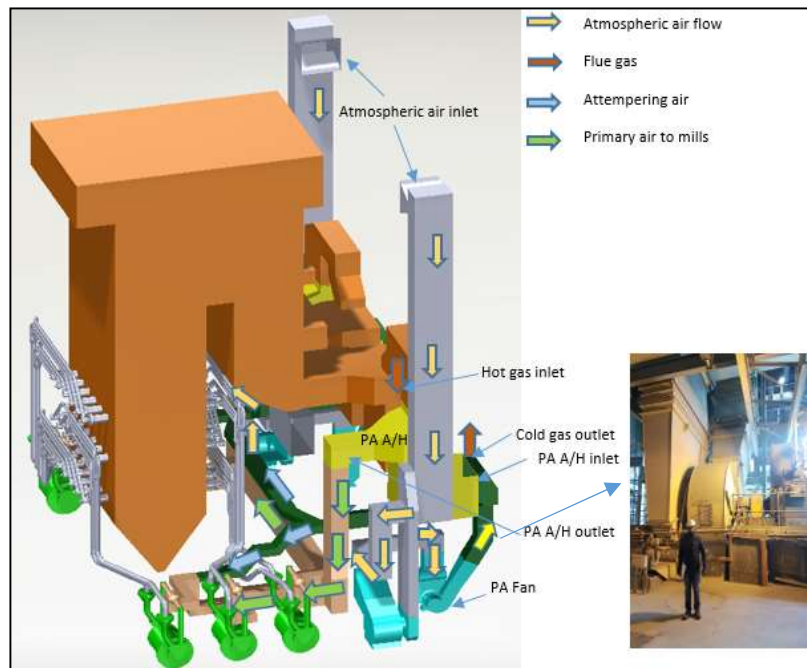


Figure 1.3: Primary air system at Power Station A (Catia 3D View)

SA System

The secondary air flow as shown in Figure 1.4 is divided into multiple streams by different ducts connected to all the burners. This allows the pulverised coal to be distributed rapidly for the combustion process in the boiler's furnace.

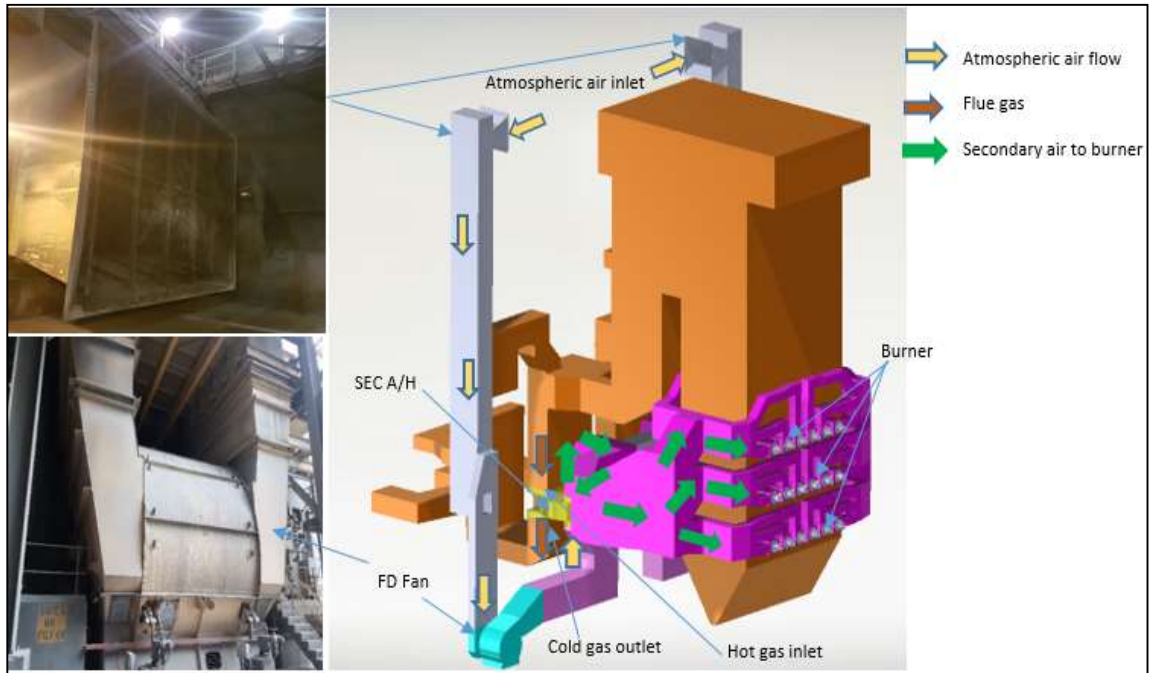


Figure 1.4: Secondary air system at Power Station A (Catia 3D view)

The secondary air at Power Station A is heated up by the Rothamule/Ljungstrom type heater (A/H) situated at the exit of the boiler's economiser on the ducting of the flue gas. The secondary air heater (SEC A/H) as shown in Figure 1.5, is a rotary heater with stationary or moving plates which extract the heat of the flue gas flowing out of the boiler. The temperature of the flue gas, at the exit of the secondary air heater, is lower than the temperature at the inlet, because of the heat recovered and transferred to the secondary air. This process increased the PF boiler efficiency by roughly 1% (Jashuva et al., 2014).

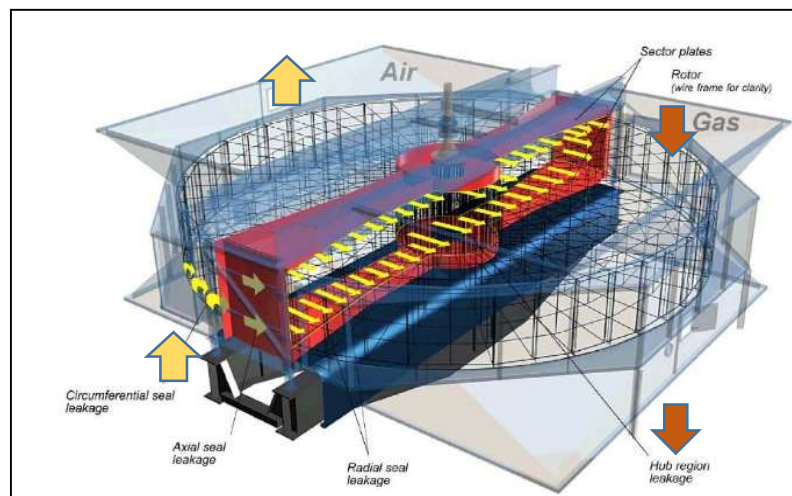


Figure 1.5: Example of a secondary air heater (Rothamule air heater) (Jashuva et al., 2014)

c) The Flue gas system at power plant A

The path of the flue gas at Power Station A as shown in Figure 1.6 starts from the furnace to the air heater's exit where the heat is extracted gradually. The flue gas passes through a series of heat exchangers from across the top of the super heater and the evaporator to the bottom of the boiler's exit. The maximum temperature of the flue gas is at the exits; of the furnace 1200°C, between 200 to 400°C of the economiser, and between 120 to 140°C of the air heater. The most important role of the flue gas is to transfer the heat produced by the combustion process to the water that is supplied to the boiler by the feed pump through the economiser, in order to generate superheated steam. The water temperature is slightly increased in the lower pressure heater (LPH) just before it is fed into the economiser which is situated at the bottom of the boiler (ESKOM, 2016).

The flue gas temperature decreases gradually while it passes through the super heater, re-heater, evaporator, economiser and air heater as the useable heat energy is recovered for boiler efficiency. At the economiser's exit, the discharge duct splits into two equal conduits supplying the left and right secondary air heaters. However, a portion of the flue gas flow bypasses the secondary air heater at the inlet from the top through to another side duct and discharges in the primary air heater. The flue gas exits the primary and secondary air heaters (left and right) in separate discharge ducting, which are connected to a main duct just before it goes through the ESP (ESKOM, 2016). The flue gas extraction from the boiler is done by two ID fans located at the ESP's exit which removes pollutant substances before it discharges through the stack to the atmosphere (Tootla, 2015).

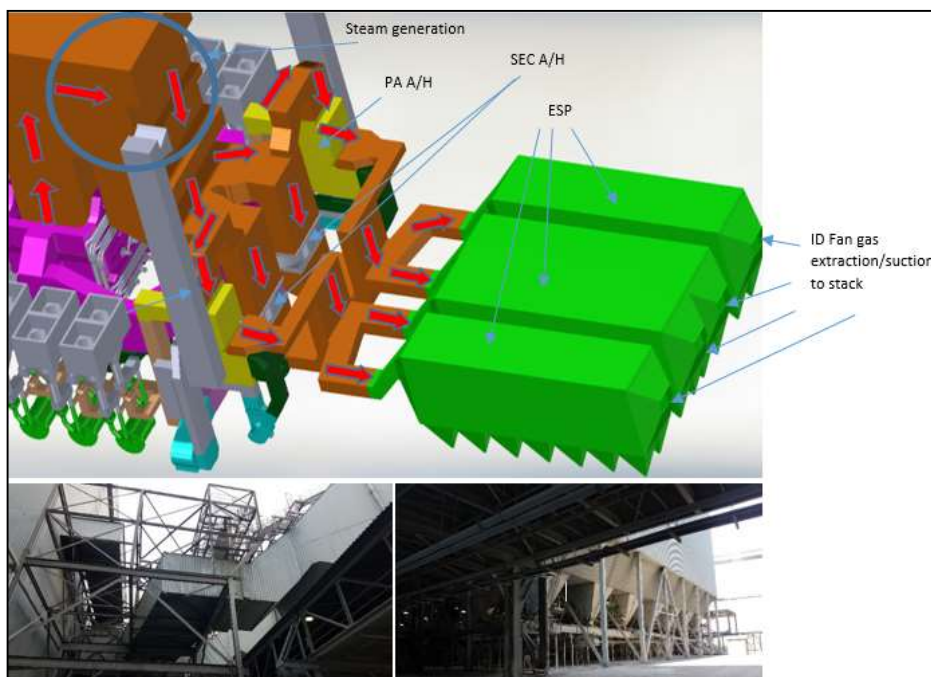


Figure 1.6: The Flue gas system at Power Station A (Catia 3D View)

1.2.2 The consumption of Coal

Electricity in South Africa is largely produced by coal power plants run by ESKOM. Inside the power station, the coal is pulverised to a fine powder by large grinding mills. Pulverised coal burns quickly, like gas, when fed into the furnace during the combustion process, producing the heat energy and steam inside the boiler to run the turbine for power generation (ESKOM, 2016).

However, competition in the production of electricity in many countries, has introduced new challenges to power plants to reduce production cost and operate more efficiently. Degrading coal quality and plants operating at maximum capacity are the main factors that reduce the efficiency of the coal-fired power stations. In effect, the coal power plant processes should be monitored constantly by means of accurate measurements of coal flow while controlling the efficiency of the boiler, which is the main component for generating steam to drive a turbine in order to produce electrical energy (Palmqvist, 2012).

The most common problem found in many coal-fired power stations in recent years is the waste of coal due to the inefficiency of the plant when operating at full load. New technology is needed for the optimal control of pulverised coal. It has been demonstrated that there is a critical need for a coal-fired power plant, to control accurately the mass flow rate of coal in order to reduce its consumption (Jing et al., 2017).

The overconsumption of coal leads to excessive increase in operating costs that affect the reliability of the power plant. When coal is supplied excessively to the burner, it causes overheating and slagging to occur on the heat exchangers' tubes such as the super-heater or the re-heater as shown by Figure 1.7. This has negative influence on the heat transfer process which is very important for steam generation. In effect, the heat transfer is reduced and this causes higher flue gas temperature that lead to heat exchanger tubes failure as well as corrosion. Therefore, the boiler's efficiency is reduced and the operating cost increased. High operating cost could lead to plant's closure and economic slowdown (Tootla, 2015).



Figure 1.7: Slagging on the super-heater's tubes (Tootla, 2015)

1.3 Problem Statement

The coal consumption at Power Station A is not monitored accurately, and there is not an exact coal flow rate quantity determined by the plant. The cost of electricity production in modern thermal coal power stations is predominantly influenced by fuel/pulverized coal consumption (Jing et al., 2017).

Over consumption of coal causes a substantial increase in operating costs, slagging of boiler tubes and unstable steam energy required to drive the turbines, while considerably reducing the efficiency of the power plant (Plamqvist 2012; Usman 2007). The boiler tubes in which steam flows are overheated by the flue gas which is at very high temperature, thus damaging the tube material (Blondeau et al., 2016; Constenla et al., 2013; Sargent, 2009).

It is difficult to measure pulverized coal and gas flow in the furnace accurately with the equipment and instrumentation available, due to the large sizes of pipe and ducting, which requires advanced technologies that are very expensive to be implemented in many coal power plants (Huang et al., 2010; Plamqvist 2012) like those operated by ESKOM in South Africa. Therefore, the mass flow rate of the coal has to be determined indirectly using a MEB calculation, taking into account the flue gas and air flows that are key relative parameters that also influence total energy output.

1.4 Objectives

The main objectives of the project are:

- ❖ Determine the heat rate of the plant using measurements (air, flue gas and steam) and MEB calculations
- ❖ Develop a 3D visual system of the different circuits like coal flow, air and flue gas that will be useful for the process/operation teams, at the coal power station, to have a better understanding of the plant and easily locate or access different measurement sensors and devices
- ❖ Compare MEB results and plant performance data
- ❖ Develop an air flow simulation to identify key measurement points

1.5 Limitations of the study

The project is limited to the analysis of the coal, flue gas and air systems inside the boiler, using thermodynamics and combustion engineering principles. Additionally, the project does not engage with development of new technology but analyses the current means of measurement used by ESKOM to determine the heat rate of the plant. Furthermore, the

research project is based only on the analysis of measurement parameters used in plant MEB calculations.

1.6 Methodology

The anticipated study was conducted in the following stages:

- ❖ The boiler MEB methodology was used in this project to calculate the heat rate of the power plant. The MEB is based on a series of thermo-fluid and coal combustion equations to calculate critical parameters like coal, gas (air and flue gas) mass flow rates in the coal-fired power plants. This is illustrated with the calculation diagram shown in Figure 1.8.

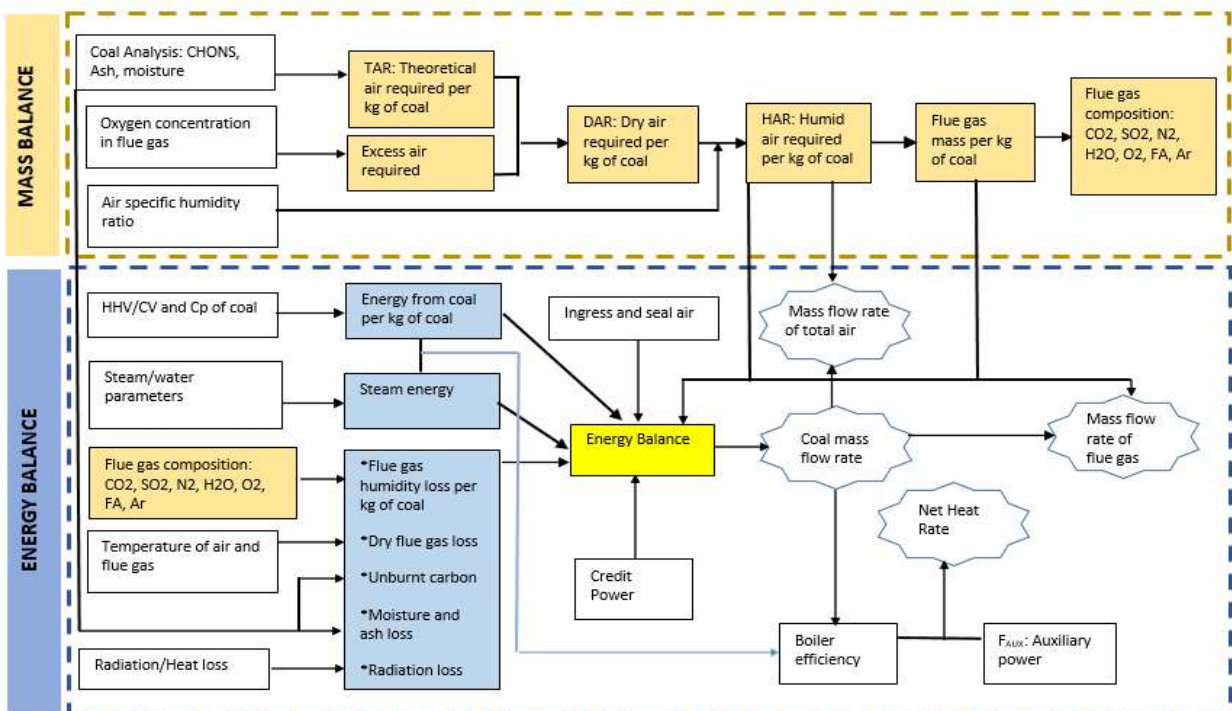


Figure 1.8: Boiler MEB calculation flow diagram

- ❖ Plant parameters were used to implement the MEB model in order to calculate the coal, air, flue gas mass flow rates and the power plant heat rate. For this project, the plant data was supplied by Power Station A run by ESKOM. A site visit was scheduled and took place during full load operation of the boiler plant at the ESKOM power station to collect the MEB data and identify measurement instruments as well as their location in the boiler plant. The plant operating parameters were extracted from the ETAPRO control system for a period of three months, as summarized by Figure 1.9 and Figure 1.10.

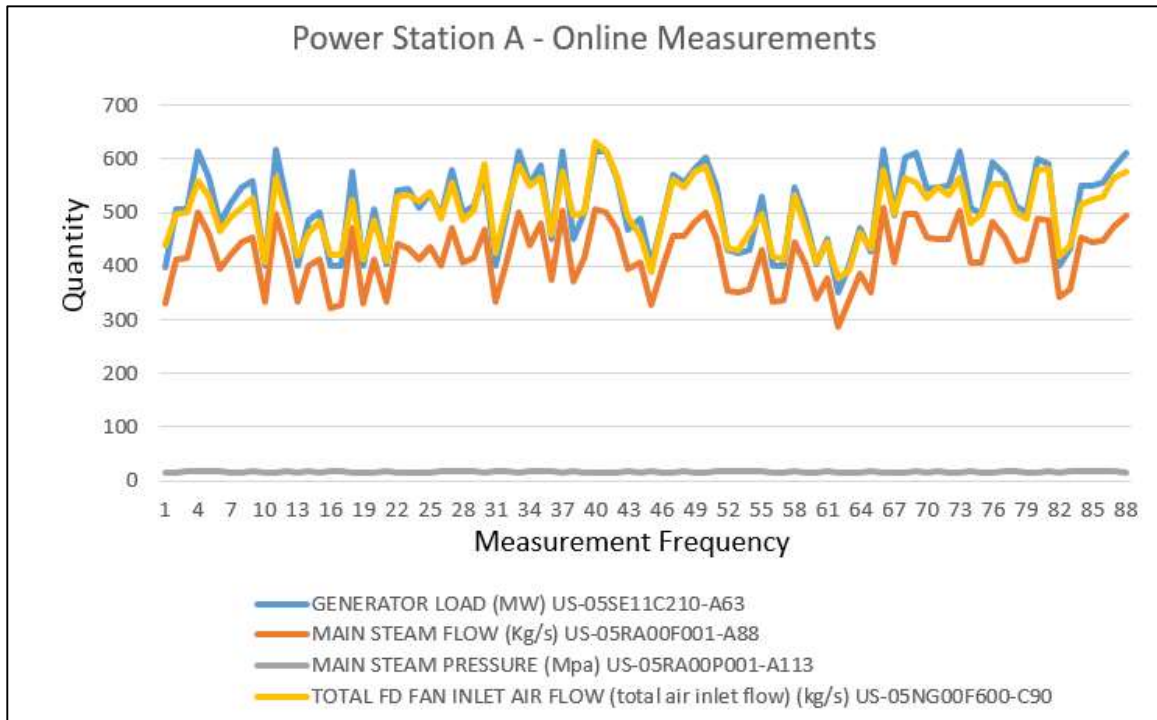


Figure 1.9: Operating parameters: flow and pressure for coal-fired Power Station A

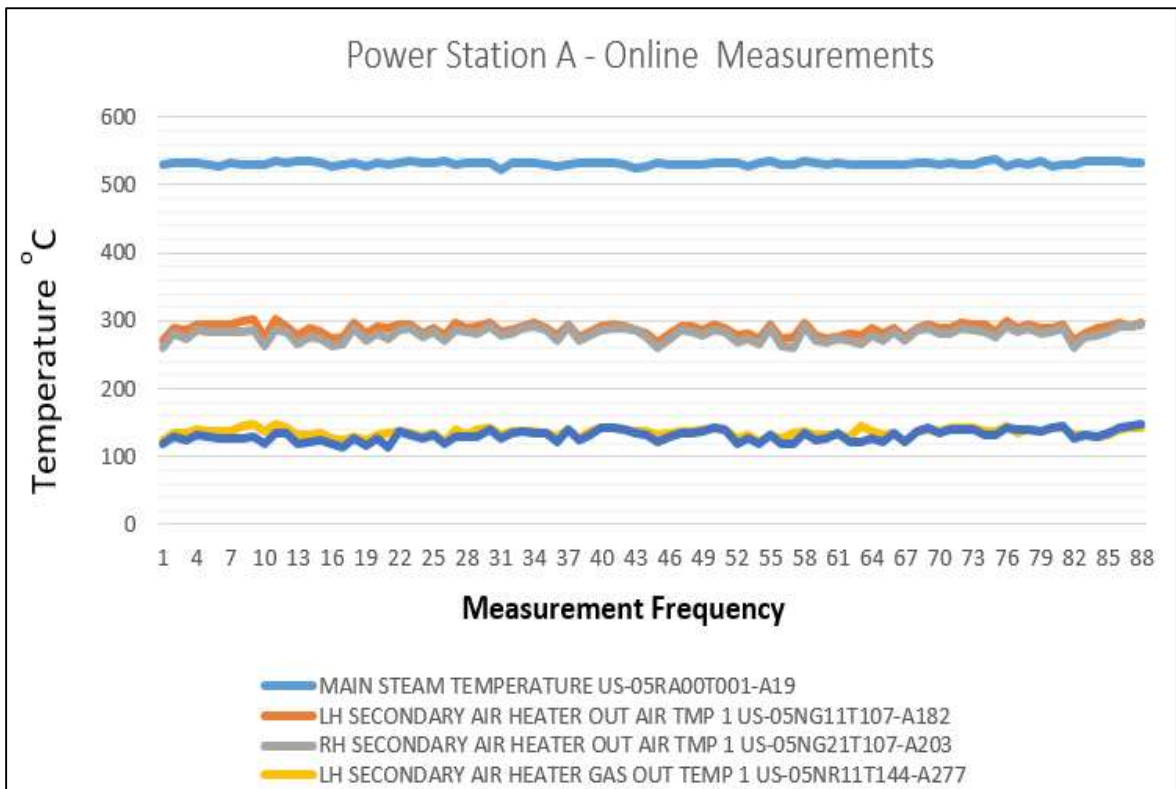


Figure 1.10: Operating parameters-Temperatures for coal-fired Power Station A

- ❖ The air flow simulation was done using ANSYS Fluent CFD. ANSYS Fluent is flow simulation software based on set of equations such as continuity, momentum and energy. Additionally, a transport equation is used by the software for turbulent flow. The process for the simulation by ANSYS Solver is illustrated in Figure 1.11.

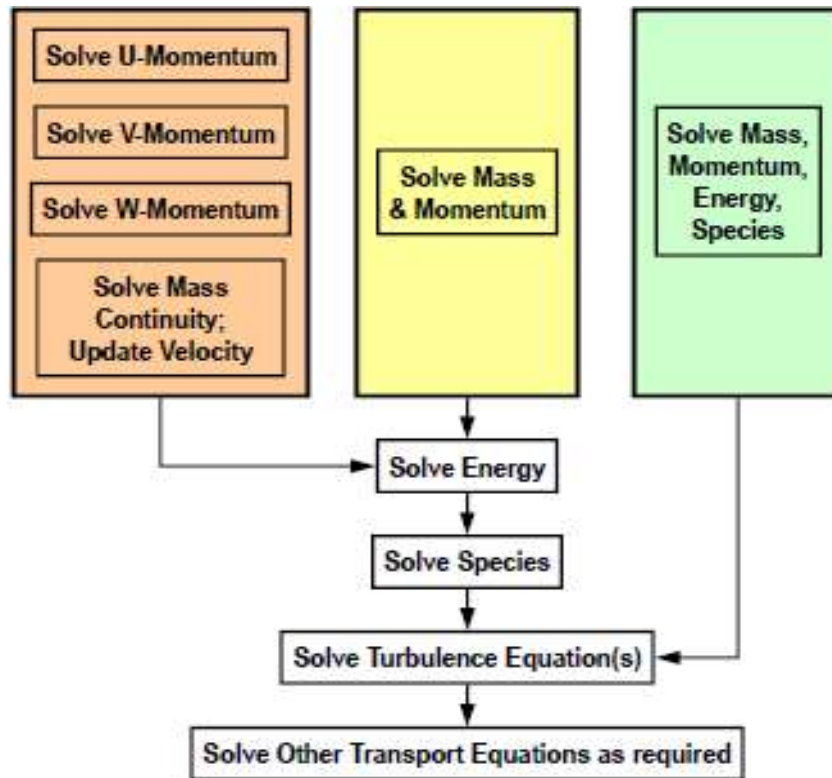


Figure 1.11: ANSYS simulation solver (ANSYS, 2015)

1.7 Chapter outline

1.7.1 Chapter One

This chapter presents the background, problem statement, objectives, limitation of study and methodology.

1.7.2 Chapter Two

The second chapter covers the literature review of the boiler flow measurements (coal, air and flue gas), and gives an overview of the MEB and CFD methodologies.

1.7.3 Chapter Three

This chapter describes the MEB methodology

1.7.4 Chapter Four

The four chapter is focused on modelling and flow simulation (CFD)

1.7.5 Chapter Five

This chapter covers the MEB results and sensitivity analysis

1.7.6 Chapter Six

This chapter discusses the CFD results

1.7.7 Chapter Seven

The seventh chapter presents the conclusion, findings and recommendation for future work

1.7.8 Appendix

This section contains the MEB calculations, CFD simulations and a 2D/3D Layout of the Plant's boiler

CHAPTER TWO LITERATURE REVIEW

This chapter is firstly focused on the different flow measurement techniques used for the coal, air and flue gas streams in a coal-fired boiler. Thereafter, the basic theory of the MEB method and CFD modelling is reviewed.

2.1 Flow Measurement in a Coal-fired plant

The demand for electrical energy worldwide has resulted in increased demand for more cost-effective power production, and tough policies to reduce pollution. In effect, the coal-fired power suppliers are searching for new solutions to optimize different processes during the production of electricity. Coal is still largely used in the production of electricity in many countries, and accounts for 40% (Constenla et al., 2013) of global electrical energy production. PF coal boilers are among the most reliable and largest suppliers of electrical energy in the world. In this regard, it is critical for the optimization of the combustion process to be implemented in order to increase boiler efficiency and reduce operational costs. The optimization of the combustion process in these power stations can be done in many ways, such as replacing old equipment with new measurement technologies, or re-calibrating the existing instruments for accurate control of all power plant operations (Constenla et al., 2013).

However, it is very difficult to accurately control the combustion processes taking place in many coal-fired furnaces due to limited measurement methodologies particularly for flow of coal. The improved stability of critical parameters for sustainable operations has been requested by many coal-fired power stations to be implemented with advanced control systems, in the last decade. There is an increasing demand for ideal and flexible operations systems in coal power plants in order for them to achieve economic and profitable performance. Many research experiments done on coal combustion process have contributed to the optimization of power plants by in-depth analyses of process input and output parameters (Huang et al., 2010).

2.1.1 The Measurement of the flow of coal

In many coal fired plants, the accuracy of measurement of the coal flow rate is a critical requirement to maintain the reliability of operations (Matthews, 2016). In effect, the efficiency of electrical power production in a thermal coal-fired power plant is indicated by the heat rate, which is the measure of the energy used to generate a kilowatt-hour per coal quantity burnt. In effect, the heat rate of the plant is a clear indicator of the plant's performance that can help to reduce coal consumption. Production cost can be reduced by continuously improving the heat rate (Walsh et al., 2015).

A power plant's heat rate is the most common indicator/parameter, used in the electrical energy generation industry, to assess their performance and efficiency. The heat rate of a power station is mainly influenced by the flow of coal at full load operation. The actual plant heat rate is generally higher than the design value in many coal-fired power plants due to operational inconsistencies that vary according to the various process systems in place (Sargent, 2009). Sharp increases in the cost of coal has led many power plants to search for ways to reduce their annual fuel bills (Edward, 2009).

Blondeau et al. (2015) conducted a study based on online monitoring of coal particle size and flow distribution in coal-fired power plants. The size of the pulverised coal and the consistency of the mass flow rate of coal supplied to the burners were critical parameters for an efficient combustion process. The project illustrated a system for online control of the PF particle distribution and flow across all burners from the coal mill outlets in a 660 MW coal-fired power plant. The results obtained when changing the speed of various mill centrifugal classifiers was analysed and the PF flow inside the burners was improved enormously.

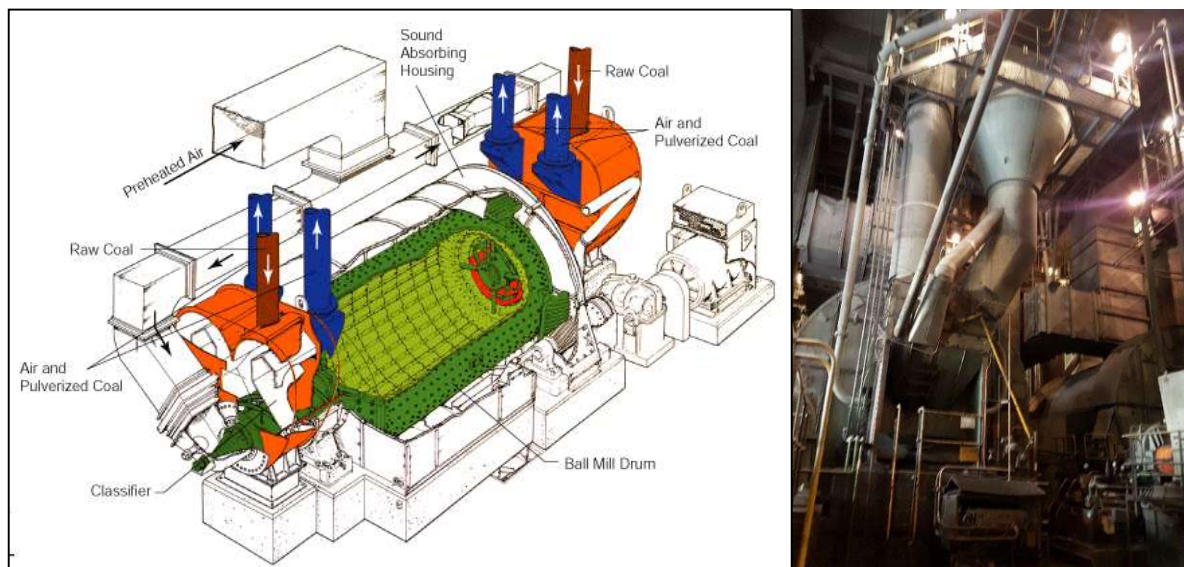


Figure 2.1: (Left) Coal ball mill (IHI Corporation, 2017), (Right) PF Coal Ball Mill (ESKOM, 2018)

However, the average size of the pulverised coal from the PF mill as shown in Figure 2.1 is in the range of 60 to 70 microns in diameter. The benefit of pulverised coal is the fast and efficient combustion rate that results, because the fine particles are highly flammable in the complete combustion when mixed up with hot air. This allows PF boiler manufacturers to design various size coal-fired boilers with the same efficient combustion process that is useful for steam generation (Tootla, 2015). The fine size of the PF particles and the consistency of the coal flow supplied to the burners are very important parameters for efficient combustion.

Coal consists of pure coal, mineral matter and moisture as detailed in Figure 2.2. The pure coal consists of fixed carbon and volatile organic matter. The mineral matter consists of volatile mineral matter with ash while the total moisture is made up of inherent moisture and surface moisture. Moisture is essentially the water contained within the coal and typically ranges between 3% and 7% for South African coals (Rousseau & Fuls, 2018).

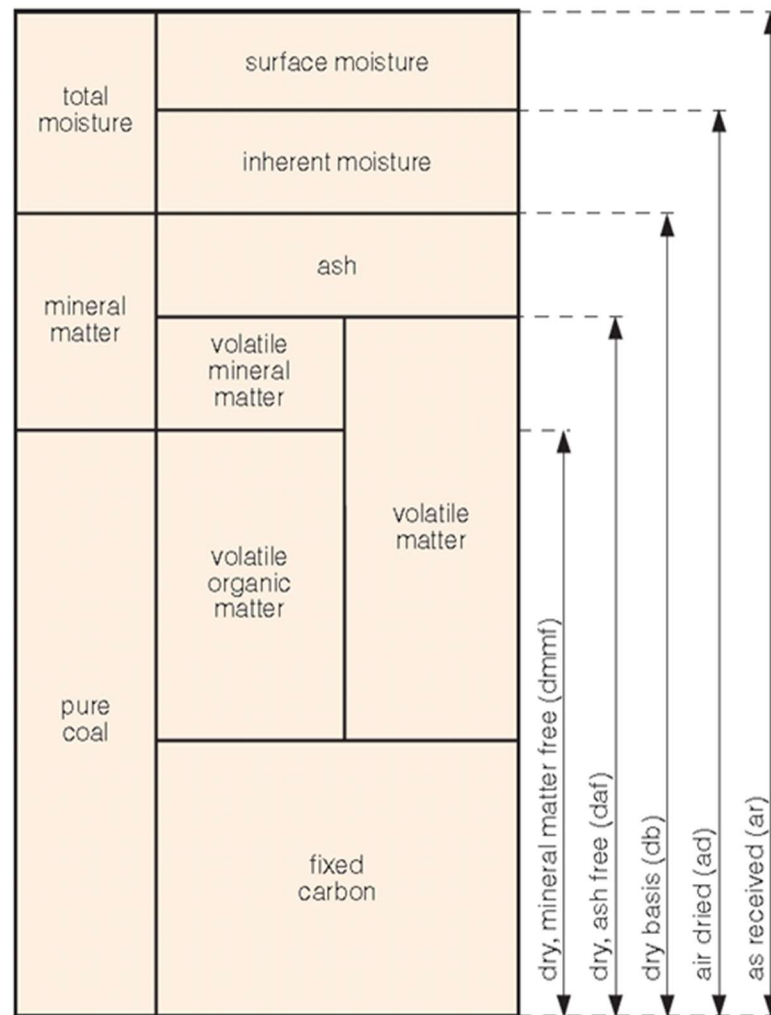


Figure 2.2: Coal composition (Rousseau & Fuls, 2018)

PF flow-meter

Coal-flow and distribution to boiler burners has, up until now, proved difficult to be measured with a dedicated instrument like the PF flow-meter. The dynamics of the flow of coal is very dependent on factors such as particle size, roping and the physical plant layout (Palmqvist, 2012).

The new generation of PF Flow-meters as shown in Figure 2.3 are capable of making continuous measurements of the flow of coal in all the burner feed pipes simultaneously. Measurements are continuously updated and hence the output signals respond accordingly.

Each sensor features a completely smooth internal bore which enables the longest possible interval between measurements (ABB, 2018).



Figure 2.3: PF Flow Meter (ABB, 2018)

Probes with Orifice Valve

The measurement system helps to monitor continuously the flow of coal from the PF pipe supply to the burners. This measurement system is designed to work continuously in a closed-loop. It can be easily integrated into an existing monitoring and control environment. A systematic series of test measurements can be done to validate the reliability of the system. The sensor probes, in combination with variable orifice valves displayed in Figure 2.4, allow simultaneous measurements of the flow of coal and hence improve the combustion process at burners' level significantly. A robust, micro-wave based system is installed to continuously measure the mass flow and velocity of the coal in all the PF pipes of the boiler (Suresh et al., 2012).

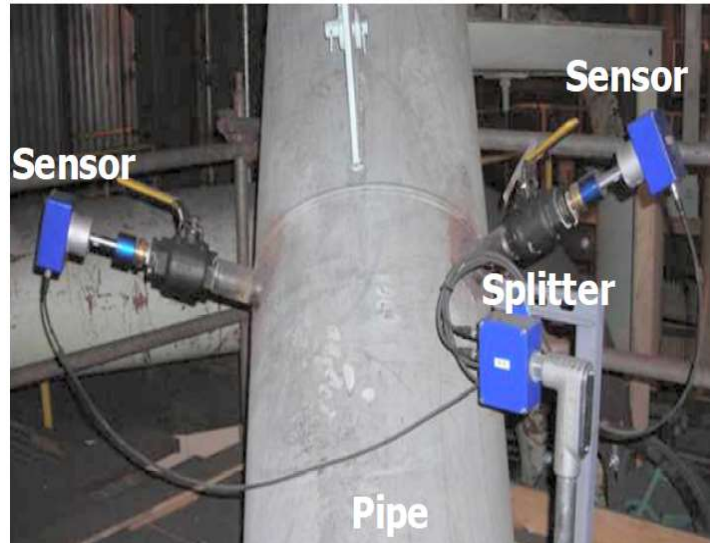


Figure 2.4: Coal Flow measurement in a PF pipe (Suresh et al., 2012)

All measurements are collected in a data acquisition unit and processed to determine the flow of coal in each pipe, in real-time. All signals are permanently monitored to identify failures in a very early stage (Suresh et al., 2012). Figure 2.5 shows the measurement of the flow of coal during operation at various loads.

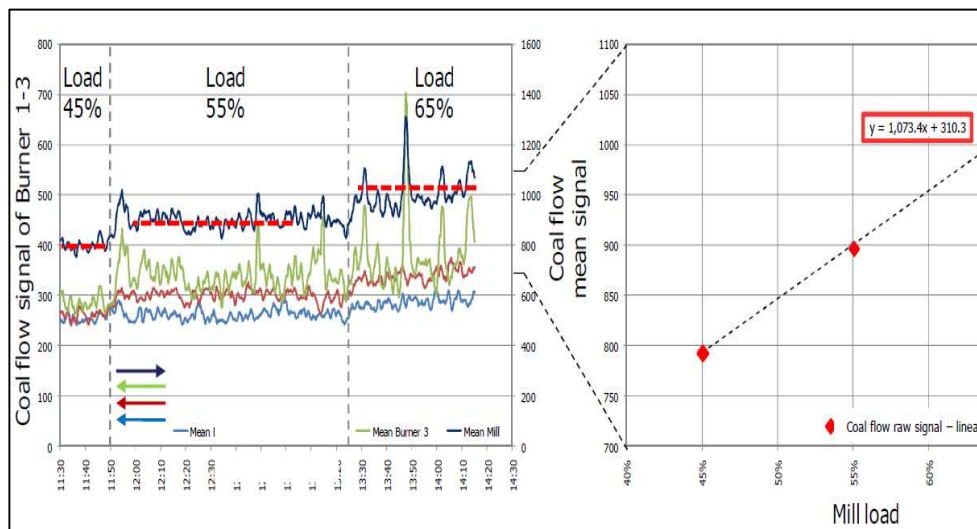


Figure 2.5: Mass flow of coal at different loads (Suresh et al., 2012)

Gravimetric Feeder – measurement of the Mass of Coal

The gravimetric feeder control system helps in compensating the variation in density and volume by facilitating precise feeding of fixed weight of coal in response to a boiler fuel demand. This ability to accurately weigh the coal provides significant improvement over

volumetric types in terms of matching the fuel delivered by the feeder to the actual process required in a coal-fired unit. The gravimetric feeder thus facilitates proper planning of coal requirement, feeding of coal as per demand and continuous monitoring of the fuel flow (Ramulu, 2017). This special type of coal feeder as shown in Figure 2.6 monitors the weight of coal and adjusts the flow speed to compensate for the change in density. This precise control of feed rate allows maintaining of proper fuel to air ratio which leads to optimum combustion (Ramulu, 2017).

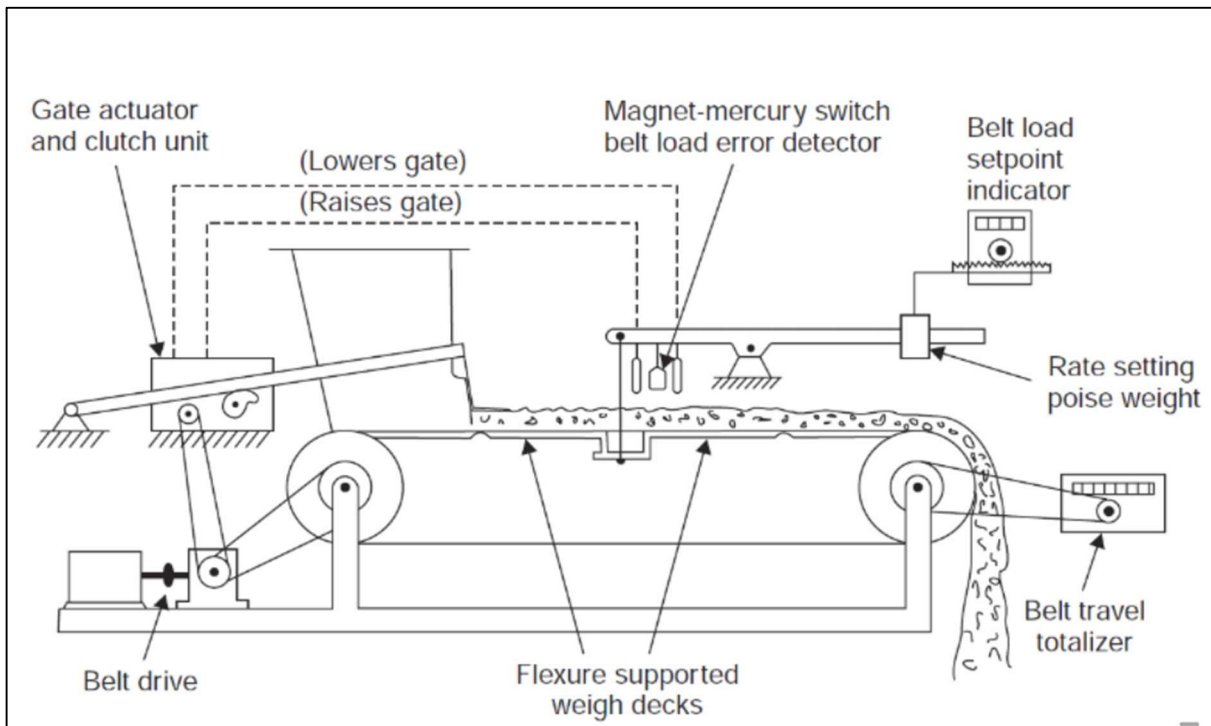


Figure 2.6 : Gravimetric feeder (Ramulu, 2017)

Online Analyser of the flow of coal

In a modern coal-fired power plant, online analysers as shown in Figure 2.7 are installed on bypass conveyor belts to control the process of coal preparation plants. The coal analysers are also installed on the main conveyor line but the accuracy of results is better on the bypass conveyor as the PF particles flow with a constant distribution along a section profile. This reduces the need for sample preparation as the PF particles in the stream are fine and are usually optimized for large material streams on the main conveyor belt. Three major components comprise the analyser system: a coal elemental analyser, a microwave moisture and a trace element analyser for heavy elements. The analyser system is designed to measure the ash content as well as the complete elemental composition of ash from sodium to strontium, moisture, sulphur, calorific value and mercury. The material is taken from the main

belt with the use of an automatic sampling system, sent to the bypass belt, crushed down to the optimal size of around 6 mm and then sent to the analyser for analysis (Klein, 2013).

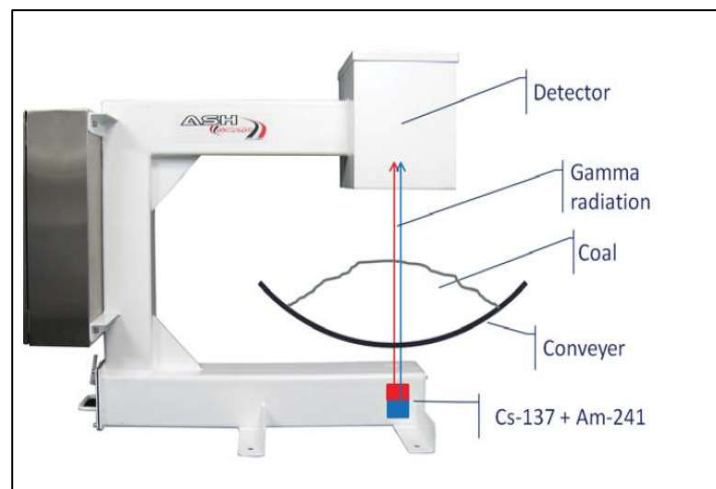


Figure 2.7: Online coal ashmeter analyser (Klein, 2013)

An online analyser is a standard instrument used to measure online the ash content on a stream of coal. It consists of a source and detector mounting that is generally installed across the conveyor line. The detector is linked to the electronic control system which consists of a computer that processes all the incoming signals from the detectors and shows the final measurement results on a screen during operation (Klein, 2013).

2.1.2 Air and Flue Gas Flow Measurement

The flow measurement of fluids like air, regularly presents challenges due to the arrangement of the boiler plant and sizes of the ducting system. Ducts in many coal power plants have an odd geometry, with dampers, expansion joints, internal restrictions, conditioning vanes and service access doors. The internal condition of ducts is always not easily accessible and not documented accurately. Standard air flow instruments' specifications usually require extension in the straight upstream and downstream portion of the duct where there are no bends or obstructions in front of the measurement point. In many coal-fired power plant units, it is difficult to install instruments at the ideal measurement points. Instruments installation in some ducts in the boiler are often obstructed by internal structures (Sabin, 2016).

In effect, to achieve an efficient combustion process, it is very important to control the flow of primary and secondary air into the boiler. This is also critical in order to achieve the correct or stoichiometric air fuel (A/F) ratio, which is an indicator of the combustion rate (Sargent, 2009).

Aerofoil

Air flow measurement in the main supply and secondary ducts of burners at power station A is accomplished by means of aerofoils which are permanently installed in these ducts (ESKOM, 2016). Aerofoils are designed to measure air and gas flow through ducting systems with a square or rectangular cross section. They are used where other flow measurement instruments like orifice plates are not suited. An aerofoil is a flow measurement instrument that has the shape of an aircraft's wing, which creates a differential pressure between the upper and lower surfaces. The aerofoil as shown in Figure 2.8 is made of a set of three foils which obstruct the flow while creating the decrease in pressure known as differential pressure (DP). It is connected to a piezo-metric system that calculates the average DP for the higher and lower side in order to determine the flow's velocity. In effect, a popular aerofoil like Eureka's AF series is a very appropriate device for the measurement of the velocity in ducting systems using air or gas. The aerofoil has an aerodynamic shape that allows the fluid to flow over it with less pressure loss (EUREKA, 2018).



Figure 2.8: Eureka AF Series Aerofoil (EUREKA, 2018)

Standard aerofoils are made of aerodynamic foils with a smooth profile on the upstream front side, and a divergent cone on the downstream side which vary in size according to the duct dimensions. They are fitted with HP and LP sensing ports as illustrated in Figure 2.9 (EUREKA, 2018).

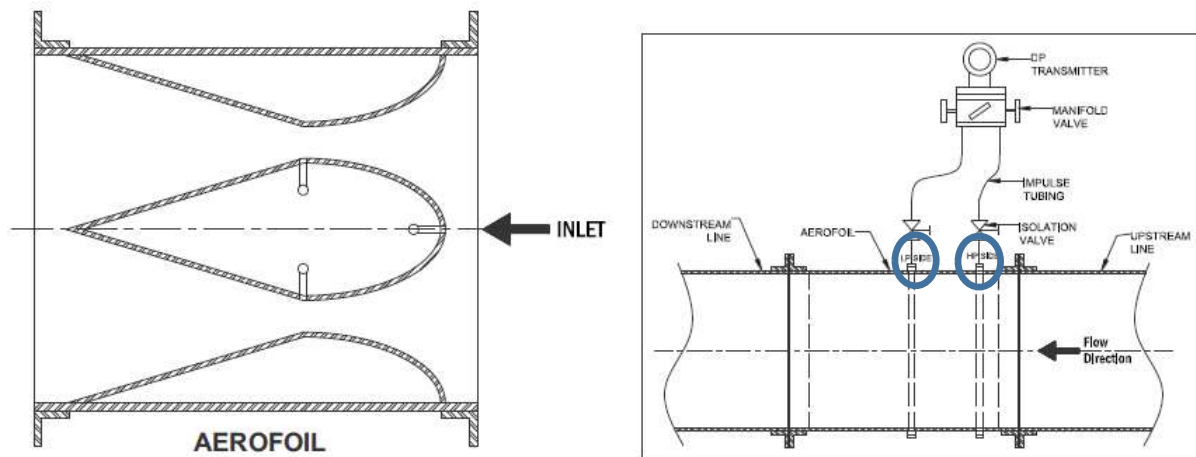


Figure 2.9: Aerofoil description (EUREKA, 2018)

In effect, the need to improve coal-fired power plant efficiency in the past few years has motivated the development of reliable and accurate measurement techniques for air flow such as the aerofoil, in order to have better control of the air-to-fuel stoichiometric ratio (Sabin, 2016).

Pitot tube

The pitot tube is a measuring device usually inserted parallel to the flow of air or gas in a duct to measure its velocity. However, turbulent flow of air can cause great difficulty in the measurement of its velocity. According to ASTM standards, pitot tubes require sufficient upstream and downstream length of duct for accurate measurement. In most power plants, there are rarely sufficient straight lengths of ducting to permit accurate measurements (Sabin, 2016).

Figure 2.10 illustrates a pitot tube mounted in a duct facing the stream in order to measure accurately the flow's velocity. This is achieved by introducing the pitot tube facing the air or gas stream through a small hole in the duct (Matthews, 2016).

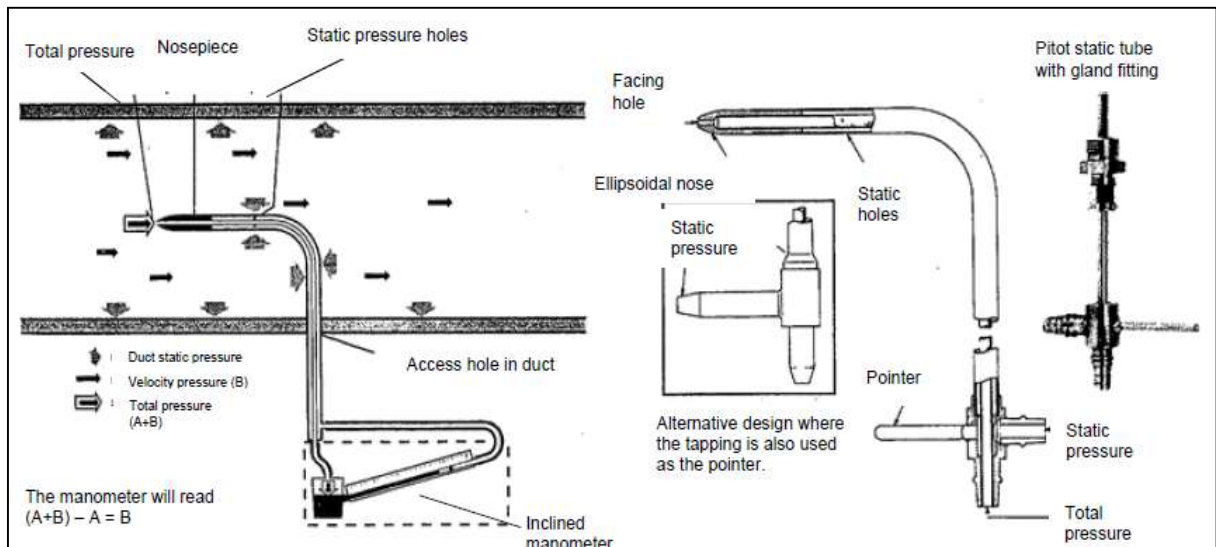


Figure 2.10: Pitot tube flow measurement in air/gas ducting (Matthews, 2016)

The advantage of the static pitot tube is that it is possible to obtain a quick measurement with reproducible results. Compared to other techniques for measuring velocity in air or gas flows, it offers another key advantage: the medium does not flow through the measurement apparatus. This eliminates the possibility of errors occurring due to changes in the system (Sabin, 2016). The fact there is no flow through the apparatus also prevents dust deposits accumulating in the pitot static tubes. This makes the method simple to use even with contaminated media like exhaust gases containing dust or combustion residues (Sabin, 2016).

Pitot tubes should be carefully calibrated when used in uncommon ducts with restricted straight lines for measurement's accuracy. The calibration can be done in-line for uncommon ducts as shown in Figure 2.11 if there is a considerable amount of the turbulence in the flow. This involves the analysis of the flow at different sampling points to determine accurate flow profile measurements in a coal-fired boiler plant system (Sabin, 2016).

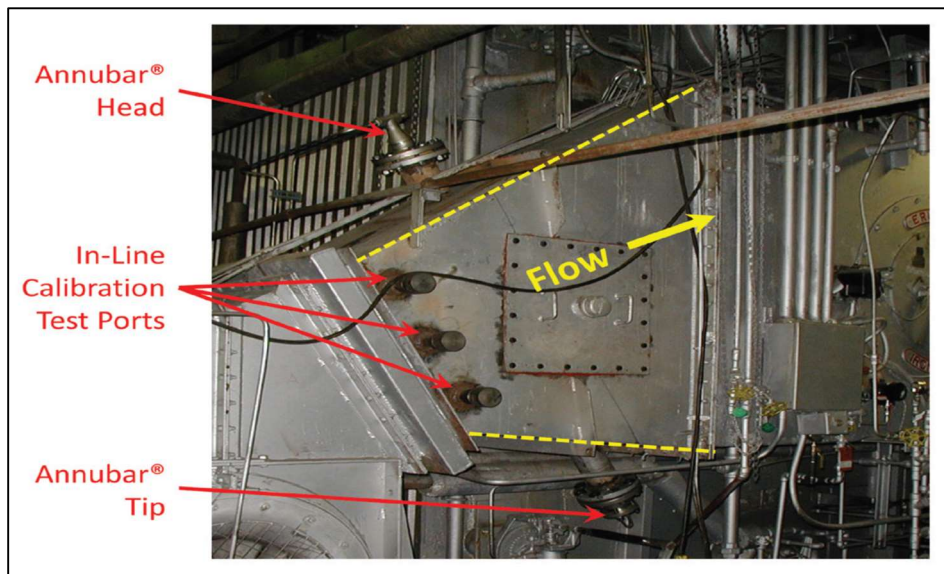


Figure 2.11: Air flow measurement in a duct with in-line calibration test ports (Sabin, 2016)

Traverse measurement with Pitot tube

Traverse measurement is a technique that consists of manually inserting instruments like a pitot tube in open points on the flue gas duct in order to measure the flow's velocity. Several points as shown in Figure 2.12 can be used in an array to increase the number of sample locations and improve the accuracy of the measurement. The number and type of instruments required for conducting traverse measurement depends on the unit being tested (ESKOM, 2016). Figure 2.12 is an illustration of the ideal location for the traverse measurement in the ducting system of the flue gas for accurate measurement. The traverse plane on the flow of the flue gas has to be as far downstream from the location of the air heater so that the air ingress from the mechanical collectors or the ESP does not slip through into the flue gas stream (ASME, 2010).

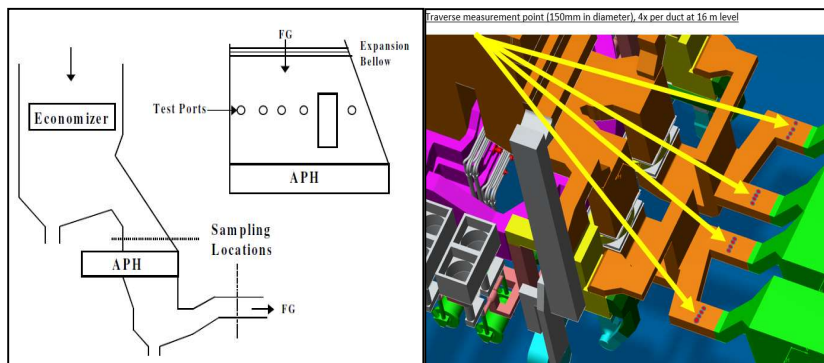


Figure 2.12: (Lft): Traverse sampling (ASME, 2010), (Right): Traverse ports measurement (Catia 3D View)

2.2 MEB (Mass and energy balance)

The MEB method is widely applied for the thermal analysis and performance test as well as to calculate the boiler's efficiency. This technique, has been detailed by both the European standard EN12952-15 and American standard ASME PTC-4-2008 for its application, in order to evaluate the boiler performance and determine the coal, air and flue gas flow rates at different power loads (Tootla, 2015).

However, the MEB method can also be used to verify the consistency of online measurements from installed/existing control system and evaluate the plant's performance as per design specification. Figure 2.13 and 2.14 illustrate the different MEB energy inputs and outputs of a coal-fired boiler (Rousseau & Fuls, 2018).

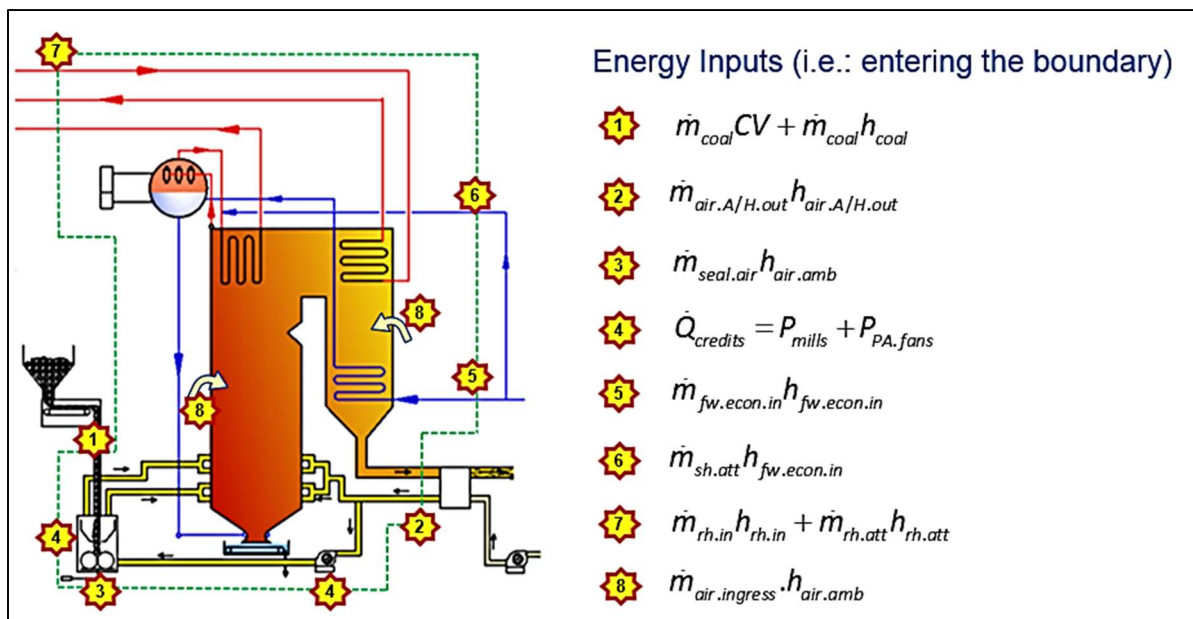


Figure 2.13: Boiler Energy Inputs (Rousseau & Fuls, 2018)

The main MEB energy inputs are the mass flow rate and enthalpy of coal, the heated ambient air from the air heater supplied to the boiler for combustion process and the water fed into the economiser. The energy outputs of the boiler as specified in Figure 2.14 are indicated by the steam energy gained from combustion flue gas and heat losses (Rousseau & Fuls, 2018).

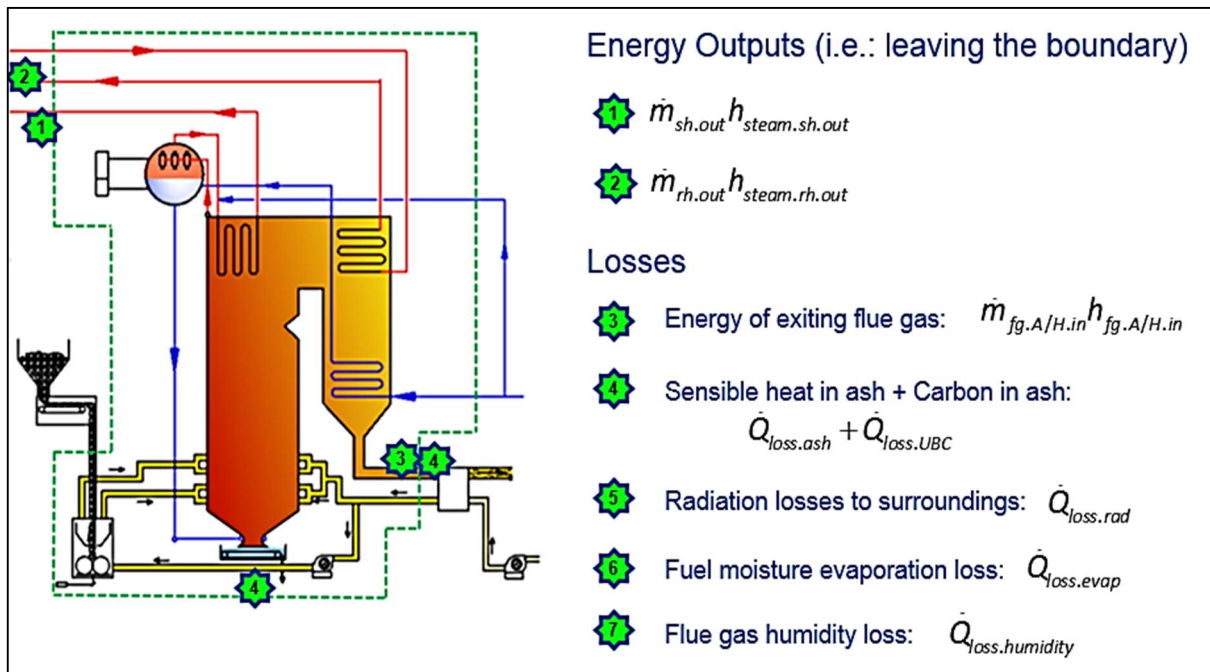


Figure 2.14: Boiler Energy Outputs (Rousseau & Fuls, 2018)

2.3 CFD Modelling

Computational fluid dynamics (CFD) is used for the evaluation of concepts and a better understanding of the complexity of fluid systems. CFD has been extensively applied in flow analysis and simulation (Scholtz, 2016).

Constenla et al. (2013) conducted a numerical CFD study of a 350MW tangentially fired pulverized coal furnace at the A's Pontes power plant. The purpose of their research was to predict the flow characteristics with actual operations' data of the boiler in order to analyse the phenomena occurring inside of the furnace and to validate the simulation model. Figure 2.15 is an illustration of the simulation done with the CFD flow software ANSYS Fluent.

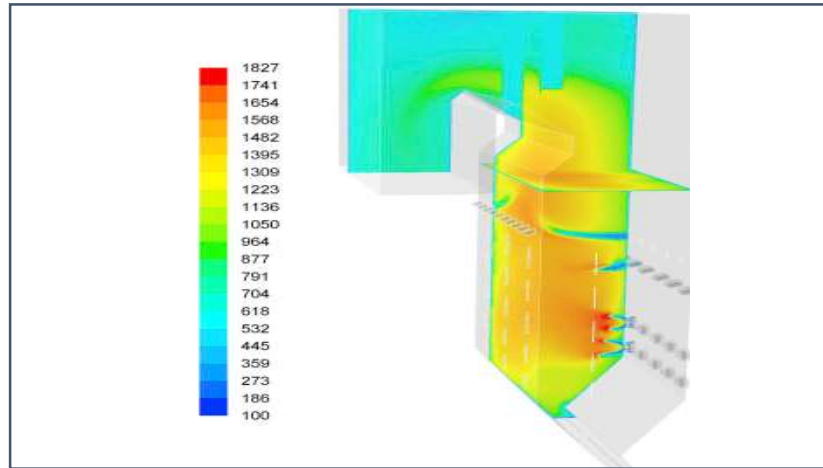


Figure 2.15: Flue gas computational flow analysis (CFD) in a coal-fired boiler (Ferreira et al., 2010)

Ferreira et al. (2010) performed a CFD study as shown in Figure 2.16 to assess the air flow in a coal-fired boiler. The simulation's solutions proved to be logically relevant to the parameters available and confirmed the efficiency of the air flow in the tertiary system running into the boiler. In their research, CFD simulations were completed in order to analyse the configuration of the ports used by the secondary and tertiary air.

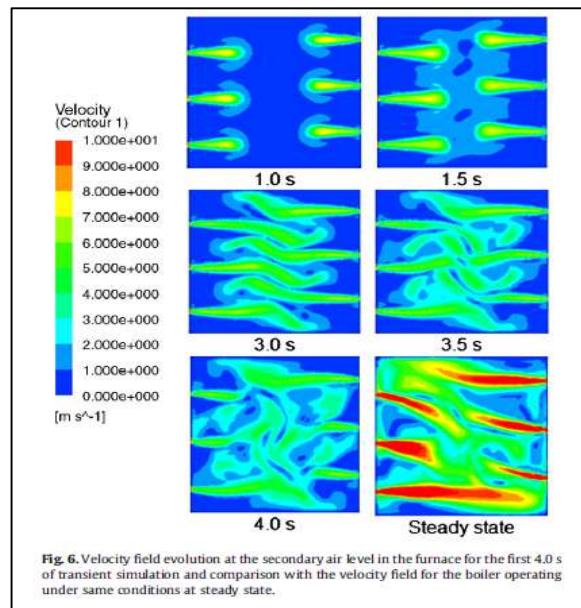


Figure 2.16: Tertiary Air Flow Simulation (Ferreira et al., 2010)

Yang et al. (2007) implemented an ideal way to perform CFD simulation modelling for a coal-fired plant furnace by means of the ANSYS Fluent software. The model represented the entire turbulent flow of air supplied to the furnace using the regular $k - \epsilon$ equations. The $k - \epsilon$ equation was selected since the flow of air in the boiler was turbulent and the simulation results indicated the points where important measurements could be taken.

Miltner et al. (2007) developed a CFD simulation of the flow of gas with ANSYS Fluent to determine the turbulent flow condition in a coal-fired boiler with 1.5 million mesh elements. The simulation's results were validated with online measurements.

In effect, CFD software like Fluent is still the most commonly used method for fluid flow analysis. It provides solver tools for the simulation of turbulent flow and uses a wide database of parameters based on the nature of the flow and process. It is a popular CFD tool for modelling and simulation of flow in coal-fired boilers (Ferreira et al., 2010).

CHAPTER THREE BOILER MASS AND ENERGY BALANCE METHODOLOGY

The mass and energy balance (MEB) method was designed to establish a coherent set of input and output data for boilers. The MEB is used to troubleshoot existing measurements from the plant, provide a foundation for future modifications to the combustion process, and also help with effective communication between various the various groups such as operating, maintenance, performance and testing at coal-fired power stations.

3.1 Boundary Selection

The MEB boundary limitation depends on the availability of installed instrumentation for the measurement of necessary inputs in order to evaluate processes at coal-fired plants.

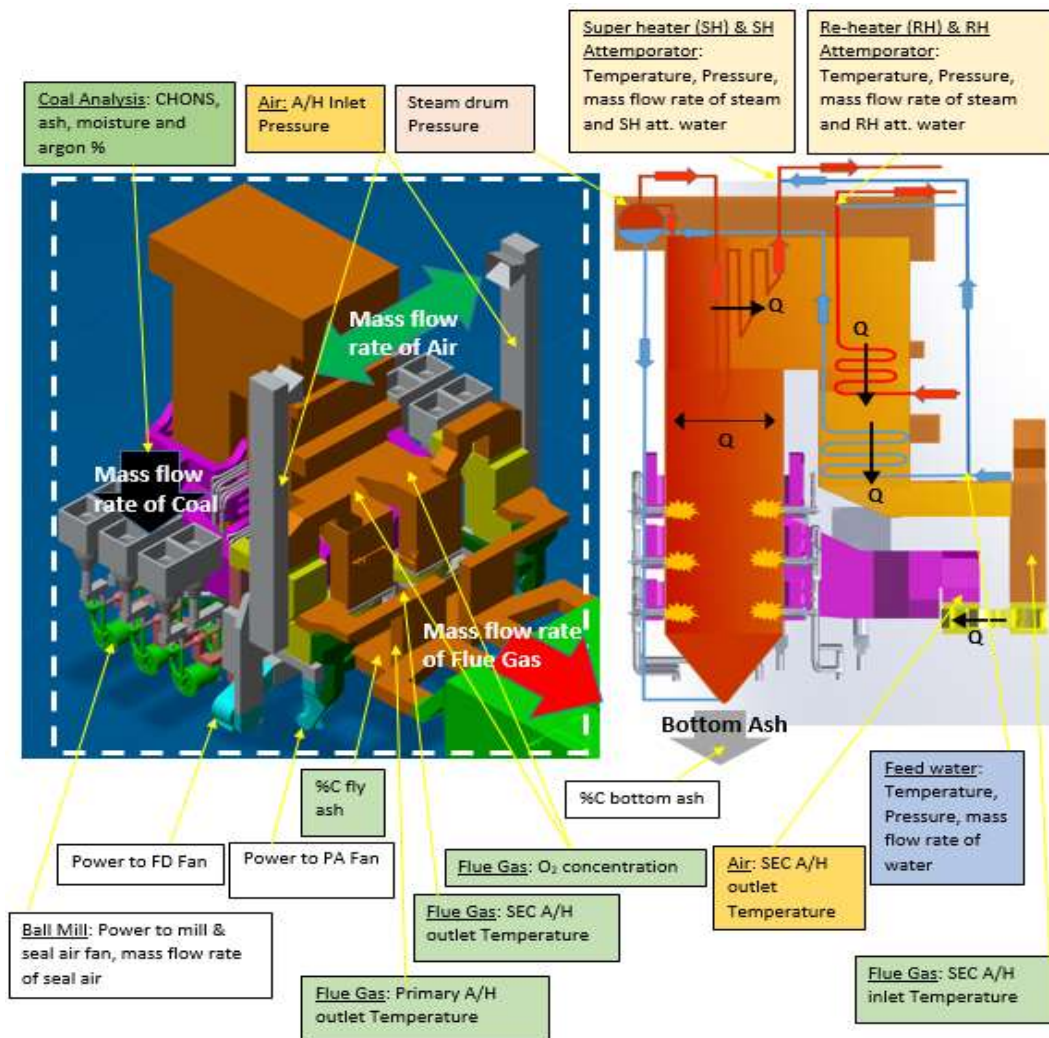


Figure 3.1: MEB boundary for a coal-fired boiler plant at Power Station A

The most important phase of the MEB methodology is to clearly define the system's boundary. The boundary limit that has been defined, shown in Figure 3.1, is also the boundary used for the MEB (as per ASME standards) to calculate the boiler's efficiency for acceptance tests. The MEB boundary includes all the coal, flue gas, air and steam systems with all respective parameters (temperature, pressure and mass flow rate).

The MEB will be applied to the C-schedule (Plant design data), acceptance tests and current operating parameters for the ESKOM coal power station. Comparison between the design specifications and operating parameters will be conducted to analyse the plant's process performance.

3.2 MEB Calculation

The main goal of the MEB is to calculate the mass flow rate of the coal in order to determine the heat rate of the plant using the measured input parameters. The MEB is also used to determine the flue gas and air flow rates that are critical boiler parameters related to the mass flow rate of the coal. In effect, the mass flow rate of air and flue gas can be expressed in terms of the mass flow rate of coal, since they are critical parameters influenced by the consumption of coal.

The 3D model of power station A in Figure 3.1 can be simplified for the derivation of the mass flow rate of coal as shown in Figure 3.2.

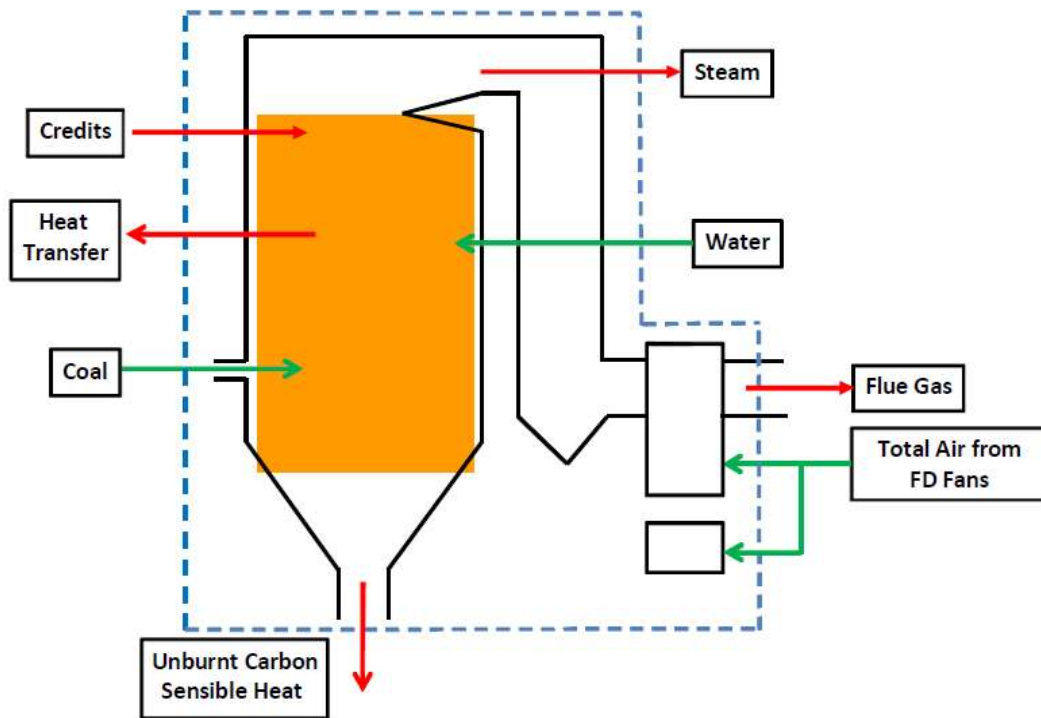


Figure 3.2: Simplified MEB boundary

3.2.1 Coal flow rate derivation

The following steps illustrate how the mass flow rate of the coal is determined based on equation 3.1 (Rousseau & Fuls, 2018):

$$E_{in} = E_{out} \quad 3.1$$

Where E_{in} is the total power inputs and E_{out} the total power outputs in MegaWatt (MW)

Equation 3.1 can also be expressed as shown:

$$Q_{in} = Q_{out} + Q_{loss} \quad 3.2$$

The inputs consist of the energy put by coal, air and feed water into the system as:

$$E_{in} = \dot{m}_{coal} CV_{pf.coal} + \dot{m}_{coal} h_{coal} + \dot{m}_{air.AH.out} h_{air.AH.out} + Q_{credits} + \dot{m}_{fw.econ.in} h_{fw.econ.in} + \dot{m}_{sh.att} h_{sh.att} + \dot{m}_{rh.att} h_{rh.att} + \dot{m}_{air.ingress} h_{air.amb} \quad 3.3$$

Where \dot{m} is the mass flow rate in kg/s and h the enthalpy in kJ/kg

The outputs consist of energy transferred to the steam and losses from the system

$$E_{out} = \dot{m}_{sh.out} h_{steam.sh.out} + \dot{m}_{rh.out} h_{steam.rh.out} + \dot{m}_{fg.AH.in} h_{air.AH.in} + Q_{loss} \quad 3.4$$

Taking into consideration all the different flows as shown by the equation below:

$$Inflows = h_{coal} + HAR \cdot \%Air_{ing} \cdot h_{T_{amb}} + (HAR - HAR \cdot \%Air_{ing}) \cdot h_{T_{air.AH.outlet}} \quad 3.5$$

$$OutFlows = -\dot{m}_{fg} \cdot h_{fg.AH.inlet} - Flow_{Ash} - X_{H2O} \cdot h_{H2O.vap} \quad 3.6$$

Where $Flow_{Ash}$ is the bottom and fly ash flow as calculated below:

$$Flow_{Ash} = (X_{Ash} \cdot \%b_{Ash} \cdot h_{ash.BA.exit}) + (X_{Ash} \cdot \%f_{Ash.fg.AH.inlet}) \quad 3.7$$

By substituting equations 3.3 to 3.7 in 3.1 and solving for \dot{m}_{coal} :

$$\dot{m}_{coal} = \frac{Q_{out} - Q_{credits}}{[CV_{pf.coal} \cdot (1 - mf_{CC} - \%Q_{insul.loss})] + \sum FRh_{flows}} \quad 3.8$$

3.2.2 Analysis of Coal

The outputs of the BMEB are highly sensitive to the input data from the coal analysis. It is thus important that time and care is taken to ensure that the analysis of the coal is correct. The analysis should be converted from an air-dried basis to an as-received basis using the formula given (Rousseau & Fuls, 2018):

$$X_i = TM \cdot \left(\frac{100 - TM}{100 - M_{ad}} \right) \quad 3.9$$

The X_i is the coal constituent elements: carbon, hydrogen, oxygen, nitrogen and sulphur, generally noted as CHONS, as well as ash. The total of the coal's elements percentages is equal to one.

$$X_C + X_H + X_O + X_N + X_S + X_{Ash} + X_{moist} = 1 \quad 3.10$$

TM stands for total moisture in the coal which is the combination of surface moisture SM and inherent moisture IM as shown

$$TM = \%SM_{ad} + \%IM_{ad} \quad 3.11$$

Energy contained in the coal comes from the HHV/CV (High heating value/Calorific value) of coal and the enthalpy of coal. The enthalpy of the coal is expressed as:

$$h_{coal} = \int_0^T C_p dT \quad 3.12$$

Where the C_p of coal is taken as 1.38kJ/kgK. The C_p of coal can vary with the coal quality and composition (moisture content, etc.). The ultimate analysis provides the elemental chemical composition of the coal in the form of percentage weight. These can be written as a mass fraction X_i for each component i (carbon, hydrogen, oxygen etc.) in kg of coal. During combustion, only pure coal which is referred as fuel, participates in the process. This leaves unburnt carbon which is not useful in the combustion analysis expressed as:

$$X_C = x_C - x_{UC} \quad 3.13$$

In the equation above only pure carbon percentage participates in combustion; it will be further used in the coal's HHV (High Heating Value) calculation to verify the CV measured at the laboratory.

Table 3.1: Heat release from combustion reaction by coal elements (Rousseau & Fuls, 2018)

Reactant	Formation heat (Qf) [kJ/kg]	Latent heat (Qlat) [kJ/kg]
C (Carbon)	32 765	0
H (Hydrogen)	119 959	21 820
N (Nitrogen)	-6 446 f_{NOX}	0
S (Sulphur)	9 256	0

The values contained in the Table 3.1 are used in the matrices with 4 rows starting from zero to three ($i = 0 \dots 3$) as illustrated below, to calculate the coal's HHV using equation 3.14.

$$Qf = \begin{pmatrix} 32765 \\ 119959 \\ -6446 \cdot f_{NOX} \\ 9256 \end{pmatrix} \frac{kJ}{kg} \quad Qlat = \begin{pmatrix} 0 \\ 21820 \\ 0 \\ 0 \end{pmatrix} \cdot \frac{kJ}{kg} \quad Xn = \begin{pmatrix} X_C \\ X_H \\ X_N \\ X_S \end{pmatrix}$$

$$HHV = \sum_{i=0}^3(Qf_i + Qlat_i).Xn_i \quad 3.14$$

Alternatively the HHV of the coal can also be calculated using the Dulong equation:

$$HHV_x = (33.83X_C + 144.25X_H - 18.04X_O + 9.42X_S) \quad 3.15$$

The total heat released per kg of coal is the mass weighted average of the heat production of all the constituent reactions. It includes the heat produced and directly utilized for evaporating any liquids, and it is generally called HHV or gross Calorific Value as determined in equation 3.14. One can also make use of the lower Heating Value (LHV), which excludes the latent heat component because it is argued that the latent heat of any moisture is not useful energy (Rousseau & Fuls, 2018).

3.2.3 Coal combustion

Table 3.2 is very important for the combustion calculation as it specifies the molar mass of the elements of the coal's composition as well as the combustion products (CHONS) contained in the flue gas such as CO₂, SO₂ and H₂O as well as dry air.

Table 3.2: Molar mass of elements of the coal's combustion (Rousseau & Fuls, 2018)

Element/Composition	Rounded [kg]	Accurate [kg]
C (Carbon)	12	12.01
H (Hydrogen)	1	1.000795
O (Oxygen)	16	15.9995
N (Nitrogen)	14	14.0065
S (Sulphur)	32	32.07
H ₂ O (Water)	18	18.015
CO ₂ (Carbon dioxide)	44	44.01
NO (Nitric oxide)	30	30.061
SO ₂ (Sulphur dioxide)	64	64.064
Air (dry)	29	28.958

To calculate the mass of unburnt carbon per kilogram of coal (if fly ash in total ash is unknown, an assumption may be made that 10 % by mass of the total ash is bottom ash and the remaining 90 % is fly ash) given the percentages of carbon in fly ash, carbon in bottom ash and the percentage of ash in the coal.

$$mf_C = X_{Ash} \cdot [(\%Cfa \cdot \%f_{Ash}) + \%Cba \cdot \%b_{Ash}] \quad 3.16$$

3.2.4 Theoretical air required

The theoretical air (TAR) required for stoichiometric combustion can be calculated per kilogram of coal using the unburnt carbon, sulphur, nitrogen and oxygen percentage (Rousseau & Fuls, 2018) as shown:

$$TAR = [11.51X_C + 34.29X_H - 4.32X_O + 4.31X_S + (4.932f_{NOX} \cdot X_N)] \quad 3.17$$

Table 3.3: Stoichiometric coefficient (Rousseau & Fuls, 2018)

Coal Element	Stoichiometric coefficient
C: Carbon	1
H: Hydrogen	1/4
O: Oxygen	-1/2
N: Nitrogen	1/2f _{NOX}
S: Sulphur	1

Alternatively, the theoretical air required can be calculated using Table 3.3 containing the stoichiometric coefficients of the coal composition elements. These coefficients are thus used in the matrices and equation below:

$$S_t = \begin{pmatrix} 1 \\ 1/4 \\ -1/2 \\ 1/2f_{NOX} \\ 1 \end{pmatrix} \begin{pmatrix} C \\ H \\ O \\ N \\ S \end{pmatrix}$$

$$TAR = \frac{M_{air}}{Y_{O_2air}} \sum_{i=0}^4 \left(St_i \frac{X_i}{M_{CO_i}} \right) \quad 3.18$$

3.2.5 Excess Air

Excess air is very critical inside the boiler to ensure that complete combustion takes place. The oxygen content in the flue gas at the boiler's exit that indicates the excess air in the combustion process (Rousseau & Fuls, 2018) can be calculated by:

$$f_{EA} = \frac{TAR + 1 - X_{Ash}}{TAR} * \frac{\%O_{2AH}f_{ginlet}}{\frac{\%mO_{air}}{Pratio} - \%O_{2AH}f_{ginlet}} \quad 3.19$$

3.2.6 Humid Air

The total humid air (HAR) required by the boiler is related to the specific humidity (ω) of the air and dry air which are influenced by the excess air and the stoichiometric air ratio (Rousseau & Fuls, 2018). This expressed in kg of air per kilogram of coal is given by:

$$HAR = (1 + \omega) \cdot DAR \quad 3.20$$

Where DAR (Dry air required)

$$DAR = TAR \cdot (1 + f_{EA}) \quad 3.21$$

3.2.7 Flue gas enthalpy

The coal combustion process produces the flue gas as the result of the coal and the air flow mixture. The flue gas contains unburnt carbon, argon, fly ash, CO₂, SO₂, NO, N₂ and H₂O (Rousseau & Fuls, 2018). The mass flow rate of flue gas per kilogram of coal can be calculated as follows:

$$FGR = HAR + 1 - X_{Ash} \cdot f_{BA} \quad 3.22$$

The percentage concentration of the flue gas composition elements is calculated using:

$$X_{i,fg} = \left(\frac{m_{i,fg}}{\sum_{i=1}^9 m_{i,fg}} \right) \quad 3.23$$

The enthalpy of various gases such as carbon dioxide (CO₂) contained in the flue gas is calculated with equation (3.24) and the corresponding constant (C_{1...4}) value as specified in table 3.4:

$$h(T) = (C_1 \cdot T + C_2 T^2 + C_3 T^3 + C_4 T^4) \text{ in kJ/kg} \quad 3.24$$

Where T is the temperature of the flue gas at the economiser at the boiler's exit.

Table 3.4: Coefficient for calculating the enthalpy of various gases at 1 bar (Rousseau & Fuls, 2018)

	O₂	N₂	CO₂	SO₂	Argon	NO
C ₁	8.974E-01	1.015E+00	8.437E-01	6.426E-01	5.205E-01	8.861E-01
C ₂	1.994E-04	1.037E-04	4.258E-04	1.850E-04	0	3.263E-04
C ₃	-7.432E-08	5.452E-09	-1.705E-07	0	0	0
C ₄	1.255E-11	-6.693E-12	2.819E-11	0	0	0

By calculating all the enthalpies of the elements in the flue gas composition, the flue gas enthalpy can thus be determined by means of the matrices with row numbers starting from zero to height ($i = 0 \dots 8$) and the following equation (3.25):

$$Hfg = \begin{pmatrix} h_{CO2} \\ h_{SO2} \\ h_{NO} \\ h_{O2} \\ h_{N2} \\ h_{H2O} \\ h_{Arg} \\ h_{UC} \\ h_{FA} \end{pmatrix} \quad Xfg = \begin{pmatrix} X_{CO2} \\ X_{SO2} \\ X_{NO} \\ X_{O2} \\ X_{N2} \\ X_{H2O} \\ X_{Arg} \\ X_{UC} \\ X_{FA} \end{pmatrix}$$

$$h_{fg} = \sum_{i=0}^8 (Xfg_i \cdot Hfg_i) \quad 3.25$$

However, there is a general formula that can be used to calculate the enthalpy and Cp of any substance. This is applicable to the flue gas as well and elements in its composition like water, ash etc.

$$hfg_{AH.inlet} = \left(\int_{T_{ref}}^{T_{fg}} Cp_{fg} dT_{fg} \right) \quad 3.26$$

Table 3.5: Cp for Typical solids (Rousseau & Fuls, 2018)

Solid	Specific heat (Cp) [kJ/kgJ]	Density [kg/m ³]
Coal	1.38	1500
Carbon (graphite)	0.71	2500
Fly Ash	0.73	2300

3.2.8 Air enthalpy:

This refers to the heat energy of air gained through the heat exchange with the flue gas in the secondary air heater as supplied to the boiler. Air enters the boiler's boundary at the secondary air heater at ambient or atmospheric temperature. Its enthalpy can however be calculated using the matrix and equation (3.27) or alternatively, using the ASHRAE equation (3.28), taking into account specific humidity and ambient temperature (Rousseau & Fuls, 2018).

$$C_{air} = \begin{pmatrix} Air \\ 9.816 \cdot 10^{-1} \\ 1.245 \cdot 10^{-4} \\ -1.308 \cdot 10^{-8} \\ -2.154 \cdot 10^{-12} \end{pmatrix}$$

$$h_{T_{amb}} = (C_{air1} \cdot T_{amb} + C_{air2} \cdot T_{amb}^2 + C_{air3} \cdot T_{amb}^3 + C_{air4} \cdot T_{amb}^4) \quad 3.27$$

$$h_{air.AH_{in}} = [1.006 T_{amb} + \omega \cdot (2501 + 1.86 T_{amb})] \quad 3.28$$

3.2.9 Credit Power load:

This load is the combination of the Electrical energy power input of the motors driving the mills and the PA/FD fans, together with the energy from the air at ambient temperature, being supplied directly to the mills in the form of seal air.

$$Q_{credits} = P_{mills} + P_{fans} + P_{othe} \quad 3.29$$

3.2.10 Steam heat energy

This refers to the energy transferred from the flue gas used to drive the turbine. It is the heat balance between the enthalpies in the economiser water, and the steam in the super-heater and re-heater (Rousseau & Fuls, 2018) calculated by:

$$Q_{sh} = [(m_{fw.econ.in} + m_{sh.}) \cdot h_{steam.sh.out}] - (m_{fw.econ.in} \cdot h_{fw.econ.in}) - (m_{sh.att} \cdot h_{sh.att}) \quad 3.30$$

Where the enthalpy (h) of steam/water at the economiser, super-heater, re-heater and attenerator's outlet is a function of pressure and temperature. This can be calculated using the MathCAD formula which extracts values from online steam tables.

$$h_{steam.sh.out} := h_{steam} (P_{steam.sh.out}, T_{steam.sh.out}, ''', ''', ''') \quad 3.31$$

3.2.11 Heat loss

This is the energy loss in the boiler's system boundary such as flue gas, ash and radiation loss to the surroundings. Even though the boilers are well insulated, the insulation cannot guarantee no heat loss. This means that a certain amount of heat is lost to the surroundings due to the temperature difference with the boiler's walls.

$$Q_{loss} = Q_{fg.AH.in} + Q_{loss.fa} + \left(\frac{1}{3}\right) Q_{insul.loss} \quad 3.32$$

3.2.12 Air and flue gas mass flow rates

The additional important boiler parameters (humid air & flue gas mass flow rates) in kg/s related to the mass flow rate of the coal can be calculated as follows:

$$\dot{m}_{air.AH.total} = HAR \cdot \dot{m}_{coal} \quad 3.33$$

$$\dot{m}_{fg.AH.in} = FGR \cdot \dot{m}_{coal} \quad 3.34$$

Where HAR is the humid air required and FGR is the mass of flue gas per kg of coal.

The specific air flow rate at the secondary air heater outlet (SEC A/H) can be calculated using the total mass flow rate of air, the percentage amount of ingress air into the boiler and the mass flow rate of seal air in the following equation:

$$m_{air.AH.out} = \dot{m}_{air.AH.total} - m_{air.ing} - m_{seal.air} \quad 3.35$$

Since the air heater leakage is simply the difference in the air flow at the air heater's inlet and exit, the mass flow rate of air at the air heater can be expressed as:

$$m_{air.AH.in} = \dot{m}_{coal} \cdot \%Air_{ing} \cdot HAR \quad 3.36$$

3.2.12 Net Heat rate

This refers to the coal energy in kJ to produce one 1 kWh of electrical energy that is supplied to the grid. The net heat rate (Rousseau & Fuls, 2018) is calculated as:

$$\eta_{boiler} = \frac{Q_{out}}{\dot{m}_{coal.HHV}} \quad 3.37$$

$$NHR = \left(\frac{1+f_{aux}}{\eta_{boiler} \cdot \eta_{cycle} \cdot \eta_{gen}} \right) \text{ in } kJ/kW.hr \quad 3.38$$

Where f_{aux} is the auxiliary power consumption percentage.

3.3. MEB implementation

The plant's inputs /parameters were selected based on three full loads to be used in MEB calculations, with the coal's analysis reports as shown in Table 3.6:

Table 3.6: List of plant measurements used for MEB at Full Loads for Power station A

Parameter	Description	Value			Unit	Source
Coal's Analysis (Air Dried)						
%IM	Inherent Moisture	5.1	5.1	4.6	%	Coal Analysis report
%Ash	Ash	40.4	40.4	40,6	%	Coal Analysis report
%C	Carbon	38.9	38.9	37.95	%	Coal Analysis report
%H	Hydrogen	1.97	1.97	2,06	%	Coal Analysis report
%O	Oxygen	4.06	4.06	4.99	%	Coal Analysis report
%N	Nitrogen	0.95	0.95	1	%	Coal Analysis report
%S	Sulphur	1.1	1.1	0.76	%	Coal Analysis report
%SM	Surface Moisture	7.52	7.52	8.04	%	Coal Analysis report
Total	Total	100	100	100	%	Coal Analysis report
CV	Calorific value	15.64	15.64	15.44	MJ/kg	Coal Analysis report
Process Parameters		Full Load (5 mills in operation)				
		@521 MW	@544 MW	@530 MW		
p_{atm}	Atmospheric Pressure	83	83	83	kPa	Weather report
T_{atm}	Atmospheric Temperature	25	25	25	°C	Weather report
$RH(\omega)$	Relative humidity	7	7	7	%	Weather report
T_{amb}	Ambient temperature inside boiler house	28	28	28	°C	Performance and Testing Total Air Flow Rate Report
$T_{air,A/H.out}$	Temperature of air at air heater exit	291.4	294.7	293	°C	ETAPRO CS
$T_{fg,A/H.in}$	Temperature of flue gas at air heater inlet	303.6	318	310	°C	ETAPRO CS/C-SCHEDULE
$T_{fg,A/H.out}$	Temperature of flue gas at air heater outlet	142.6	134	133	°C	ETAPRO CS
$\%O_{2,A/H.fg.in}$	Volume percent oxygen in flue gas at air heater flue gas inlet	4.08	4.08	4.08	% v/v	ETAPRO CS/C-SCHEDULE
$\%C_{fa}$	Carbon content in fly ash	3.41	3.41	3.4	% m/m	Coal Analysis report
$\%C_{ba}$	Carbon content in bottom ash	3.41	3.41	3.4	% m/m	Coal Analysis report

$\dot{m}_{fw.econ.in}$	Mass flow rate of feed water	414.55	416.6	421.29	kg/s	ETAPRO CS
p_{fw}	Pressure of feed water	18.19	18.05	18.13	MPa	ETAPRO CS
$T_{fw.econ.in}$	Temperature of feedwater at economiser inlet	226.8	230	229	°C	ETAPRO CS
$T_{fw.econ.out}$	Temperature of feedwater at economiser outlet	277	277	277	°C	C-SCHEDULE Plant Technical Specification
m_{steam}	mass of sh steam out	427.73	434.47	429.2	kg/s	ETAPRO CS
$p_{steam.drum}$	Pressure of steam/water inside drum	19	19	19	MPa	C-SCHEDULE Plant Technical Specification
$T_{steam.sh.out}$	Temperature of steam at final superheater outlet	533.2	534.4	535.8	°C	ETAPRO CS
$p_{steam.sh.out}$	Pressure of steam at final superheater outlet	16.37	16.24	16.3	MPa	ETAPRO CS
$m_{sh.att}$	Mass flow rate of super heater attemporator spray water	10.29	10.3	10.3	kg/s	C-SCHEDULE Plant Technical Specification
$p_{sh.att}$	Pressure of super heater attemporator spray water	17.88	17.5	17.6	MPa	ETAPRO CS
$T_{sh.att}$	Temperature of attemporator spray water	249	249	249	°C	C-SCHEDULE Plant Technical Specification
$P_{steam.rh.out}$	Pressure of re-heater steam out	2.89	3.02	2.91	MPa	ETAPRO CS
$T_{steam.rh.out}$	Temperature of re-heater steam out	532.4	533.5	531.5	°C	ETAPRO CS
$P_{rh.att}$	Pressure of re-heater attemporator	4.1	4.1	4.09	MPa	C-SCHEDULE Plant Technical Specification
$T_{rh.att}$	Temperature of re-heater attemporator	165	165	164	°C	C-SCHEDULE Plant Technical Specification
$m_{rh.steam}$	Mass flow rate of re-heater steam out	468	467.9	468	kg/s	ETAPRO CS
$m_{rh.att}$	Mass flow rate of re-heater attemporator spray water	10.86	10.8	10.3	kg/s	C-SCHEDULE Plant Technical Specification
P_{mills}	Mill A	1459.7	1451.5	1453.6	kW	ETAPRO CS

	Mill B	1448.2	1451.3	1460.6	kW	ETAPRO CS
	Mill C	1444.6	1427.6	1460	kW	ETAPRO CS
	Mill D	0	1437.207	0	kW	ETAPRO CS
	Mill E	1448.8	0	1463.2	kW	ETAPRO CS
	Mill F	1440.5	1455.4	1457.5	kW	ETAPRO CS
$P_{PA,fans}$	Power to PA fan	1850	1850	1850	kW	C-SCHEDULE Plant Technical Specification
$P_{fd,fan}$	Power to FD Fan	3148	3148	3148	kW	C-SCHEDULE Plant Technical Specification
$P_{seal,fans}$	Power to mill seal air fans	75	75	75	kW	C-SCHEDULE Plant Technical Specification
$V'_{seal,air}$	Volumetric flow rate of seal air	2,65	2,65	2,65	m ³ /s	C-SCHEDULE Plant Technical Specification

The analysis of the coal was carried out at the ESKOM central coal laboratory. The analysis was performed on an air-dried basis for each sample received at the lab. The amount of carbon contained in the coal was adjusted by various iterations until the laboratory measured CV matched the calculated HHV. The oxygen content was calculated by difference.

Table 3.7 specified other additional parameters beside the extracted data from the plant's control system to complete the MEB calculations.

Table 3.7: ESKOM MEB Assumptions

Parameter	Description	Value	Unit
$f_{.AUX}$	Auxiliary power	12	%
$f_{.NOX}$	NOX coefficient	30	%
$\eta_{.cycle}$	Rankine cycle efficiency	42.3	%
$\eta_{.gen}$	Generator efficiency	98.7	%
%FA	Percentage of fly ash in total ash	80	%
$T_{BA,exit}$	Temperature of bottom ash	790	°C

All specified in Tables 3.6 and 3.7 depend on coal-fired boiler operating conditions, such as load, as well as the configuration of the coal milling plant and the arrangement of the burners in the furnace. In the global MEB, it was estimated that the ingress air accounts for a percentage, $\%Air_{ingress}$, of the total humid air entering the boiler.

CHAPTER FOUR COMPUTATIONAL FLUID DYNAMICS (CFD)

4.1 Introduction

This chapter focuses on the simulation of the secondary air system's flow which is very critical for coal combustion. The air system was analysed with the method of computational fluid dynamics (CFD) using ANSYS Fluent Workbench. Figure 4.1 illustrates the secondary air system used for the CFD method.

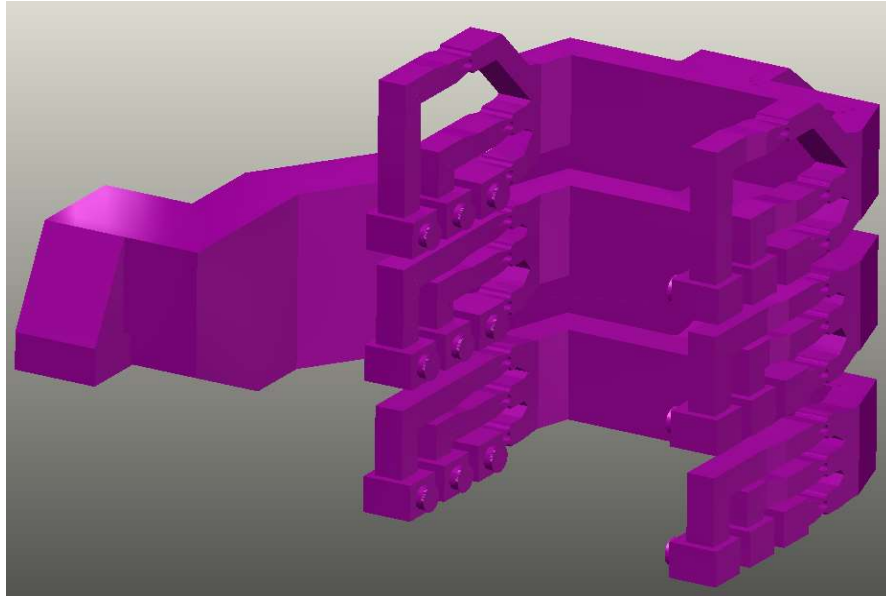


Figure 4.1: Secondary Air Ducting to boiler (Catia 3D View)

Secondary Air System - Inlet

The ambient air, after being heated by the air heater, enters the secondary duct at the inlet, as highlighted in green in the 3D model in Figure 4.2 at 283 kg/s, at a temperature of 273°C at 520.56 MW full load.

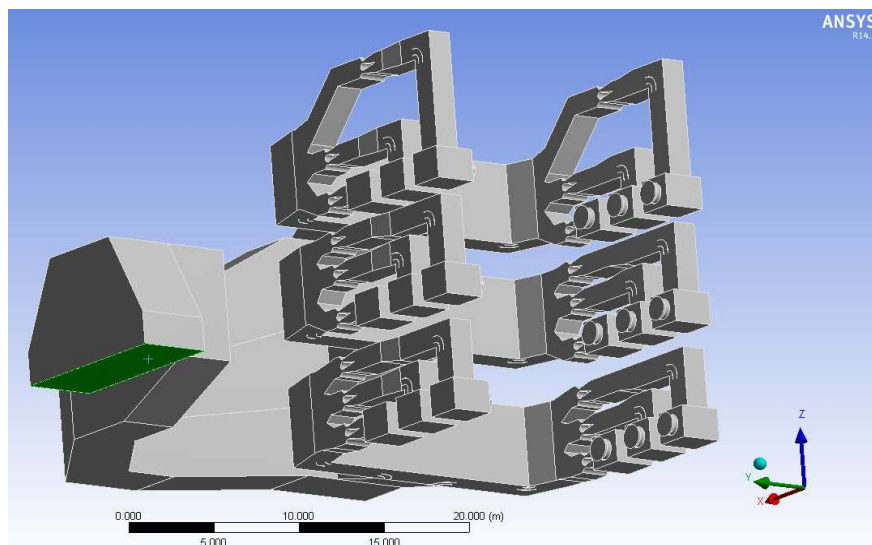


Figure 4.2: Air flow system's inlet boundaries

Secondary Air System - Outlet

Figure 4.3 specifies the outlets of the system where the secondary air is supplied to the burners.

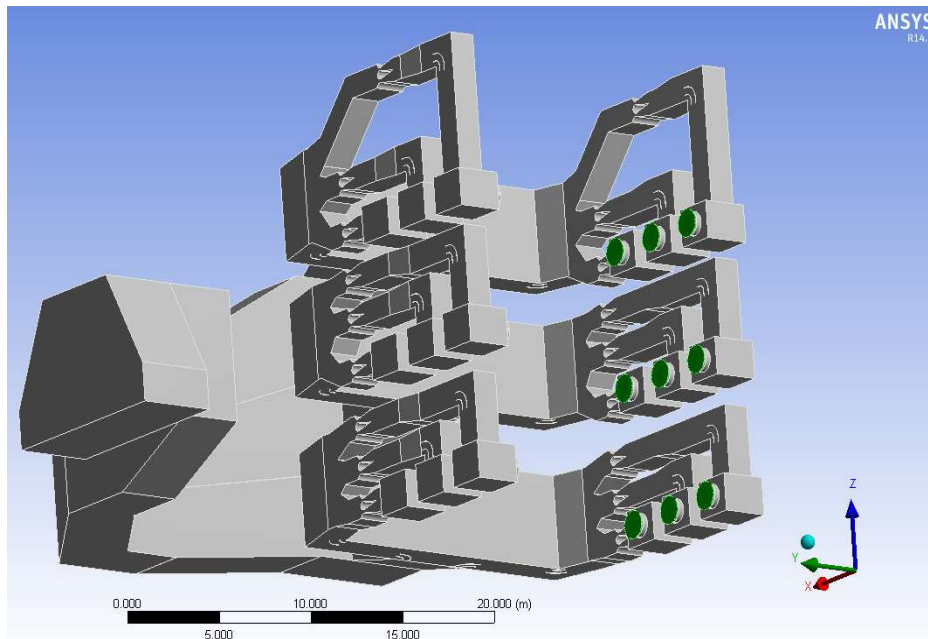


Figure 4.3: Air flow system's outlet boundaries

4.2 Simulation process

ANSYS Fluent is a finite volume method using a flow numerical solution technique. In effect, the computational domain is meshed into cells representing finite control volumes for which the combination of the main equations for fluid flow are applied. The resulting equations are then substituted into a system of algebraic equations so that they can be solved iteratively (ANSYS, 2015).

The finite volume method considers a fluid element (see Figure 4.4) through which the fluid flows.

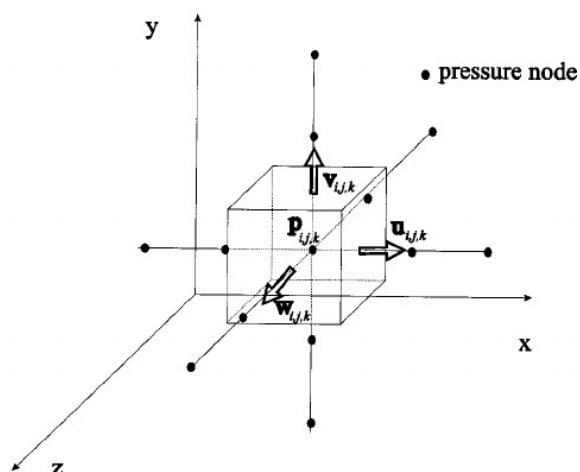


Figure 4.4: Fluid element for pressure and flow analysis (ANSYS, 2015)

4.2.1 Meshing Process

ANSYS Fluent uses a dynamic mesh as shown in Figure 4.5 to model flows where the shape of the domain varies in part due to motion on the domain's boundaries. The dynamic mesh model can also be applied for a steady state solution. The volume mesh can be updated automatically by ANSYS Fluent when necessary, depending on the new locations of the boundaries (ANSYS, 2015). The application of the dynamic mesh model is facilitated by a starting volume mesh that needs to be provided and the specification of the motion of the moving zones in the model.

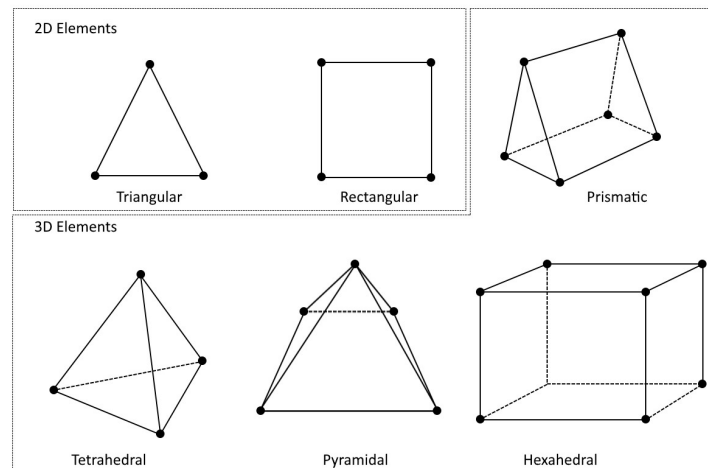


Figure 4.5: Fluid element mesh type (ANSYS, 2015)

The motion can however be described using either boundary profiles to specify the inlets and outlets of the fluid flow in the system. The description of the motion can also be specified on either face or cell zones. If the model contains moving and non-moving regions, the respective face or cell zones in the starting volume mesh should be identified. Furthermore, areas that are deformed due to motion in their adjacent regions must be grouped into separate zones in the starting volume mesh.

Meshing is an integral part of the computer-aided engineering simulation process that influences the accuracy, convergence and speed of the solution. Furthermore, the time it takes to create and mesh a model is often a significant portion of the time it takes to get results from the flow simulation. Thus, the automated tools available during the meshing process gives a better simulation solution. The tools also offer the flexibility to produce meshes that range in complexity. The right mesh can be selected to ensure that the simulation will accurately validate the physical model (ANSYS, 2015).

However, ANSYS has a variety of meshing types such as tetrahedral (triangular) or cut cell (square). The tetrahedron type is mostly used due to its high level of accuracy in the fluid flow

simulation. The mesh size varies from coarse, medium and fine; the type size of mesh selected depends on the accuracy needed for the flow simulation.

ANSYS Fluent offers meshing solutions for fluid flow simulation that provides unstructured tri- and quad-surface elements determined by curvature, proximity, smoothness and quality, combined with a high level of capability that automatically removes unimportant features. The mixture of automated surface meshing, boundary layer technology and an advancing front mesh algorithm ensures high-quality, push-button meshing for fluid flow analysis. Extended sizing, matching, mapping and sweep controls provide additional flexibility, if required (ANSYS, 2015).

4.2.2 Simulation Calculation

ANSYS Fluent is commonly used for flow simulation and uses a set of equations such as continuity, momentum and energy equation. Additional transport equation is used when the flow is turbulent. Figure 4.6 illustrates the basic workflow for any flow simulation in ANSYS.

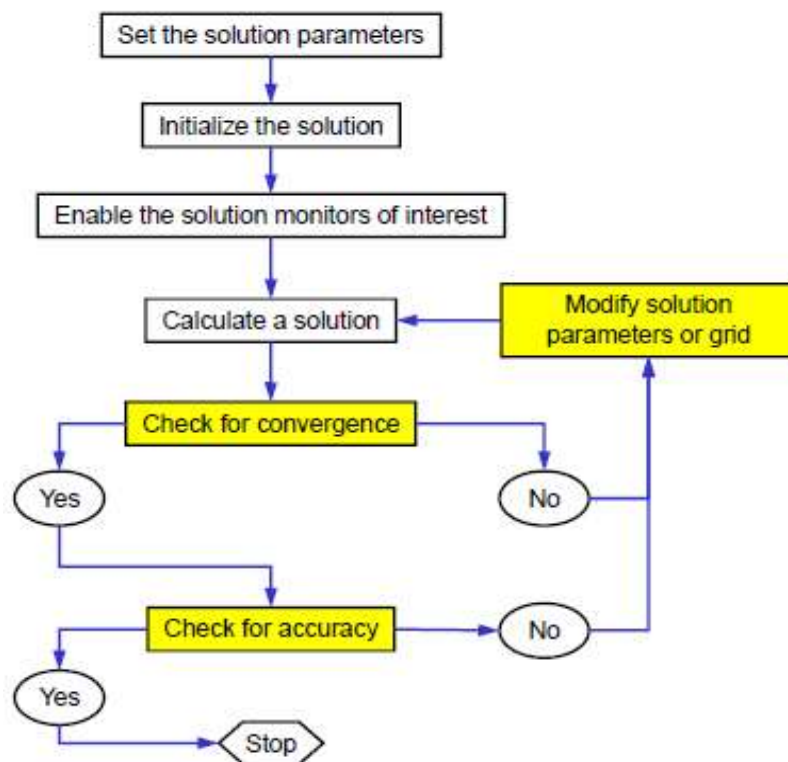


Figure 4.6: ANSYS Simulation Process Flow Diagram (ANSYS, 2015)

The flow simulation process as shown in Figure 4.6 always starts with the setting of important parameters of the fluid system and CFD equations. This is followed by the initialization of the simulation solution and calculation with multiple iterations until the solution converges for accuracy of results.

Continuity equations

The continuity equation commonly known as conservation of mass used by ANSYS can be described as follows (Versteeg & Malalasekera, 2007):

$$\frac{\partial \rho}{\partial t} + \nabla \cdot (\rho \vec{v}) = S_m \quad 4.1$$

Where the term S_m represents the mass added to the continuous phase from the distributed second phase.

The conservation of mass law can be applied so that the net flow of mass into the fluid element is equal to the rate of increase of mass in the fluid element. The continuity equation for unsteady three-dimensional (3D) mass conservation in a fluid element is in compact vector notation (Versteeg & Malalasekera, 2007).

The continuity equation used for 2D axisymmetric geometries, is given by:

$$\frac{\partial \rho}{\partial t} + \frac{\partial}{\partial x} (\rho v_x) + \frac{\partial}{\partial r} (\rho v_r) + \frac{\rho v_r}{r} = S_m \quad 4.2$$

Where x is the axial coordinate, r the radial coordinate, v_x is the axial velocity and v_r is the radial velocity.

Momentum Equations

The momentum equation used by ANSYS Fluent is based on Newton's second law. The rate of increase of momentum of a fluid particle is equal to the sum of the forces on the fluid particle. For three-dimensional flow (3D), the flow equation can be used with respect to x , y and z axis. The x -components of the momentum equation is calculated by:

$$\rho \frac{Du}{Dt} = \frac{\partial(-p + \tau_{xx})}{\partial x} + \frac{\partial \tau_{yx}}{\partial y} + \frac{\partial \tau_{zx}}{\partial z} + S_{Mx} \quad 4.3$$

The y -component of the equation is:

$$\rho \frac{Dv}{Dt} = \frac{\partial(-p + \tau_{yy})}{\partial y} + \frac{\partial \tau_{yx}}{\partial x} + \frac{\partial \tau_{zy}}{\partial z} + S_{My} \quad 4.4$$

The z-component of momentum is:

$$\rho \frac{D\omega}{Dt} = \frac{\partial(-p+\tau_{zz})}{\partial z} + \frac{\partial\tau_{yz}}{\partial y} + \frac{\partial\tau_{xz}}{\partial x} + S_{Mz} \quad 4.5$$

The momentum equation of a fluid flow including contribution to the body forces is shown by the equation 4.6, Fluent uses a modified equation in the conservative form (ANSYS, 2015):

$$\frac{\partial}{\partial t}(\rho\vec{v}) + \nabla \cdot (\rho\vec{v}\vec{v}) = -\nabla p + \nabla \cdot (\bar{\tau}) + \rho\vec{g} + \vec{F} \quad 4.6$$

Where p is the static pressure ($\bar{\tau}$) is the stress tensor and $\rho\vec{g}$ vector and \vec{F} vector are the gravitational body force and external body forces respectively.

The stress tensor is defined as

$$\bar{\tau} = \mu[(\nabla\vec{v} + \nabla\vec{v}^T) - \frac{2}{3}\nabla \cdot \vec{v}I] \quad 4.7$$

With μ is the molecular viscosity, I is the unit tensor, and the second term on the right-hand side is the effect of volume dilation.

Energy equation

The energy equation used by the ANSYS fluent solver applies the first law of thermodynamics. The rate of increased energy of a fluid particle is equal to the sum of the net rate of heat added and the net rate of work done on the conservation of energy.

The energy equation of the 3D flow is described as follows:

$$\rho \frac{DE}{Dt} = -\nabla \cdot (\rho\vec{v}) + \left[\frac{\partial(u\tau_{xx})}{\partial x} + \frac{\partial(u\tau_{yx})}{\partial y} + \frac{\partial(u\tau_{zx})}{\partial z} + \frac{\partial(v\tau_{xy})}{\partial x} + \frac{\partial(v\tau_{yy})}{\partial y} + \frac{\partial(v\tau_{zy})}{\partial z} + \frac{\partial(\omega\tau_{xx})}{\partial x} + \frac{\partial(\omega\tau_{yz})}{\partial y} + \frac{\partial(\omega\tau_{zz})}{\partial z} \right] + \nabla \cdot (k \nabla T) + S_E \quad 4.8$$

With S_E being the source term for the potential energy changes and k the thermal conductivity.

Fluent solves the energy equation presented in the following conservative form as:

$$\frac{\partial}{\partial t}(\rho E) + \nabla \cdot (\vec{v}(\rho E + p)) = -\nabla \cdot (k_{eff}\nabla T - \sum_j h_j \vec{j}_j + (\bar{\tau}_{eff} \cdot \vec{v})) + S_h \quad 4.9$$

With \vec{j}_j the diffusion flux of species j , k_{eff} the effective conductivity $k + ki$ (with ki dependent on the turbulence model used) and the first three terms on the right hand side being energy transfer due to conduction, species diffusion and viscous dissipation respectively. The source term S_h is made up of the heat of chemical reactions as well as other heat sources where applicable (ANSYS, 2015).

Turbulence equation

For turbulent flow the instantaneous continuity and momentum equations are simplified into the mean and fluctuating components and represented in the Cartesian tensor form as (ANSYS, 2015):

$$\frac{\partial \rho}{\partial t} + \frac{\partial}{\partial x_i} (\rho u_i) = 0 \quad 4.10$$

$$\frac{\partial}{\partial t} (\rho u_i) + \frac{\partial}{\partial x_j} (\rho u_i u_j) = -\frac{\partial p}{\partial x_i} + \frac{\partial}{\partial x_j} \left[\mu \left(\frac{\partial u_i}{\partial x_j} + \frac{\partial u_j}{\partial x_i} - \frac{2}{3} \delta_{ij} \frac{\partial u_k}{\partial x_k} \right) \right] + \frac{\partial}{\partial x_j} (-\rho \bar{u}'_i \bar{u}'_j) \quad 4.11$$

These are the Reynolds-averaged Navier-Stokes equations; or with velocities representing mass-averaged values they can be interpreted as the Favre-averaged Navier-Stokes equations for variable density compressible flow. In order to close the RANS equations, the additional Reynolds stresses $(-\rho \bar{u}'_i \bar{u}'_j)$ that appear need to be modelled. This involves solving the two additional transport equations given below. The wall boundary conditions as used in the k-w models is the enhanced wall treatment method (ANSYS, 2015).

The k-w model turbulent kinetic energy transport equation with k the turbulence kinetic energy is shown as:

$$\frac{\partial}{\partial t} (\rho k) + \frac{\partial}{\partial x_i} (\rho k u_i) = -\frac{\partial}{\partial x_j} \left(r_k \frac{\partial k}{\partial x_j} \right) + \bar{G}_k - Y_k + S_k \quad 4.12$$

The specific dissipation rate transport equation with w the specific dissipation rate is shown in Equation 4.13

$$\frac{\partial}{\partial t} (\rho \omega) + \frac{\partial}{\partial x_j} (\rho \omega u_j) = -\frac{\partial}{\partial x_j} \left(r_\omega \frac{\partial \omega}{\partial x_j} \right) + \bar{G}_\omega - Y_\omega + D_\omega + S_\omega \quad 4.13$$

Transport equation RNG k-ε model

ANSYS Fluent uses The RNG k-ε model equation to increase the accuracy for rapidly strain flows. The RNG k-ε model is derived from the instantaneous Navier-Stokes equations, using a mathematical technique called renormalization group (RNG) methods.

The effect of swirl on turbulence is included in the RNG model, enhancing accuracy for the swirling flows. The RNG theory provides an analytical formula for turbulent Prandtl numbers while the k-ε model uses user-specified constants values. The RNG theory provides an analytically derived differential formula for effective viscosity that accounts for the effects of low-Reynolds number. Effective use of this equation does, however, depend on an appropriate treatment of the near wall region (ANSYS, 2015).

The RNG k-ε model has a similar form to the standard k-ε model as shown:

$$\frac{\partial}{\partial t} (\rho k) + \frac{\partial}{\partial x_i} (\rho k u_i) = \frac{\partial}{\partial x_j} \left(\alpha_k u_{eff} \frac{\partial k}{\partial x_j} \right) + \bar{G}_k + G_b - \rho \epsilon - Y_M + S_k \quad 4.14$$

$$\frac{\partial}{\partial t}(\rho \epsilon) + \frac{\partial}{\partial x_i}(\rho \epsilon u_i) = \frac{\partial}{\partial x_j} \left(\alpha_e u_{eff} \frac{\partial \epsilon}{\partial x_j} \right) + C_{le} \frac{\epsilon}{k} (G_k + C_{3e} G_b) - C_{2e} \rho \frac{\epsilon^2}{k} - R_e + S_e \quad 4.15$$

In these equations G_k represents the turbulence kinetic energy generated due to the mean velocity gradients. G_b is the generation of kinetic to buoyancy in the k-E model. Y_M represents the contribution of the fluctuation dilatation in the compressible turbulence to the overall dissipation rate. The quantities α_k and α_e are the inverse effective Prandtl numbers for the k and ϵ , respectively. S_k and S_e are user-defined source terms.

Enhanced Wall Treatment equation

Enhanced wall treatment is a near-wall modelling method used by ANSYS Fluent, which combines a two-layer model with enhanced wall functions. If the near-wall mesh is fine enough to be able to resolve the viscous sublayer (typically with the first near-wall node placed $y^+ = 1$), then the enhanced wall treatment will be identical to the traditional two-layer zonal model. However, the restriction that the near-wall mesh must be sufficiently fine everywhere might impose too large a computational requirement. Ideally, it is better to have a near-wall formulation that can be used with coarse meshes (wall function meshes) as well as fine meshes (low-Reynolds number meshes). In addition, excessive error should not be incurred for the intermediate meshes where the first near-wall node is placed neither in the fully turbulent region, where the wall functions are suitable, nor in the direct vicinity of the wall at $y^+=1$, where the low-Reynolds-number approach is adequate. To achieve the goal of having a near-wall modelling approach that will possess the accuracy of the standard two-layer approach for the fine near-wall meshes and that, at the same time, will not significantly reduce accuracy for wall functions meshes, ANSYS Fluent combines the two-layer model with enhanced wall functions as described the following sections (ANSYS, 2015).

The viscosity affected near wall region is completely resolved all the way to the sublayer. The two-layer approach is an integral part of the enhanced wall treatment; it is used to specify the turbulent viscosity in the near wall cells. In this approach, the whole domain is subdivided into viscosity-affected regions. The demarcation of the two regions is determined by a wall distance-based, turbulent Reynolds number, Re_y , defined as:

$$Re_y = \frac{\rho y \sqrt{k}}{\mu} \quad 4.16$$

Where y is the wall-normal distance calculated at the cell centres, which is interpreted in ANSYS Fluent as the distance to the nearest wall. y is the wall-normal distance calculated at the cell centres and nearest wall

$$y = \min_{\vec{r}_w \in r_\omega} \|\vec{r} - \vec{r}_\omega\| \quad 4.17$$

Where vector \vec{r} is the position vector at the filed point, and \vec{r}_ω is the position vector of the wall boundary. This interpretation allows y to be uniquely defined in the flow domain of complex shape involving multiple walls. Furthermore, y defined in this way is independent of the mesh topology. The two-layer formulation for turbulent viscosity is used as part of the enhanced wall treatment, in which the two-layer definition is smoothly blended with the High-Reynolds number.

$$\mu_{t,enh} = \lambda_c \mu_t + (1 - \lambda_c) \mu_{t,2laye} \quad 4.18$$

The enhanced thermal wall function used by ANSYS is calculated using the equation below:

$$T^+ = \frac{(T_\omega - T_p) \rho C_p u_T}{q} = e^r T_{lam}^+ + e^{\frac{1}{r}} T_{turb}^+ \quad 4.19$$

The equation can be further specified as laminar or turbulent b the following equations:

$$T_{lam}^+ = \text{Pr} \left(\mu_{lam}^+ + \frac{\rho u}{2.q} u_*^2 \right) \quad 4.20$$

$$T_{turb}^+ = \text{Pr} \left\{ \mu_{turb}^+ + P + \frac{\rho u}{2.q} \left[u^2 - \left(\frac{Pr}{Pr_t} - 1 \right) (u_c^+)^2 (u_*)^2 \right] \right\} \quad 4.21$$

Where the quantity u_c^+ is the value of u^+ at the fictitious cross between the laminar and the turbulent region in the flow simulation.

4.3 Sensitivity study on the mesh

Mesh's sensitivity is very critical as it defines the convergence of the simulation results. These results are sensitive to the size of the mesh that can be coarse, medium or fine. Finer mesh results converge to provide an accurate solution however they need more elements that require a lot of computational time. Therefore, it is ideal to find out the suitable mesh size that will give accurate results (Kulkani et al., 2016).

The sensitivity study on the mesh is necessary to analyse the variation depending on the mesh type selected in order to compute the air flow simulation throughout the secondary air ducting. This CFD will help to visualize the flow velocity in different sections of ducting to identify where useful measurements can be taken. Figure 4.7 is an illustration of the secondary air system's meshing using a coarse type for the simulation process.

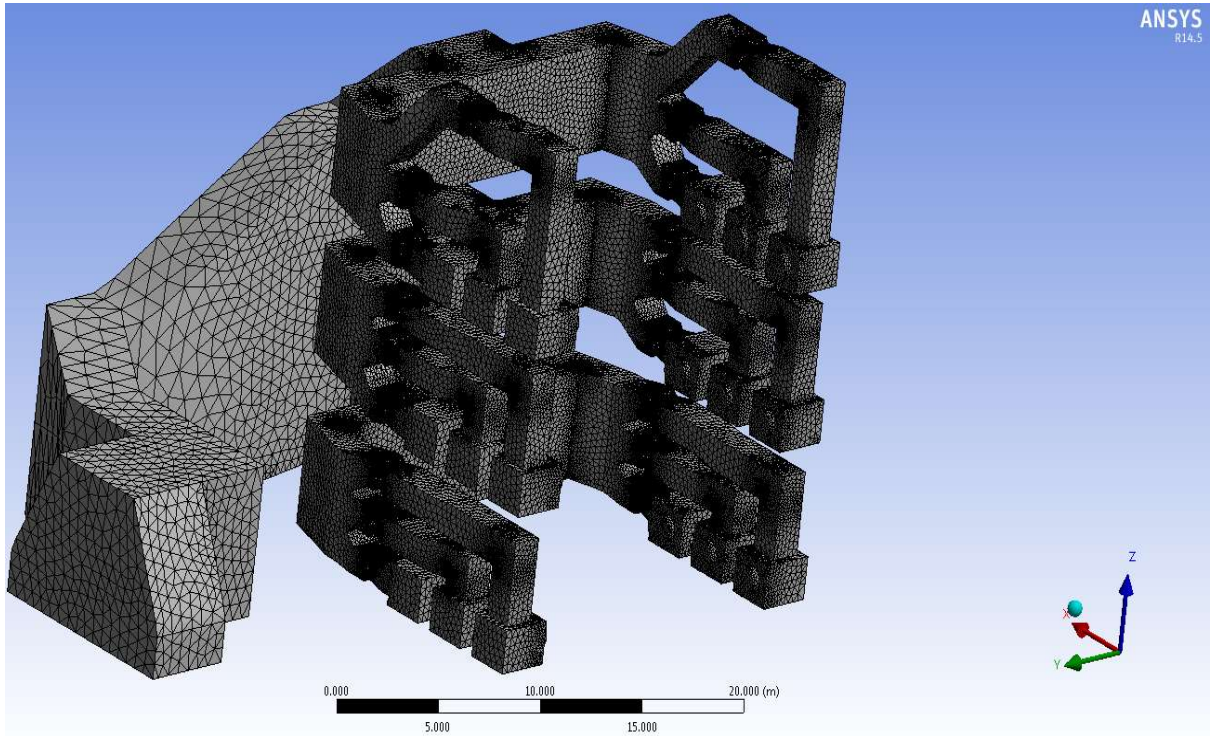


Figure 4.7: Air flow system's meshing for the simulation process

The different mesh type that will be used for air flow simulation process are illustrated in Table 4.1.

Table 4.1: Mesh size used for the air flow simulation

Mesh	Min Size(m)	Max Face size (m)	Max Size (m)	Node	Elements	Type
Coarse	4.1335e-002	5.29090	1.850	148515	668573	Tetrahedrons
Medium	1.3227e-002	1.32270	2.64540	180373	870037	Tetrahedrons
Fine	7.7481e-003	0.774810	1.54960	182875	880250	Tetrahedrons

CHAPTER FIVE MEB CALCULATION RESULTS AND SENSITIVITY ANALYSIS

5.1 The boiler's MEB Results

The main results of the boiler's MEB using the different inputs at full load are listed in Table 5.1:

Table 5.1: MEB calculation results

Description	Symbol	Unit	@521MW	@544MW	@530MW
Mass flow rate of coal	<i>m.coal</i>	kg/s	80.25	81.07	82.88
Mass flow rate of air at A/H inlet	<i>m.air.AH.total</i>	kg/s	541.2	545	542.7
Mass flow rate of flue gas at A/H inlet	<i>mf.fg.AH.in</i>	kg/s	611.7	616.3	615.5
Net Heat Rate	<i>NHR</i>	kJ/kWh	3.191	3.22	3.207

The results as illustrated above are based on the input parameters of a boiler unit at ESKOM coal-fired power station A and will be further compared to the plant's C-Schedule to determine if the plant is performing as per technical specifications. Additionally, it is to ensure accuracy of online measurements.

Table 5.2 and 5.3 show a comparison of the different values of mass flow rate of coal, air and flue gas. This is further displayed on graphs in Figure 5.1 and 5.2.

Table 5.2: Comparison MEB results with ETAPRO Plant operation Data

Description	Symbol	Unit	Load	MEB Results	Plant operation Data-Etapro CS	%Difference
Mass flow rate of coal (Total flow of 5 mills)	<i>m.coal</i>	kg/s	@521MW	80.25	91.24	13.69%
		kg/s	@544MW	81.07	85.5	5.46%
		kg/s	@530MW	82.88	89.5	7.99%
Mass flow rate of air at A/H inlet	<i>m.air.AH.total</i>	kg/s	@521MW	541.2	498.4	7.89%
		kg/s	@544MW	545	531.4	2.49%
		kg/s	@530MW	542.8	498.6	8.13%
Mass flow rate of flue gas at A/H inlet	<i>mf.fg.AH.in</i>	kg/s	@521MW	611.7	615.2	0.58%
		kg/s	@544MW	616.3	608.2	1.31%
		kg/s	@530MW	615.5	599.5	2.61%

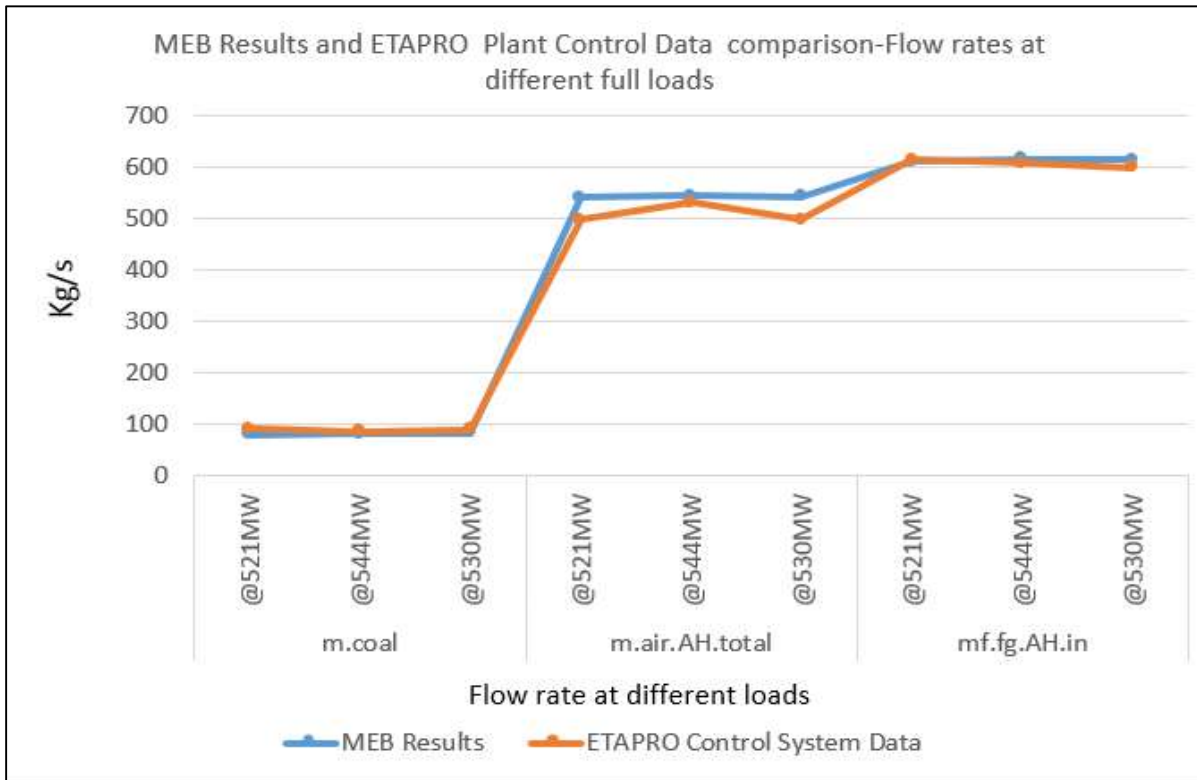


Figure 5.1: Flow rates comparison between MEB results and Etapro Control System Data

Table 5.3: Comparison between MEB results and plant design specification data

Description	Symbol	Unit	Load	MEB Results	Plant Design Specification-C Schedule	%Difference
Mass flow rate of coal (Total flow of 5 mills)	<i>m.coal</i>	kg/s	@521MW	80.25	71.97	10.32%
		kg/s	@544MW	81.07	71.97	11.23%
		kg/s	@530MW	82.88	71.97	13.16%
Mass flow rate of air at A/H inlet	<i>m.air.AH.total</i>	kg/s	@521MW	541.2	504.9	6.70%
		kg/s	@544MW	545	504.9	7.36%
		kg/s	@530MW	542.8	504.9	6.97%
Mass flow rate of flue gas at A/H inlet	<i>mf.fg.AH.in</i>	kg/s	@521MW	611.7	598.3	2.19%
		kg/s	@544MW	616.3	598.3	2.92%
		kg/s	@530MW	615.5	598.3	2.80%

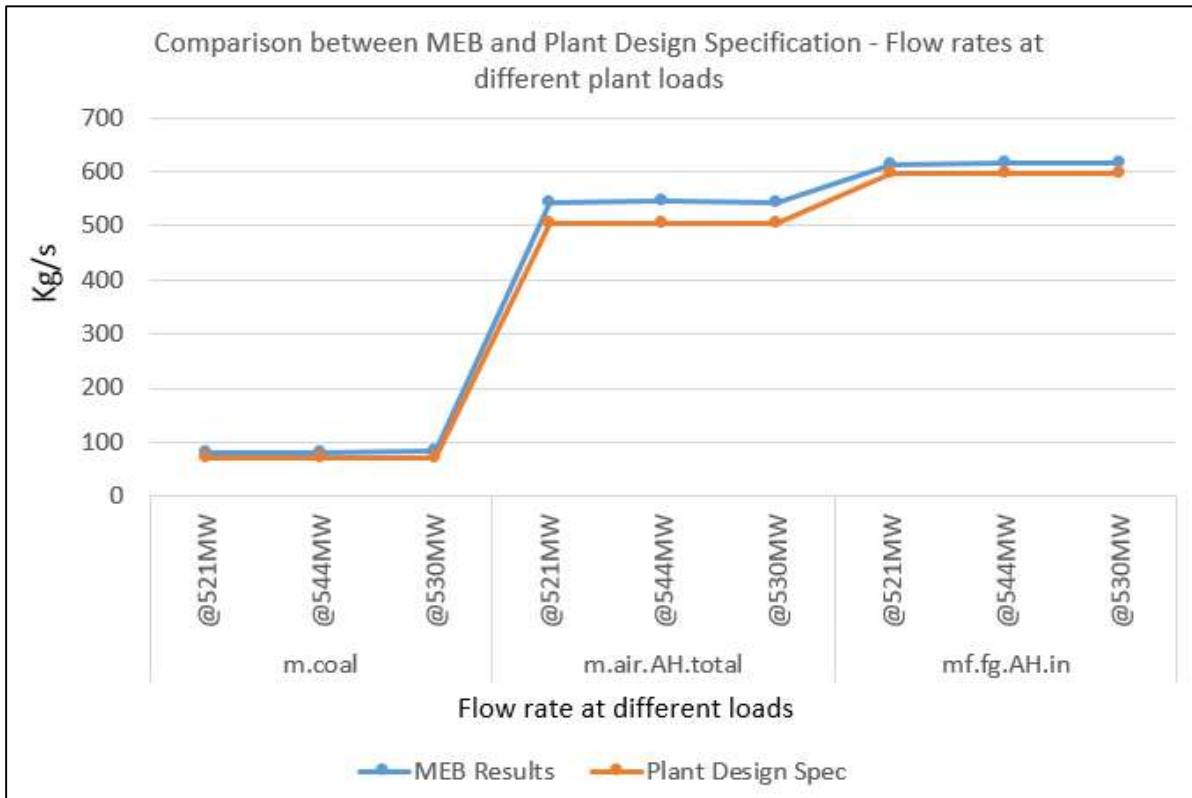


Figure 5.2: Flow rates comparison between MEB results and plant design specifications

The MEB results have been calculated by means of a Mathcad model that was developed using boiler mass energy balance methodology to facilitate traceability of different calculations. However it was found that there is between 5.46 % to 13.69 % difference of the mass flow rates extracted from the ETRAPRO control system and those obtained from mass balance calculations. The mass flow rate of coal is the total flow supplied by the five mills to the boiler unit when the plant operates at full load. The mass flow rate of coal obtained from the MEB calculation is between 10.32 % to 13.16 % more than the one specified in the C-Schedule/Plant specification. This can be caused by many factors such as overall plant efficiency, inputs variation depending on the measurement instruments, or test applied. The MEB results will be further analysed with a sensitivity study for input parameters at 521MW full load.

5.2 Sensitivity Analysis

The sensitivity analysis is very important to test the level of accuracy of measurement input parameters, as well as consistency of assumptions and the effect on the outputs in normal coal power plant operation. There are recognised approaches for the calculation of the systematic uncertainty transmitted in a calculated result from the separate uncertainties of the input parameters (Tootla, 2015).

However, by considering a set of data inputs $x_1, x_2 \dots x_N$ with uncertainties $u_{x1}, u_{x2} \dots u_{xN}$ respectively, if y is a plant output such as coal, air or flue gas mass flow rate and a function of these inputs, the uncertainty of $Y = f(X_1, X_2, \dots, X_N)$ can be calculated as follows:

$$\mu_y = \sqrt{\left(\frac{\partial Y}{\partial X_1}\right)^2 u_{x1}^2 + \left(\frac{\partial Y}{\partial X_2}\right)^2 u_{x2}^2 + \dots + \left(\frac{\partial Y}{\partial X_N}\right)^2 u_{xN}^2} \quad 5.1$$

Where the partial derivatives are calculated as illustrated in the equation below:

$$\frac{\partial Y}{\partial X_i} = \frac{Y(X_i + u_{xi}) - Y(X_i - u_{xi})}{2u_{xi}} \quad 5.2$$

This is to be applied to the plant's operation parameters that were used as inputs in the Mathcad calculations, as well as output values.

The main objective of the sensitivity analysis is to increase awareness of output parameters that are highly sensitive to input variations. This is achieved by varying the input parameters one at the time into the developed model by means of Mathcad and Excel programs. The output values impacted by this variation is carefully observed and recorded. The variations of output parameters as a result of autonomous changes in input variables are arranged to determine the most sensitive parameters. In the case of the sensitivity analysis, a $\pm 1\%$ variation is applied to each of the input parameters. Although the sensitivity analysis provides understanding of how sensitive the outputs are relative to the variation in the inputs, it does not account for what the actual uncertainties of the inputs are, which may be less or even more than $\pm 1\%$ (Tootla, 2015).

The MEB calculation input data will however be used for the sensitivity analysis with uncertainty given as percentage variation, as specified in Table 5.4. In effect, the sensitivity analysis of all of the MEB inputs are varied by 1% of the value. These uncertainties are valued bearing in mind the expected accuracy level of the measurement's instrumentation as well as the variation of the tests used in the process' evaluation of the coal-fired power plant.

Table 5.4: Input parameters at 521 MW Full load values for MEB sensitivity analysis

Input Number	Parameter	Value	Unit	Uncertainty Value
X1	%Ash	40.4	%	0.404
X2	%C	38.9	%	0.389
X3	%H	1.97	%	0.0197
X4	%O	4.06	%	0.0406
X5	%N	0.95	%	0.0095
X6	%S	1.1	%	0.011
X7	%TM	12.5	%	0.125
X8	Total	99.88	%	0.9988
X9	CV	15.64	MJ/kg	0.1564
X10	p_{atm}	83	kPa	0.83
X11	T_{atm}	25	°C	0.25
X12	$RH(\omega)$	7	%	0.07
X13	T_{amb}	28	°C	0.28
X14	$T_{air,A/H.out}$	291.5	°C	2.915
X15	$T_{fg,A/H.in}$	303.6	°C	3.036
X16	$T_{fg,A/H.out}$	142.6	°C	1.426
X17	%O _{2,A/H,fg.in}	4.08	% v/v	0.0408
X18	%C _{fa}	3.41	% m/m	0.0341
X19	%C _{ba}	3.41	% m/m	0.0341
X20	$\dot{m}_{fw,econ.in}$	414.5	kg/s	4.145
X21	p_{fw}	18.19	MPa	0.1819
X22	$T_{fw,econ.in}$	226.8	°C	2.268
X23	$T_{fw,econ.out}$	277	°C	2.77
X24	\dot{m}_{steam}	427.7	kg/s	4.277
X25	$p_{steam.drum}$	19.02	MPa	0.1902
X26	$T_{steam.sh.out}$	533.2	°C	5.332
X27	$p_{steam.sh.out}$	16.37	MPa	0.1637
X28	$\dot{m}_{sh.att}$	10.29	kg/s	0.1029
X29	$p_{sh.att}$	17.88	MPa	0.1788
X30	$T_{sh.att}$	249	°C	2.49
X31	$P_{steam.rh.out}$	2.89	MPa	0.0289
X32	$T_{steam.rh.out}$	532.4	°C	5.324
X33	$P_{rh.att}$	4.1	MPa	0.041
X34	$T_{rh.att}$	165	°C	1.65
X35	$\dot{m}_{rh.steam}$	467.9	kg/s	4.679

X36		$m_{rh.att}$	10.86	kg/s	0.1086
X37		P_{mills}	1459.7	kW	14.597
X38			1448.2	kW	14.482
X39			1444.6	kW	14.446
X40			1448.8	kW	14.488
X41			1440.5	kW	14.405
X42		$P_{PA.fans}$	1850	kW	18.5
X43		$P_{fd.fan}$	3148	kW	31.48
X44		$P_{seal.fans}$	75	kW	0.75
X45		$V'_{seal.air}$	2.65	m ³ /s	0.0265
X46		%FA	80	%	0.8
X47		$T_{BA.exit}$	790	°C	7.9
X48		$Q_{insul.loss}$	0.8	%	0.008
X49		%Air _{ing}	10	%	0.1
X50		%Ingress _{furnace}	100	%	1

As a result of the sensitivity analysis, the graphs illustrated in Figure 5.3, 5.4 and 5.5 present the variation of the outputs based on +/-1 % variation input. The result on each graph is focused on the most influential inputs on the different output parameters.

Mass flow rate of coal

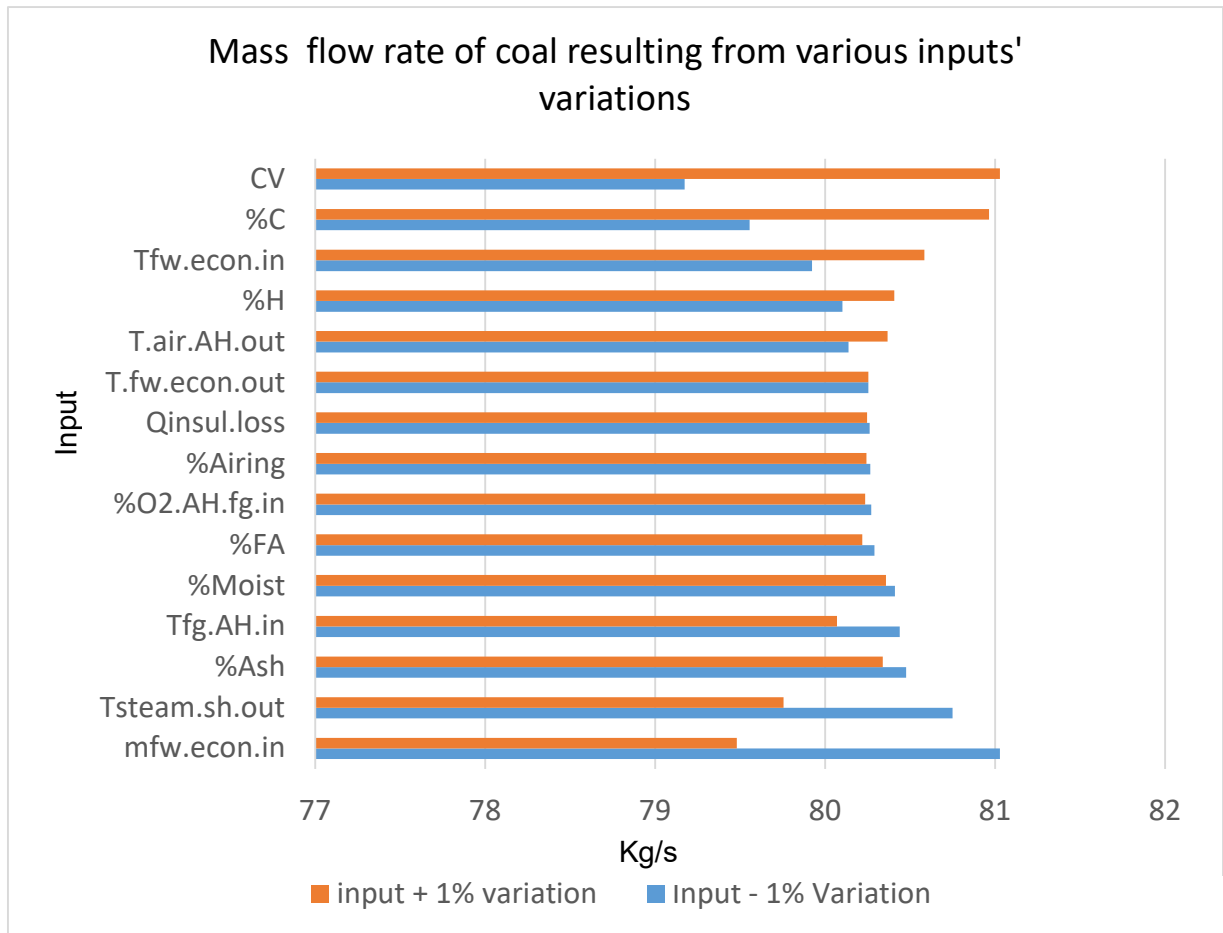


Figure 5.3: Coal mass flow rate sensitivity variation

It can be seen in Figure 5.3 that the mass flow rate of coal is most sensitive to the CV of the coal and the water flow in the economiser of the boiler. Table 5.5 below shows the variations of the mass flow rate of coal when each input parameter with +/- 1 % variation is substituted in the Mathcad model.

Table 5.5: Sensitivity variation of mass flow rate of coal

Value	Xi	Uxi	y(Xi+Uxi)	y(Xi-Uxi)
CV	15.64	0.1564	79.17	81.03
mfw.econ.in	414.5	4.1455	81.028	79.48
Tsteam.sh.out	533.2	5.332	80.749	79.755
Tfw.econ.in	226.7	2.267	79.923	80.584
Tfg.AH.in	303.6	3.036	80.438	80.07
T.air.AH.out	291.5	2.915	80.138	80.368
%FA	80	0.8	80.29	80.218
Qinsul.loss	0.8	0.008	80.262	80.246

%O2.AH.fg.in	4.08	0.0408	80.272	80.236
%Airing	10	0.1	80.265	80.243
T.fw.econ.out	277	2.77	80.254	80.254
%C	38.9	0.389	79.556	80.965
%H	1.97	0.0197	80.101	80.407
%Ash	40.4	0.404	80.476	80.339
%Moist	12.5	0.125	80.41	80.358

Mass flow rate of Air

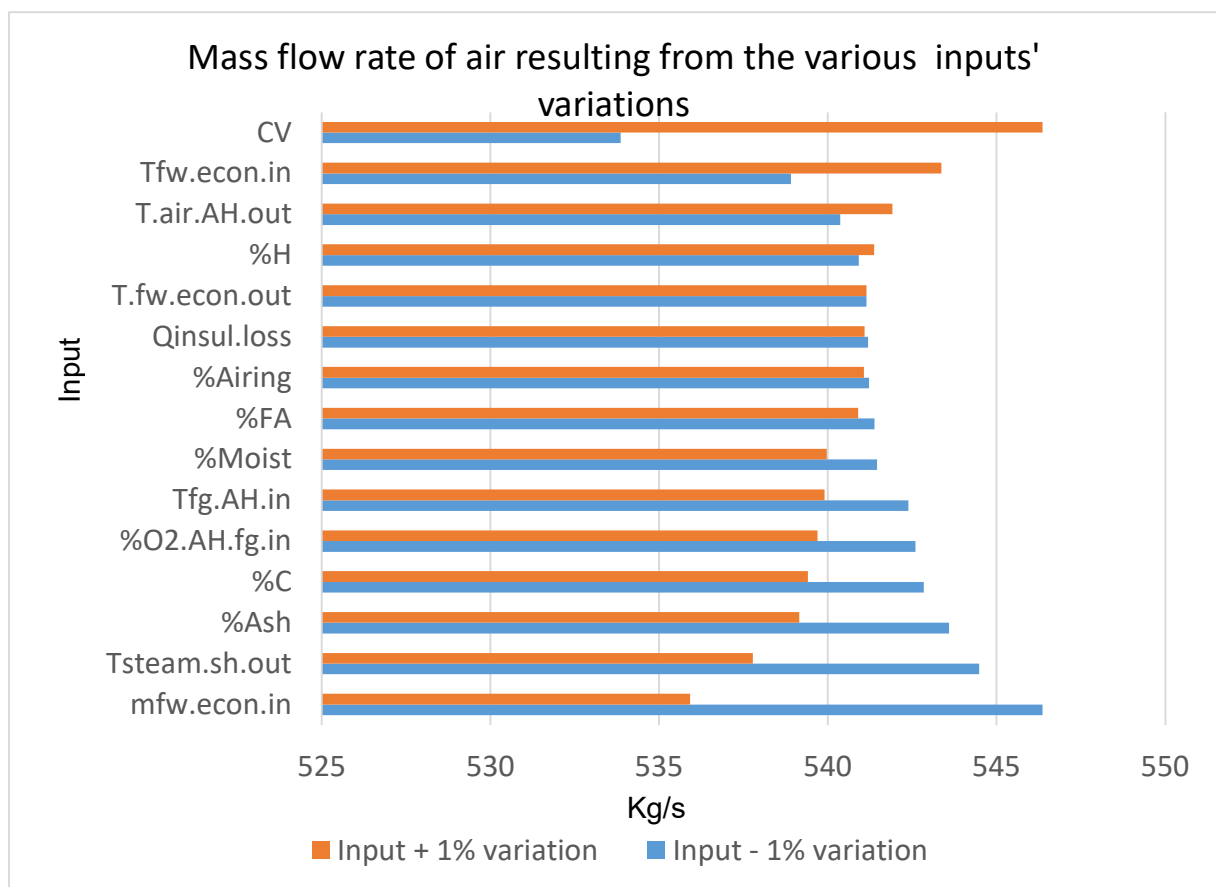


Figure 5.4: Air mass flow rate sensitivity variation

The graph shown in the Figure 5.4 illustrates the air flow sensitivity analysis, which is mostly influenced by inputs such as CV, mass flow rate of water in the economiser, ash percentage and oxygen concentration at the economiser's exit. In effect, the combined uncertainty of the air mass flow rate is 541 ± 9.764 Kg/s using equation 5.2. For example, CV input value is 15.64 ± 0.1564 MJ/kg which gives 533.9 and 546.4 kg/s of total mass flow rate of air when substituted in the Mathcad model, as shown in Table 5.6.

Table 5.6: Sensitivity variation of mass flow rate of air

Value	X_i	U_{xi}	$y(X_i+U_{xi})$	$y(X_i-U_{xi})$
CV	15.64	0.1564	533.7	546.4
mfw.econ.in	414.5	4.145	546.4	535.9
Tsteam.sh.out	533.2	5.332	544.5	537.8
Tfw.econ.in	226.8	2.268	538.9	543.4
Tfg.AH.in	303.6	3.036	542.4	539.9
T.air.AH.out	291.5	2.915	540.4	541.9
%FA	80	0.8	541.4	540.9
Qinsul.loss	0.8	0.008	541.2	541
%O2.AH.fg.in	4.08	0.0408	542.6	539.7
%Airing	10	0.1	541.2	541
T.fw.econ.out	277	2.77	541.1	541.1
%C	38.9	0.389	542.8	539.4
%H	1.97	0.0197	540.9	541.4
%Ash	40.4	0.404	543.6	539.2
%Moist	12.5	0.125	541.5	540

Mass flow rate of flue gas

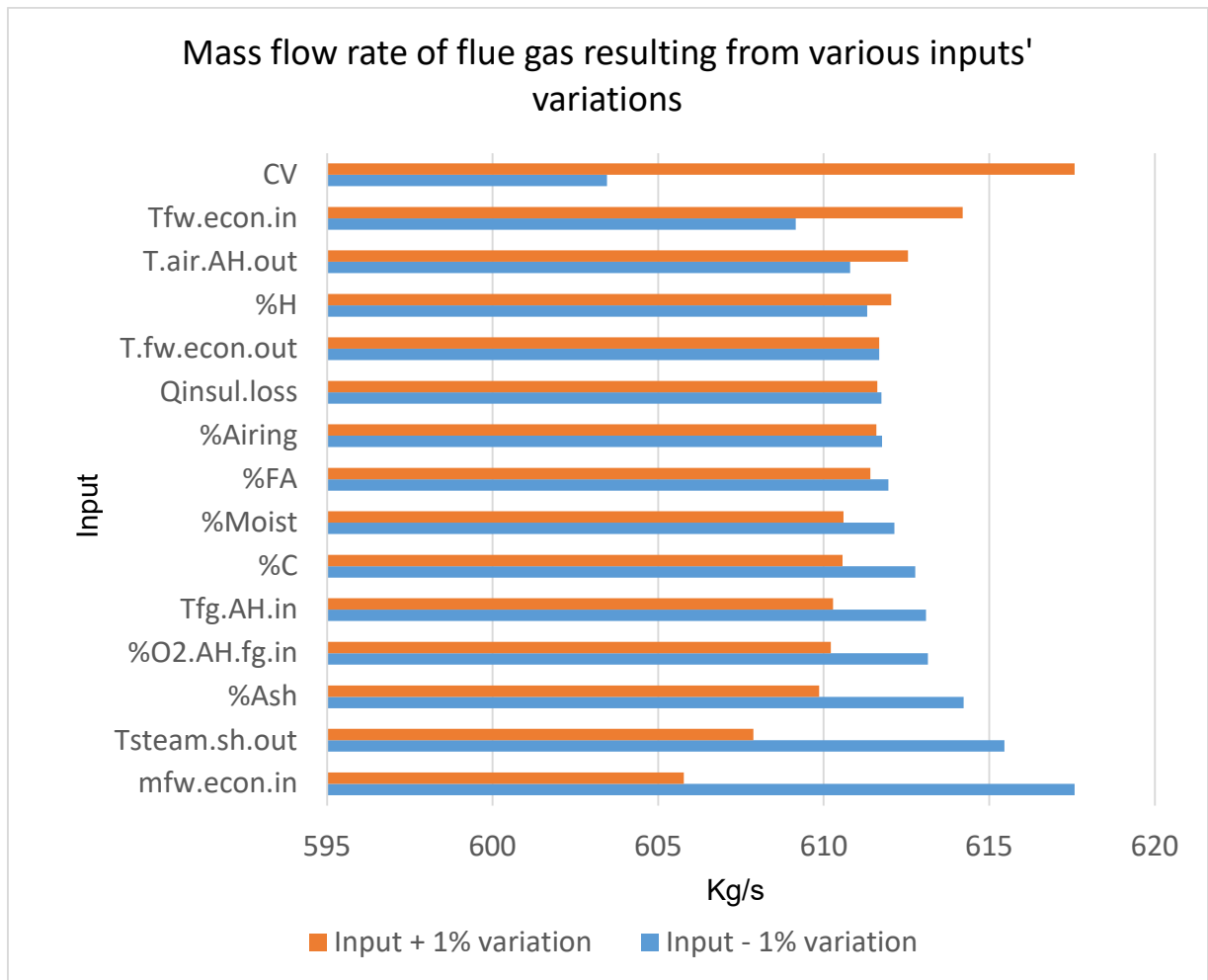


Figure 5.5: Flue gas mass flow sensitivity variation

Similarly to air flow, the mass flow rate of flue gas is also very sensitive to the coal CV, mass flow rate of water in the economiser, temperature of flow gas at the boiler economiser's exit or secondary air heater's inlet, as well as oxygen concentration and carbon content percentage in the coal. Table 5.7 below is an illustration of the different value of the mass flow rate of flue gas when each input parameter with +/- 1 % variation is substituted in the Mathcad model.

Table 5.7: Sensitivity variation of mass flow rate of flue gas

Value	X_i	U_{xi}	$y(X_i+U_{xi})$	$y(X_i-U_{xi})$
CV	15.64	0.1564	603.5	617.6
mfw.econ.in	414.5	4.145	617.6	605.8
Tsteam.sh.out	533.2	5.332	615.5	607.9
Tfw.econ.in	226.8	2.268	609.2	614.2
Tfg.AH.in	303.6	3.036	613.1	610.3
T.air.AH.out	291.5	2.915	610.8	612.5
%FA	80	0.8	612	611.4
Qinsul.loss	0.8	0.008	611.7	611.6
%O2.AH.fg.in	4.08	0.0408	613.1	610.2
%Airing	10	0.1	611.8	611.6
T.fw.econ.out	277	2.77	611.7	611.7
%C	38.9	0.389	612.7	610.6
%H	1.97	0.0197	611.3	612
%Ash	40.4	0.404	614.2	609.9
%Moist	12.5	0.125	612.1	610.6

The MEB output variations from the sensitivity analysis are summarized in Table 5.8 with the respective values of the mass flow rates of coal, air and flue gas.

Table 5.8: Sensitivity variation of MEB outputs

Description	Symbol	Unit	Value
Mass flow rate of coal	<i>m.coal</i>	kg/s	80.25 +/- 1.545
Mass flow rate of air at A/H inlet	<i>m.air.AH.total</i>	kg/s	541.1 +/- 9.764
Mass flow rate of flue gas at A/H inlet	<i>mf.fg.AH.in</i>	kg/s	611.7 +/- 10.823

CHAPTER SIX CFD RESULTS

6.1 Results from the CFD model

The different simulation results for the different type of mesh have been grouped by sections to give a better overview of the mesh sensitivity study and shown the Figure 6.1, 6.2, 6.3 and 6.4.

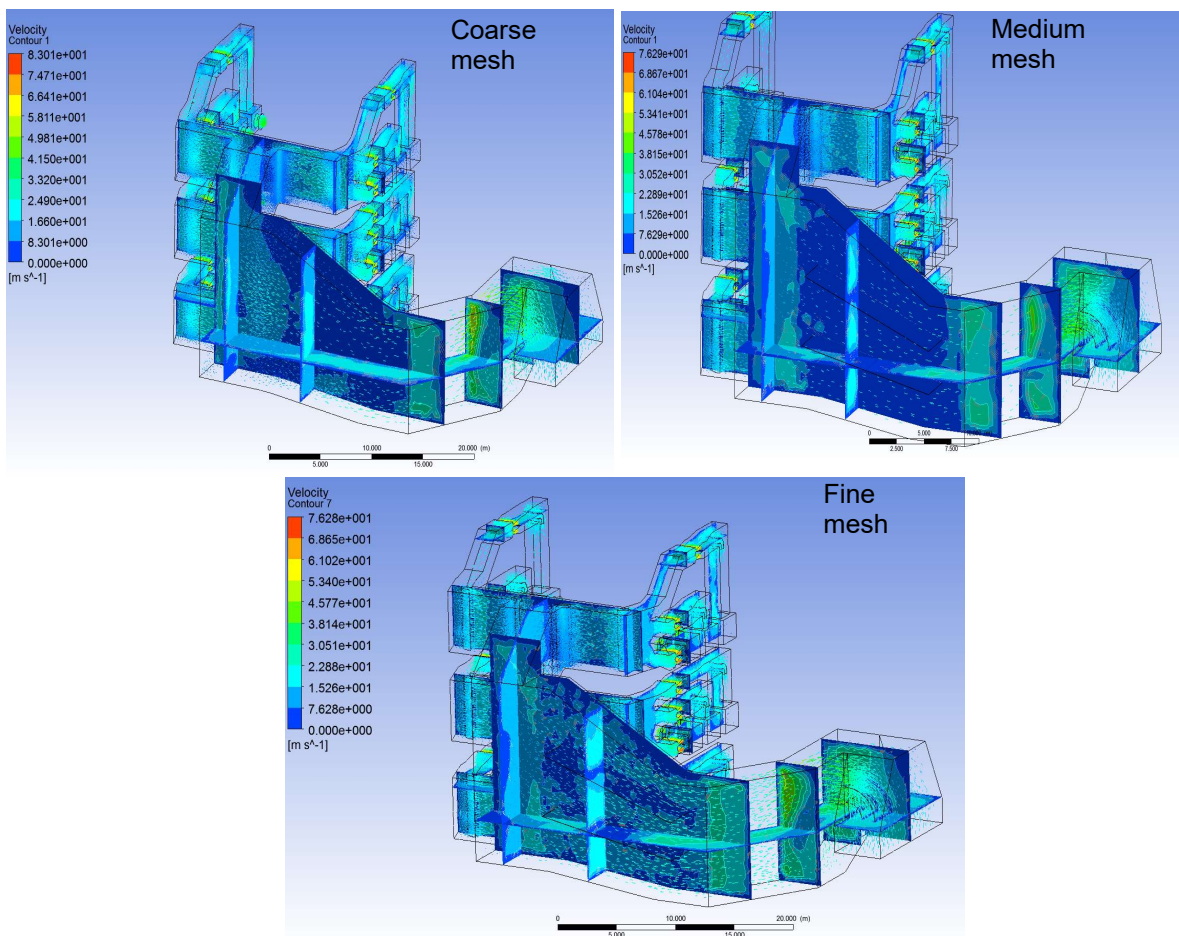


Figure 6.1: Air flow simulation in Main Ducting (3D View)

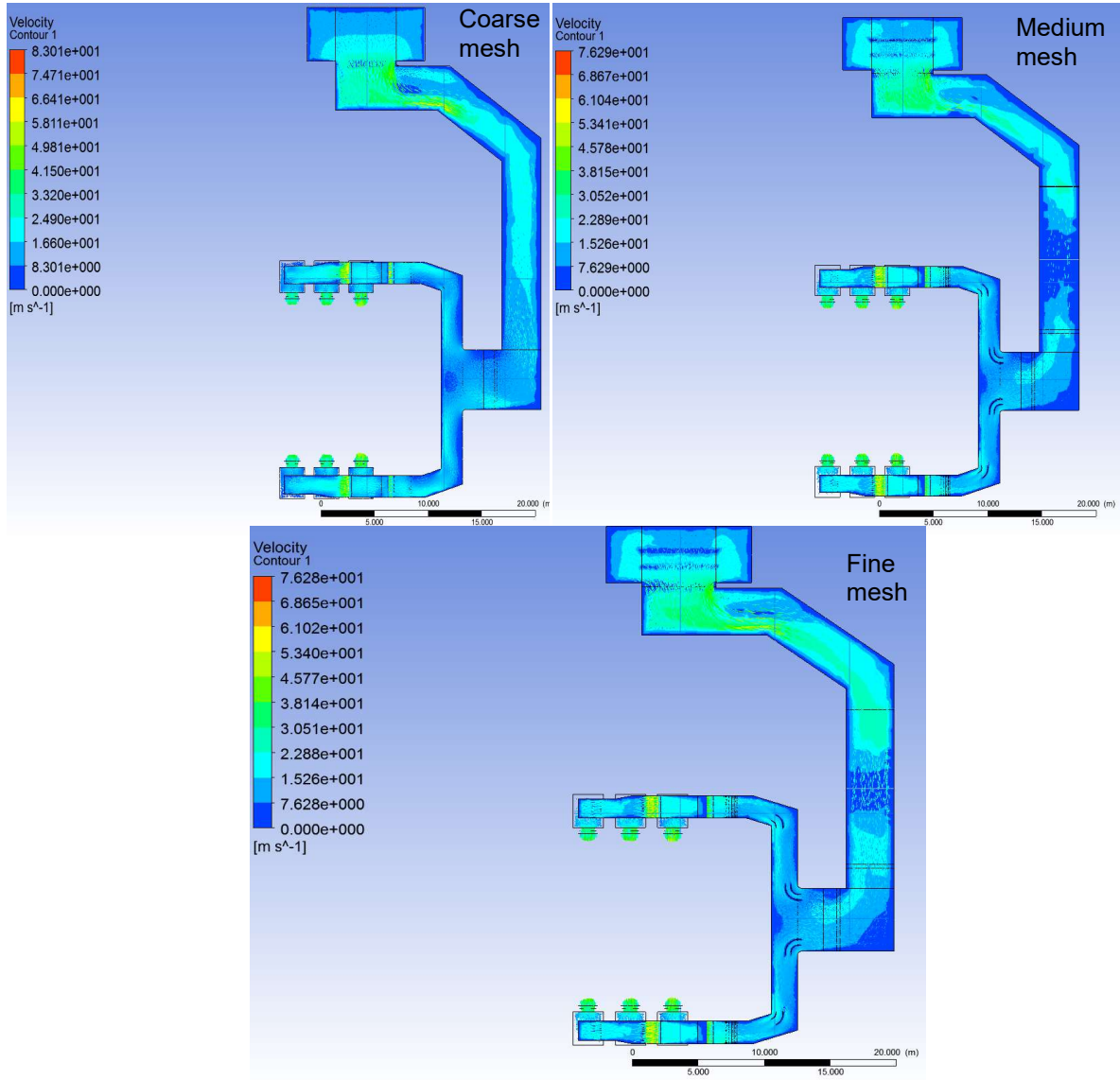


Figure 6.2: Air flow simulation in Main and distribution Ducting (Top View)

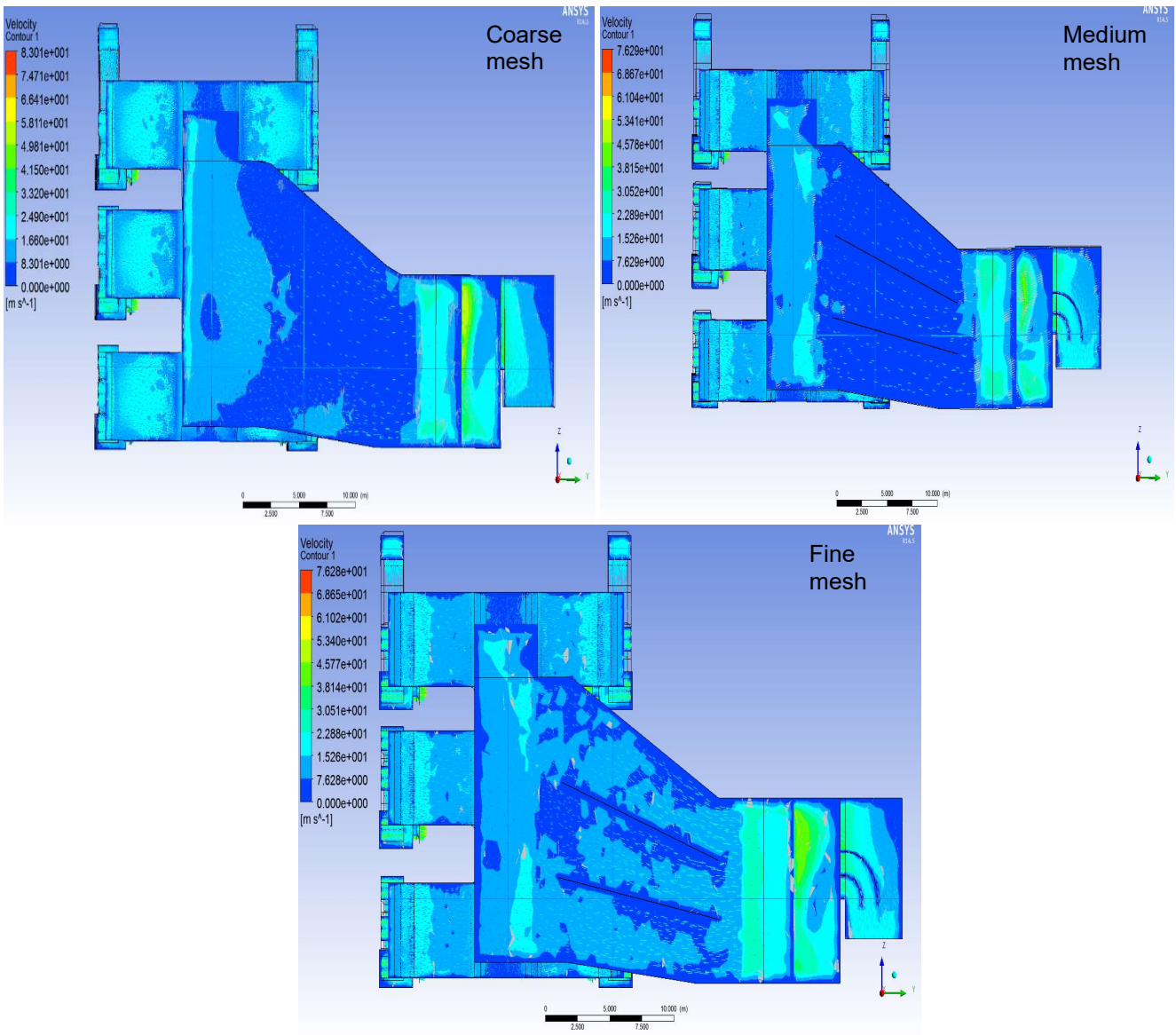


Figure 6.3: Air flow simulation in Front Main and distribution Ducting (Front View)

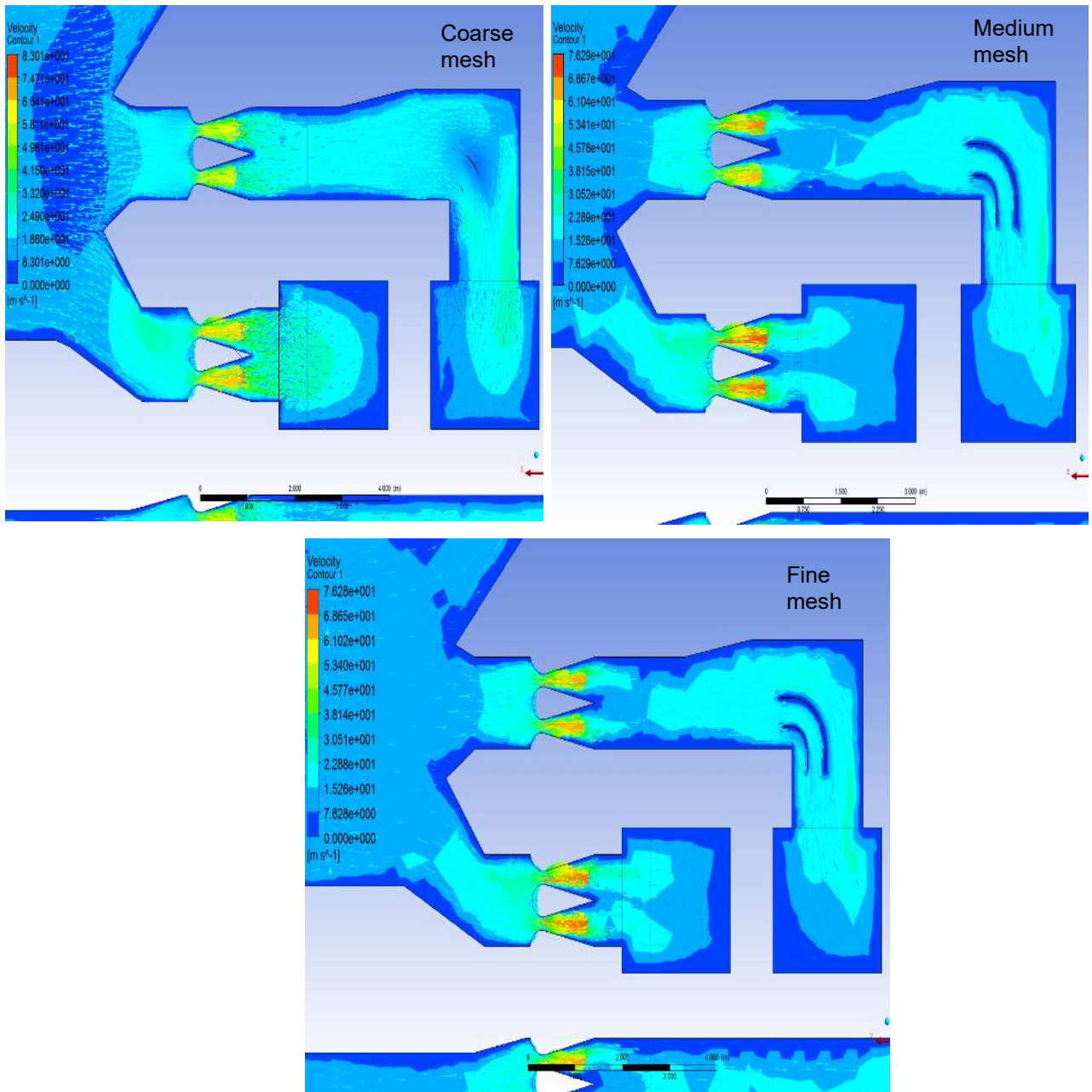


Figure 6.4: Air flow simulation across airfoil

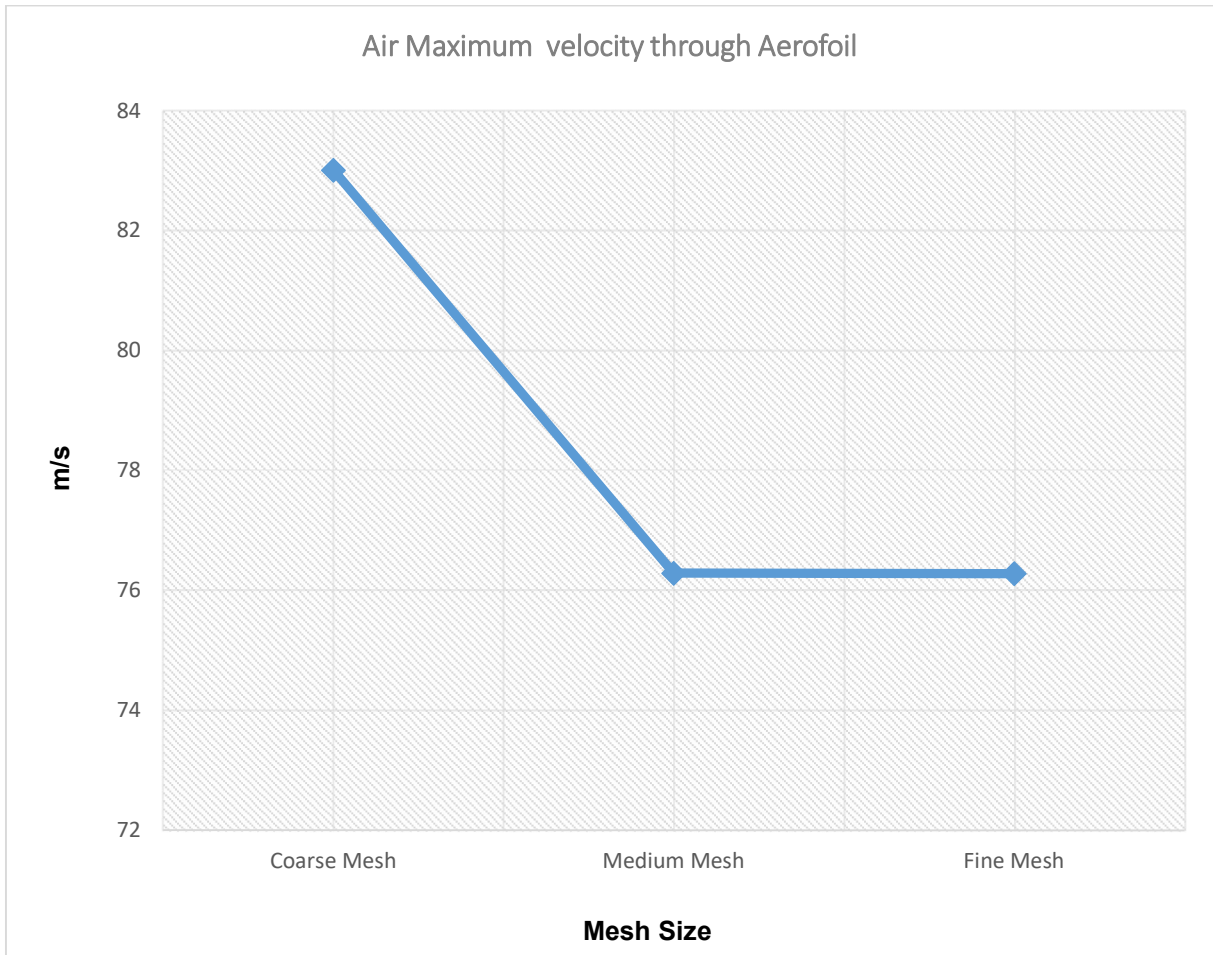


Figure 6.5: Results of the analysis of the size of mesh in the air flow simulation

Figure 6.5 illustrates the simulation results using coarse, medium and fine mesh across the aerofoil in the distribution air duct. The result using a coarse mesh differs significantly from the medium mesh whereas there is no change when changing from medium to fine meshing. A fine mesh was, however, used throughout to ensure that we have a more accurate result.

Iso-Velocity Diagram – Fine mesh

The velocity profile after the aerofoil at the location shown by the yellow line in Figure 6.6 is illustrated on the XY axis where Z is the vertical distance in meters with respect to the yellow line across the ducting; the X axis represents the corresponding velocity of points along the yellow line. The extreme point on the yellow line has a velocity of 4.5 m/s and the centre point 9.5 m/s.

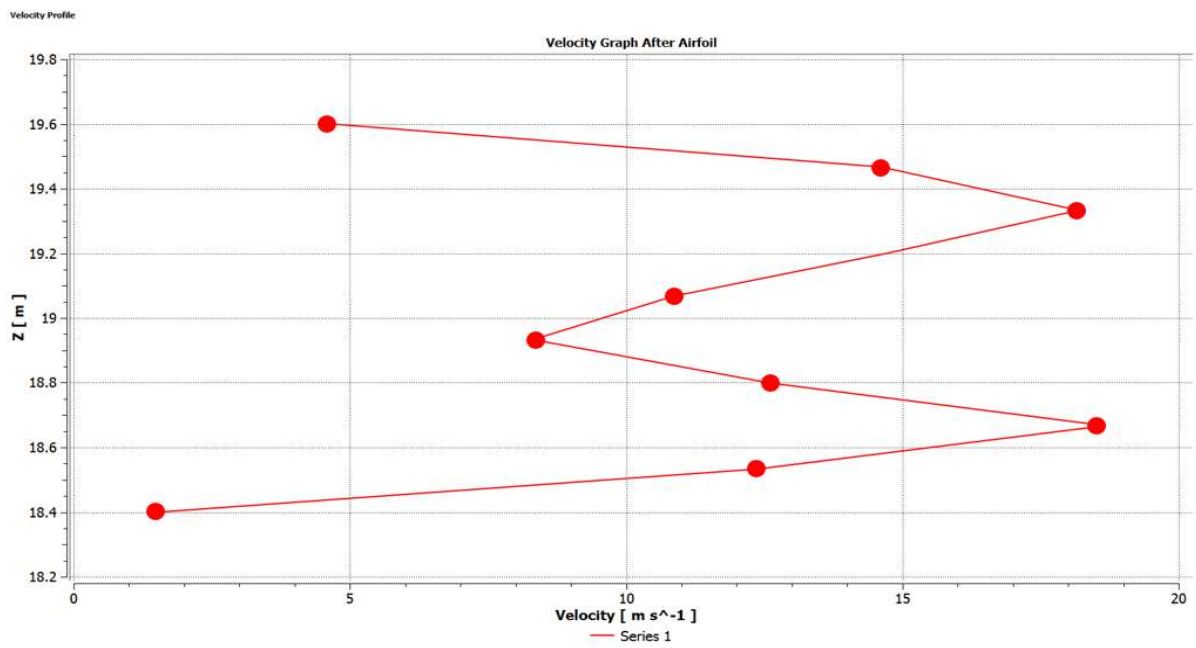
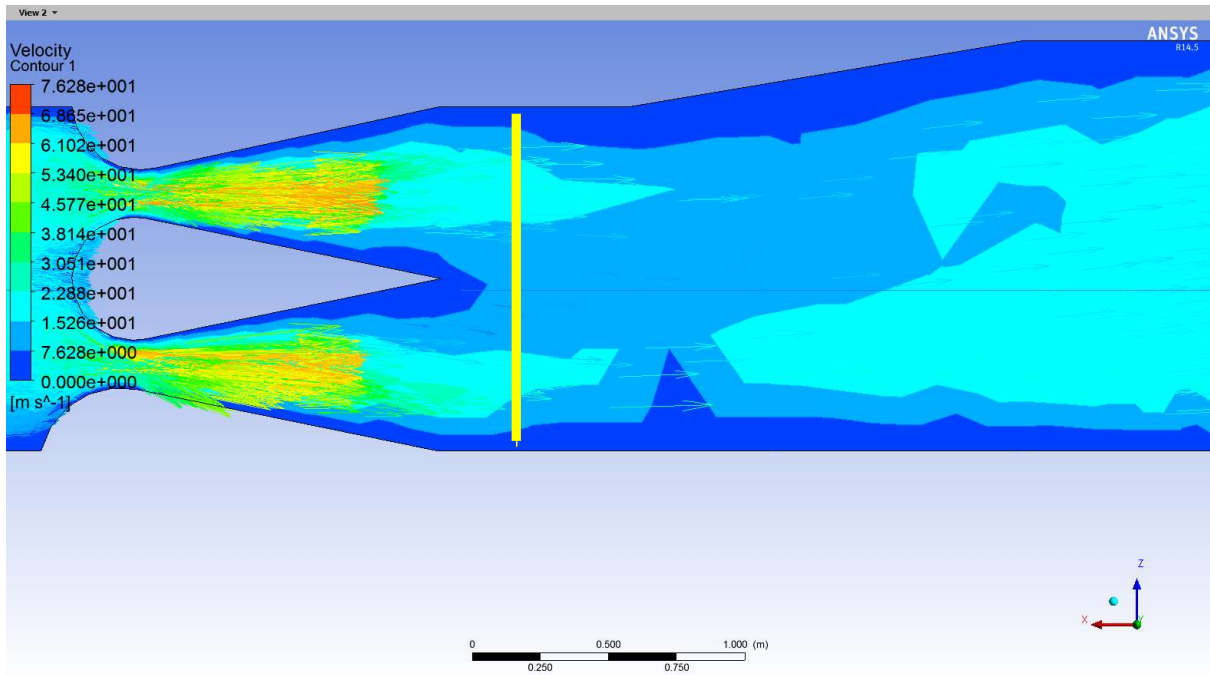


Figure 6.6: Iso-velocity diagram after the aerofoil in the burners' ducting

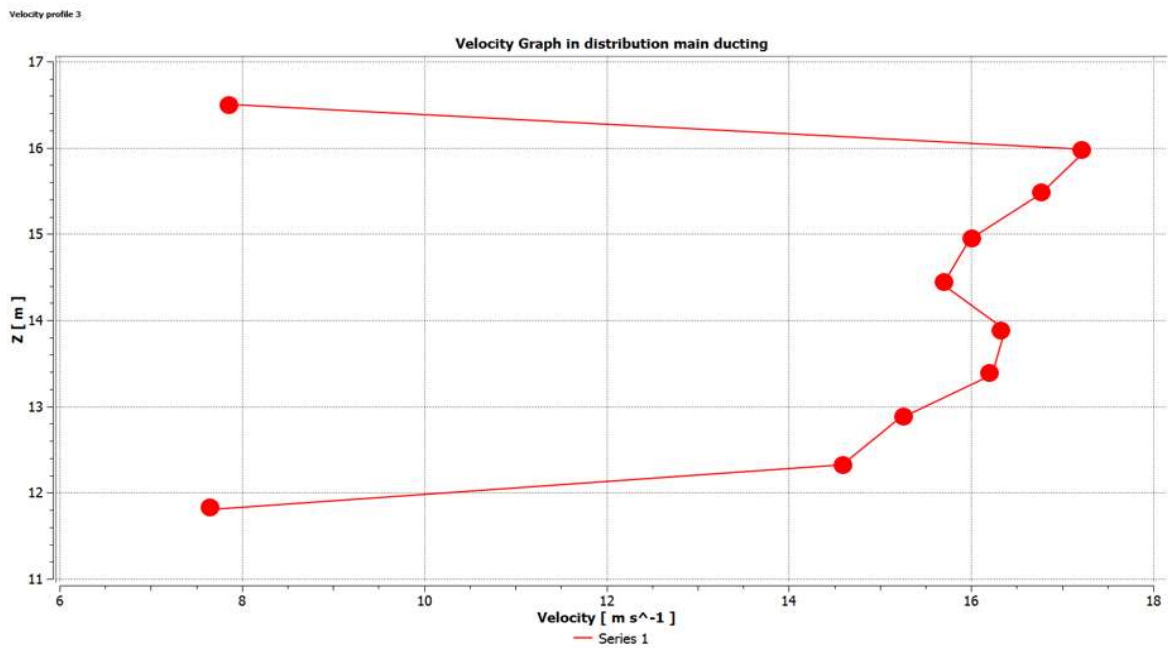
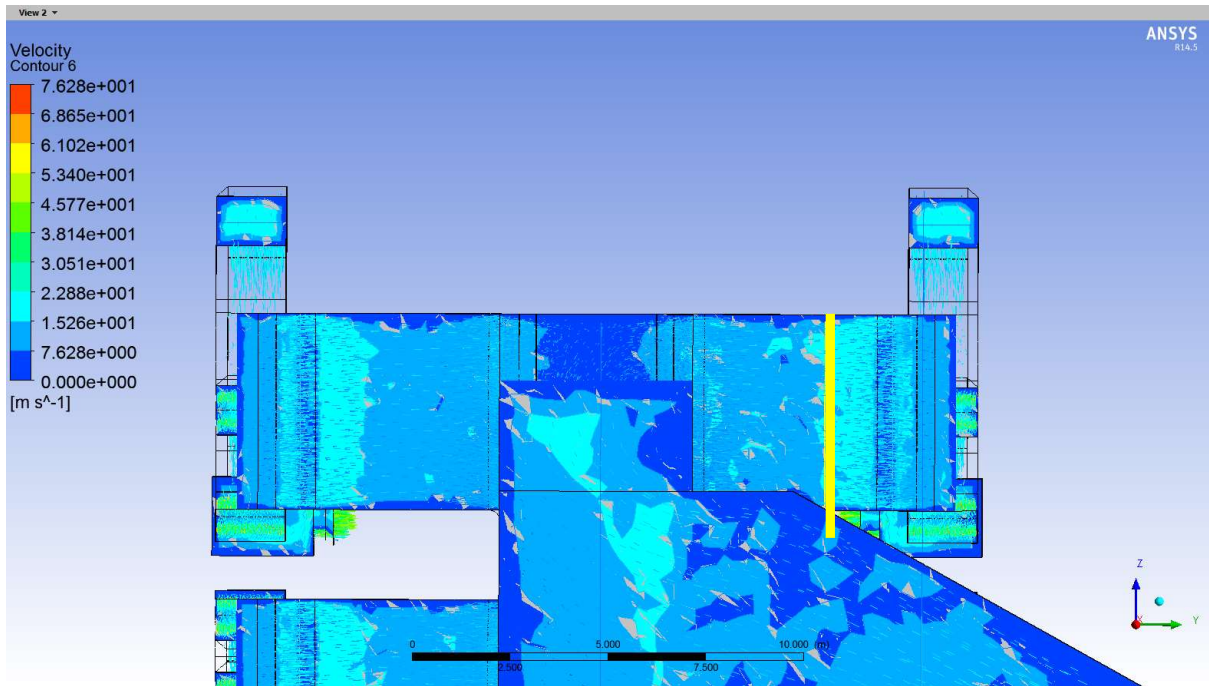


Figure 6.7: Iso-velocity diagram in the distribution ducting

The velocity profile in the distribution ducting at the location shown by the yellow line in Figure 6.7 is illustrated on the XY axis where Z is the vertical distance from 11 to 17 m with respect to the yellow line across the ducting. The corresponding velocity of each point, which varies from 7.5 to 17.5 m/s along the yellow line, is displayed by the X axis. The extreme point on the yellow line has a velocity of 7.6 m/s and the centre point 16.3 m/s.

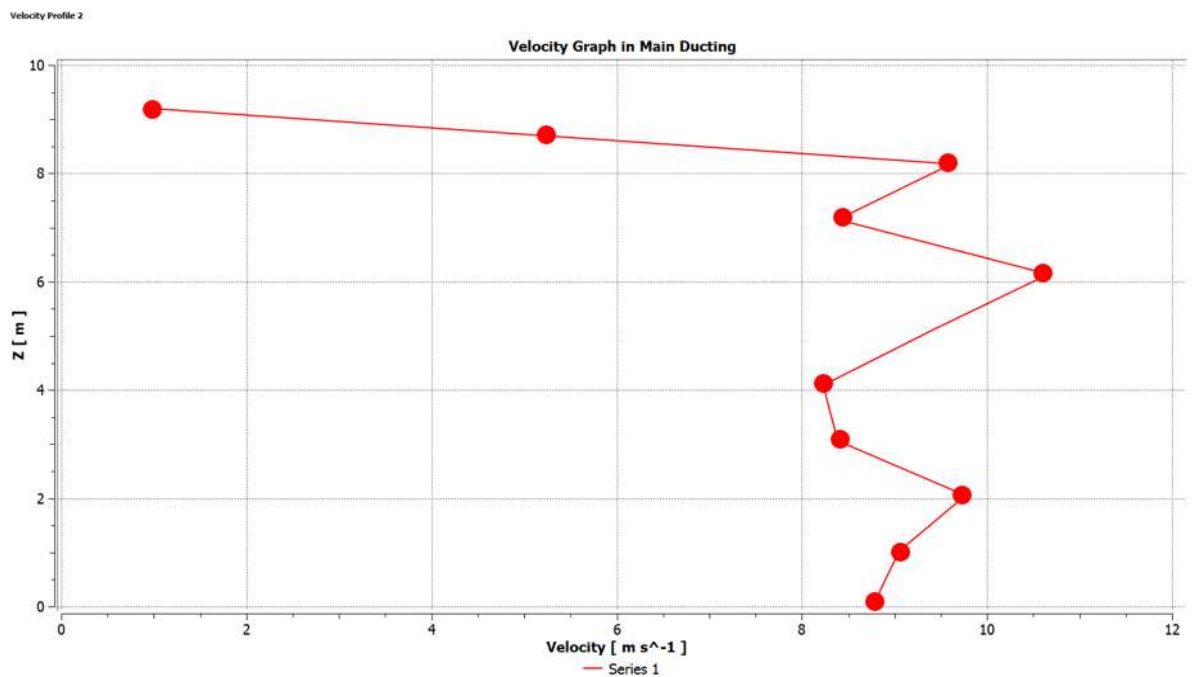
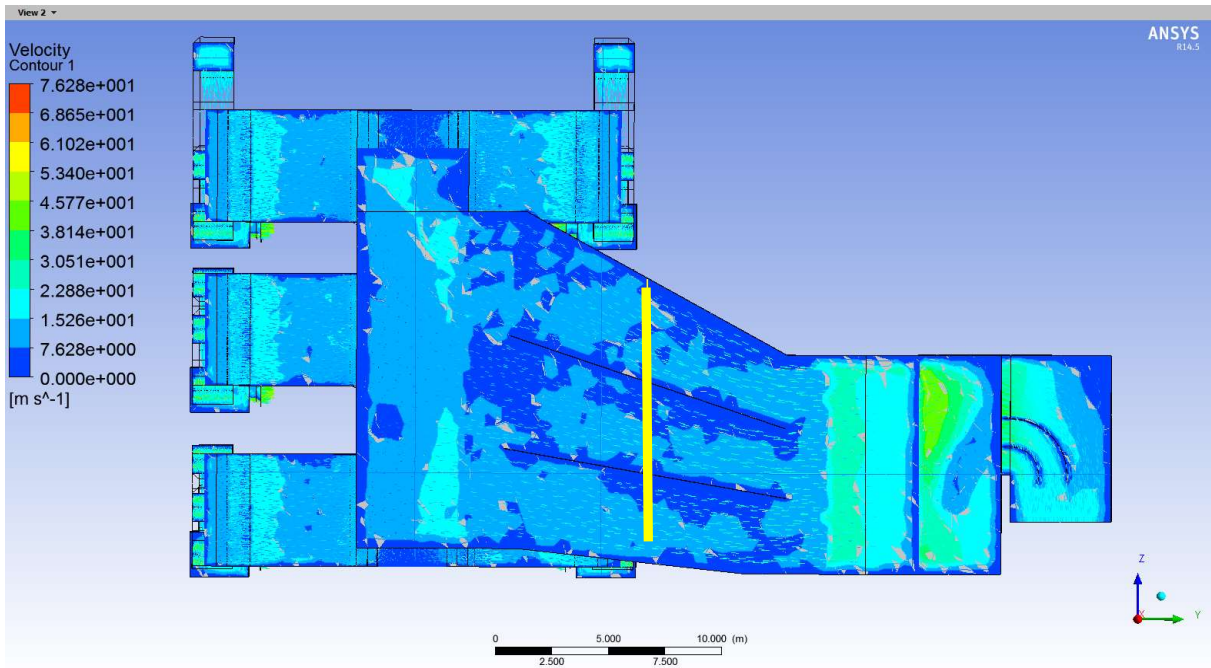


Figure 6.8: Iso-velocity diagram in the main ducting

The velocity profile in the main ducting at the location shown by the yellow line in Figure 6.8 is illustrated on the XY axis where Z is the vertical distance from 0 to 10 m with respect to the yellow line across the main ducting. In effect, the velocity at the points along the yellow line varies from 1 to 12.5 m/s. The highest point on the yellow line has the velocity of 1 m/s and the centre point is 9.7 m/s.

6.2 Discussion

The sensitivity study that was conducted to determine the level of mesh needed also included additional local refinement in areas that have higher rates of change in the solution, such as the velocity of the air flow in the secondary air duct. It was found that the results from the air flow simulation in the main duct were not as accurate when using the coarse mesh, compared to those when using the medium and fine mesh.

The results using a coarse mesh were significantly different from the medium mesh ones, whereas there was no change when changing from medium to fine meshing. The results were converging, and this gave an indication that accurate results have been simulated for the air flow system.

The velocity of the air flow simulated in the distribution ducts supplied to the burners, (that is critical for the combustion process) was found to be in the range of 22.8 to 30.51 m/s during full load operation. However, there is a lot of turbulence in the main air duct due to internal flow guide plates separating the flows to the distribution ducts supplying the burners. The CFD results indicated that the ideal location for measurement points necessary for an analysis of the air flow required for combustion, is in the distribution duct because of the high level of turbulence that could be better controlled. Measurements can be taken as well on the main duct to investigate any eventual internal structure obstructions that can affect the required air flow for the combustion process. An insufficient secondary air supply contributes to very poor combustion, resulting in PF coal waste and loss of heat energy for steam generation.

Figure 6.9 illustrates the measurement points on the secondary air ducting system that resulted from the flow simulation.

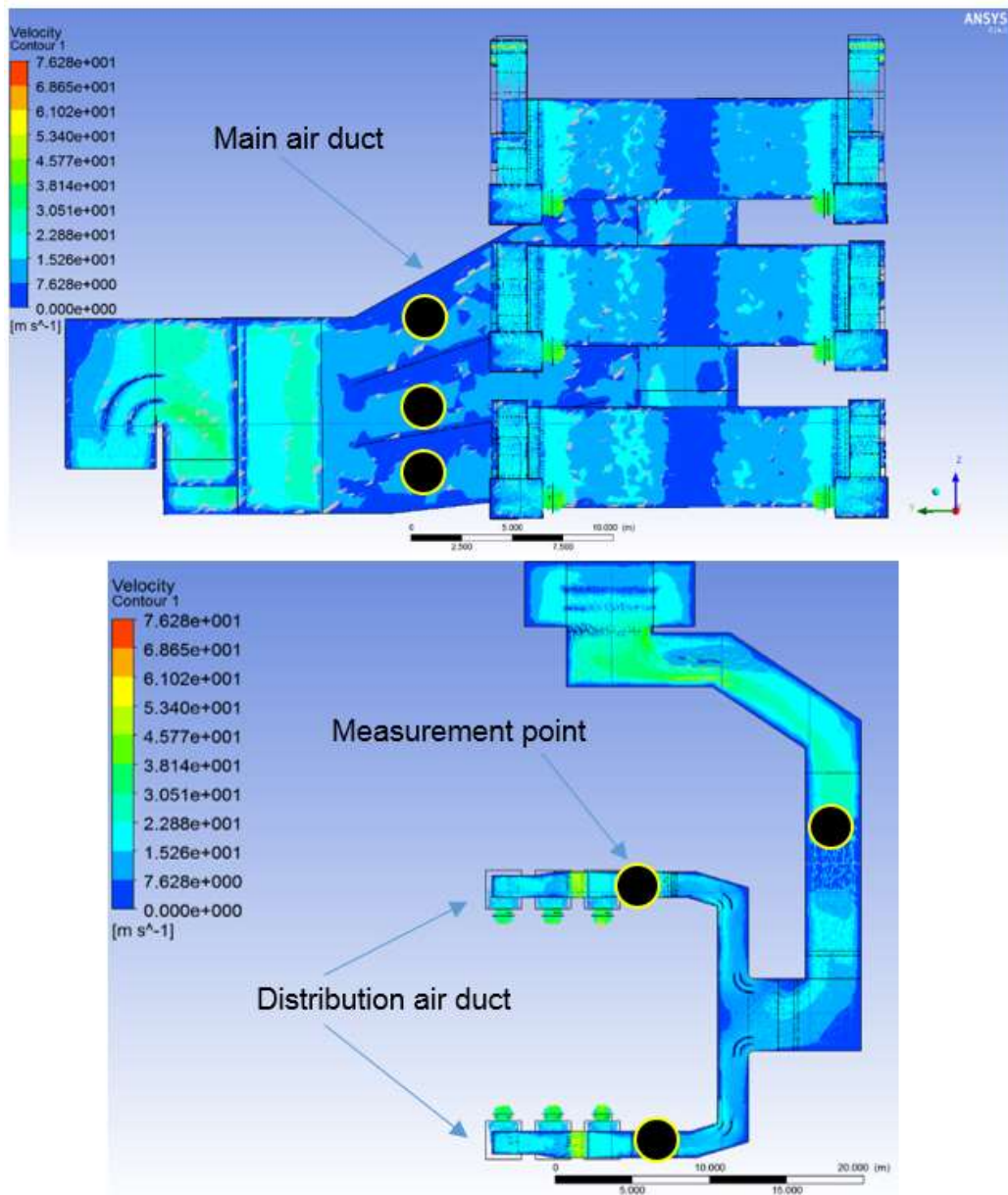


Figure 6.9: Measurement points for the analysis of secondary air flow

7. CONCLUSIONS, RECOMMENDATIONS AND FUTURE STUDY

7.1 Conclusions

The primary objective of this study was to determine the heat rate of the plant using measurements and MEB calculations. An additional goal of the project was to determine with MEB the flue gas and air mass flow rates which also influence the efficiency of the coal power plant. Furthermore, CFD was used for air flow simulation as part of the 3D plant visual system implemented to analyse the flow velocity in the different sections of the secondary air ducts and to identify where useful measurements could be taken.

Initially, the fundamental concepts of the boiler and its auxiliaries were studied to lay the foundations of the coal, air and flue gas systems in a coal-fired boiler plant. From literature survey emerged that coal consumption is defined as a critical indicator of plant performance in terms of cost and efficiency. The different methods used for flow measurements (coal, air and flue gas) in a coal-fired boiler plant, MEB and CFD were further reviewed. The MEB method was used to determine coal, air, and flue gas mass flow rates and the plant's heat rate. Furthermore, CFD was used for air flow visualization and optimization in the secondary air system. The air flow in the secondary ducting system (extracted from the 3D plant layout) was simulated with CFD, using ANSYS Fluent. This was done in order to visualize the velocity of the air flow in each section of the ducting system and at burners' exits. As part of the simulation process, the type of mesh used was tetrahedral, and the simulation calculation was done using a continuity, momentum and energy equations solver. The simulation process was done gradually using coarse, medium and fine mesh sizes with respect to the boundaries of the secondary air duct, which has an inlet located at the air heater's exit and 18 outlets, each supplying 18 burners.

The velocity of the air in the distribution ducts (supplied to the burners) is critical for the fuel (PF coal) mixture ratio during the combustion process. It was found to be in the range from 22.8 to 30.51 m/s during operation under full load. There was significant turbulence in the main air duct due to internal flow guide plates separating the flows to the distribution ducts supplying the burners. The CFD indicated that the ideal location for measurement points necessary for the analysis of the air flow required for combustion, is the distribution duct. Measurements can be taken as well on the main duct to investigate any eventual internal structure obstructions that can affect the required air flow for the combustion process, as insufficient secondary air supply contributes to very poor combustion, PF coal waste and loss of heat energy for steam generation.

In effect, the MEB method was used to establish a coherent set of input and output data for the boiler, as well as to troubleshoot the existing data of the coal-fired power plant. The MEB, which primarily focused on the calculation of coal, air and flue gas mass flow rates, was studied in detail, and expanded to allow reliable results. The entire MEB method was applied using actual plant data extracted from the plant's operating control system, and the MEB results were further analysed with the plant's C-Schedule to determine if the plant is performing as per technical specifications. The plant's coal consumption and heat rate results were calculated by means of a Mathcad model that was developed using boiler MEB methodology.

However, it was found that there was between 5.46% to 13.69% difference in the coal's mass flow rates extracted from the ETRAPRO control system and those obtained from the mass balance calculations. The mass flow rate of coal is supplied by the five mills to the boiler unit, when the plant operates at full load. The mass flow rate of coal obtained from the MEB calculation was between 10.32 to 13.16% more than the values indicated in the C-Schedule/Plant specification, due to many factors such as overall plant efficiency and measurement variations.

This variation was further analysed with a sensitivity study to increase awareness which of the output parameters such as coal mass flow rate were sensitive to variations of the inputs. This was done by varying the input parameters to the model independently, one at a time, and observing the impact on the outputs. Using the Mathcad model and Excel program, the changes in an output variable as a result of independent changes in input variables were then ranked to determine the most sensitive parameters. In the case of the sensitivity analysis, a $\pm 1\%$ variation was applied to each of the input parameters. Although the sensitivity analysis provides understanding of how sensitive the outputs are relative to the variation of the inputs, it did not account for what the actual uncertainties of the inputs are, which may be less or even more than $\pm 1\%$. As result of the sensitivity analysis, it was found that the variation in the mass flow rate of coal at 520.56 MW full load was 80.254 +/- 1.545 kg/s. The air and flue gas mass flow rate variations were 541.145 +/- 8.431 kg/s, and 611.68 +/- 10.823 kg/s respectively. The MEB has proven that it is a very important tool for the analysis of the plant's performance based on the actual input parameters and the design specifications. Since the outputs from the MEB method are key indicators for plant performance, they can be used to advise the power plant operators on heat rate and fuel consumption, which affect enormously the operation costs.

7.2 Recommendation and future project

Future work arising from this research study could comprise the following:

1. The entire MEB methodology should be applied to develop standard models for coal power stations of different load configurations.
2. The MEB method can be applied to the new supercritical boilers, utilising measurements of temperature of the furnace's walls to better determine the heat transfer
3. Further improvements to the CFD model for the power plant that could be done:
 - Include the effect of heat transfer between air and flue gas through the rotary air heater.
 - The secondary air flow through the coal burner
 - Flue gas flow across boiler tubes during steam generation

The topics suggested above and the outcomes of these investigations can form part of EPPEI's inter-university project to improve overall plant condition monitoring.

8. BIBLIOGRAPHY

- ABB, 2018. *Coal Flow Online Measurement*, s.l.: Powergen.
- ANSYS, 2015. *ANSYS Theory Guide*. 14.0 ed. s.l.:s.n.
- ASME, 2010. *Air Heaters, Flue and Exhaust Analysis*. PTC.
- Baylar, A., Cihan, A., Mehmet, U. & Fahri, O., 2009. *Numerical modeling of venturi flows for determining air injection rates using FLUENT V6. 2. Mathematical and Computational Applications*,14(2),97-108, Elazig, Turkey: ASR.
- Bhatt, S., 2007. *Effect of air ingress on the energy performance of coal fired thermal power plants*. s.l., Energy Conservation.
- Bhatt, S. & Rajkumar, N., 2015. EFFECT OF SURFACE MOISTURE COAL ON UNIT HEAT RATE AND OPERATING COSTS FOR INDINA THERMAL POWER PLANTS. *Central Power Research Institute*.
- Blondeau, J. et al., 2016. *Online monitoring of coal particle size and flow distribution in coal-fired power plants: Dynamic effects of a varying mill classifier speed*. *Applied Thermal Engineering*,98,449-454 ed. s.l.:s.n.
- Briggs, B., 2015. The Factor That Impact Venturi Meter Accuracy, Primary Signal. <http://www.primaryflowsignal.com/images/stories/whitepapers/PFS White paper Venturi Meter Accuracy.pdf> [2 April 2018].
- Constenla, I., Ferrin, J. & Saavedra, L., 2013. Numerical study of a 350MW tandentially fired pulverized coal furnace of the A Pontes Power Plant. *Elsevier-Fuel Processing Technology*, pp. 116,189-200.
- Edward, L., 2009. *REDUCING HEAT RATES OF COAL-FIRED POWER PLANTS*, s.l.: Lehigh Energy.
- Eskom Power Plant Boiler, E., 2010. *Boiler Mass and Energy Balances Guideline and user Manual-V1.15*, Sunninghill: Eskom Generation Business Engineering.
- ESKOM, 2012. *Fossil Fuel Fire Regulations edn, Coal Fired Stations*.
- ESKOM, 2016. *HOW ELECTRICITY IS PRODUCED AT A COAL FIRED STATION*. JOHANNESBURG: ESKOM Fact Sheet.
- ESKOM, 2016. *HOW ELECTRICITY IS PRODUCED AT A COAL FIRED STATION*. Johannesburg, ESKOM Fact Sheet.
- ESKOM, 2018. *COAL- FIRED POWER PLANT SITE VISIT*. s.l., ESKOM FACT SHEET.
- EUREKA, 2018. *Aerfoil for industrial applications*. Powegen.
- Ferreira, D., Cardoso, M. & Park, S., 2010. *Gas flow analysis in a Kraft recovery boiler*, Madrid: Elsevier.
- Gordon, L., 2016. *Basic principles and design of industrial Thermocouples*. *EDN Network*.

- Halstrup, W., 2017. Pitot tube for industrial applications. *Stegener Strabe*.
- Huang, B. & Haichun, Z., 2015. Online monitoring of coal particle size and flow distribution in coal-fired power plants. *Elsevier*, pp. 449-454.
- Huang, B., Zixue, L. & Huaichun, Z., 2010. Optimization of combustion based on introducing radiant energy signal in pulverized coal-fired boiler. *Elsevier*, pp. 660-668.
- Innami, Y., Murata, A., Yuki, Y. & Yoshimura, E., 2011. *Real-time CO measurement in a coal fired boiler with a TDLS analyser*. Tokyo, SICE Annual Conference (SICE), 2011 pp.92-96.
- Jashuva, N., Mallikarjuna, V. & Rama Bhupal, B., 2014. IMPROVING BOILER EFFICIENCY BY USING AIR PREHEATER. *International Journal of Advanced Research in Engineering and Applied Sciences*, Issue ISSN:2278-6252.
- Jing, X., Yujiong, G., Dongchao, C. & Qianqian, L., 2017. Data mining based plant-level load dispatching strategy for the coal-fired power plant coal-saving. *Elsevier*, pp. 553-559.
- Klein, A., 2013. *An Improved Concept for Online Coal Analysis*. Istanbul, Proceedings of the 17th International Coal Preparation Congress.
- Kulkani, S., Craig, C. & Hanifa, S., 2016. *Computational Fluid Dynamics (CFD) Mesh Independency Study of A Straight Blade Horizontal Axis Tidal Turbine*, Birmingham: Birmingham City University.
- Lin, C., Rosendahl, L. & Condra, T., 2003. Further study of the gas temperature deviation in large-scale tangentially coal-fired boilers. *Fuel*, pp. 1127-1137.
- Matthews, 2016. How to measure pressure and flow. https://www.tsi.com/getmedia/668b4c26-9783-4bc8-9dd3-c921b557bf71/how_to_determine_air_flow?ext=.pdf. [10 April 2018].
- Miltner, M., Miltner, A., Harasek, M. & Friedl, A., 2007. Process simulation and CFD calculations for the development of the innovative bale biomass-fired combustion chamber. *Applied Thermal Engineering*, pp. 1138-1143.
- Naeem, E., 2015. *Investigation into methods for the calculations and measurement of pulverised coal boiler flue gas exit temperature*, Cape Town: University of Cape Town.
- Palmqvist, O., 2012. *Dynamic Modelling of Heat Transfer in a Supercritical Steam Power Plant*. Goteborg: Chalmers University.
- Ramulu, J. T., 2017. Implementation of Gravimetric Control System for Efficient Coal Feeding in Thermal Power Plants. *JSERBR*, pp. 507-512.
- Rodriguez, F. et al., 2014. *Performance Monitoring and Combustion Optimization Technologies to Reduce Emissions and Enhance Boiler Efficiency*, Johannesburg: Powergen-Africa.
- Rousseau, P. & Fuls, W., 2018. *Power Plant System Analysis*, Cape Town: University of Cape Town.
- Sabin, B., 2016. 4 Key measurements for optimal boiler control. *Flow Control Solutions for Fluid Movement, Measurement & Containment*. Available:

<https://www.flowcontrolnetwork.com/4-key-measurements-for-optimal-boiler-control/>. [10 March 2018].

Sargent, L., 2009. *COAL-FIRED POWER PLANT HEAT RATE REDUCTIONS*, Chicago: SL-009597.

Schena, E., Stefano, C. & Sergio, S., 2013. *An orifice meter for bidirectional air flow measurement: Influence of gas thermo-hygrometric content on static response and bidirectionality*. Rome, Elsevier.

Scholtz, K. B., 2016. *Optimisation of Solid Rocket Motor Blast Tube and Nozzle Assemblies using Computational Fluid Dynamics*, Bellville: CPUT.

Sharler, R. et al., 2004. *Advanced CFD Analysis of Large Fixed Bed Biomass Boilers with Special Focus on the Convective Section*. Rome: Biomass Energy.

Shuk, P., 2010. Process Zirconia Oxygen Analyser measuring Technology. *Technisches Messen*.

Staudt, J. & Macedonia, J., 2014. *Evaluation of Heat Rates of coal Fired electric Power Boilers*, Baltimore: MEGA.

Suresh, G., Francesco, T., Reinhardt, K. & Michael, H., 2012. Online Coal Flow Measurement System for Combustion Optimisation in a Thermal Boiler. *CPRI*.

Tootla, N., 2015. *Investigation into methods for the calculation and measurement of pulverised coal boiler flue gas exit temperature*, Cape Town: University of Cape Town.

Usman, M., 2007. Simulation Model of Flue Gas Condensation Unit And Complete Process Plant Simulation"Case Study of ENA Energy". *Malarden University*.

Versteeg, H. & Malalasekera, W., 2007. *An Introduction to Computational Fluid Dynamics: the Finite Volume Method*, India: Pearson Education.

Walsh, K., Lesneski, D., Carl, T. & Jay, R., 2015. *Analysis of Heat Rate Improvement Potential at Coal-Fired Power Plants*, s.l.: Energy Information Administration:<https://www.eia.gov/analysis/studies/powerplants/heatrate/pdf/heatrate.pdf>. [8 February 2018].

Yang, Y. et al., 2007. Mathematical modelling of coal combustion in 38MWe power plant furnace and effect of operating conditions. *Fuel*, pp. 129-142.

9. APPENDIX / APPENDICES

APPENDIX A: MEB-MATHCAD CALCULATIONS

Reference: C:\Users\andr\Desktop\MathCAD UCT\MathCAD\Water-Steam IAPWS-IF97 rev 1.0.xmcd

MEB Calculations - @ FULL LOAD 520.56 MW

Coal Analysis Parameters-Air Dried Basis:

	<u>% in Coal</u>
Inherent Moisture:	$\%IM_{ad} := 5.1\%$
Ash:	$\%Ash_{ad} := 40.4\%$
Carbon :	$\%C_{ad} := 38.9\%$
Hydrogen :	$\%H_{ad} := 1.97\%$
Oxygen :	$\%O_{ad} := 8.36\%$
Nitrogen :	$\%N_{ad} := 0.95\%$
Sulphur :	$\%S_{ad} := 1.1\%$
Calorific Value:	$CV_{ad} := 15.64 \cdot 10^6 \frac{J}{kg}$
Surface Moisture:	$\%SM_{ad} := 7.52\%$
Specific Heat Capacity:	$Cp_{coal} := 1.38 \frac{10^3 J}{kg}$

Coal Analysis Parameters-As received:

$$\begin{aligned} \text{Total Moisture: } TM &:= \%SM_{ad} + \%IM_{ad} & M_{ad} &:= \%IM_{ad} \\ X_C &:= \%C_{ad} \cdot \left(\frac{100 - TM}{100 - M_{ad}} \right) = 38.871\% & X_i &:= TM \cdot \left(\frac{100 - TM}{100 - M_{ad}} \right) \\ X_{Ash} &:= \%Ash_{ad} \cdot \left(\frac{100 - TM}{100 - M_{ad}} \right) = 40.37\% \\ X_{moist} &:= TM \cdot \left(\frac{100 - TM}{100 - M_{ad}} \right) = 12.611\% \\ CV_{Coal} &:= CV_{ad} \cdot \left(\frac{100 - TM}{100 - M_{ad}} \right) = 15.628 \cdot \frac{10^6 J}{kg} \end{aligned}$$

$$X_H := \%H_{ad} = 1.97\%$$

$$X_N := \%N_{ad} = 0.95\%$$

$$X_S := \%S_{ad} = 1.1\%$$

$$X_O := 100\% - X_C - X_{Ash} - X_{moist} - X_H - X_N - X_S = 4.129\%$$

Coal HHV (High heating Value):

$$f_{NOX} := 30\%$$

$$Q_f := \begin{pmatrix} 32765 \\ 119959 \\ -6446 \cdot f_{NOX} \\ 9256 \end{pmatrix} \frac{kJ}{kg} \quad Q_{lat} := \begin{pmatrix} 0 \\ 21820 \\ 0 \\ 0 \end{pmatrix} \frac{kJ}{kg} \quad X_n := \begin{pmatrix} X_C \\ X_H \\ X_N \\ X_S \end{pmatrix}$$

$$HHV := \sum_{i=1}^3 [(Q_f)_i + (Q_{lat})_i] \cdot X_{n,i} = 15.612 \times 10^3 \frac{kJ}{kg}$$

$$\text{Fly Ash: } \%f_{Ash} := 80\%$$

$$\text{Bottom Ash: } \%b_{Ash} := 20\%$$

Unburnt Carbon in fly Ash:

$$\%C_{fa} := 3.4\%$$

Unburnt Carbon in bottom Ash:

$$\%C_{ba} := 3.4\%$$

MASS BALANCE

Combustion products

Mass of Unburnt Carbon kg/kg Coal

$$m_{fC} := X_{Ash} \cdot [(\%C_{fa} \cdot \%f_{Ash}) + (\%C_{ba} \cdot \%b_{Ash})] = 0.014 \frac{kg}{kg}$$

Mass of unburnt Carbon per kg of Carbon

$$m_{fCC} := \frac{m_{fC}}{X_C} = 0.035 \frac{kg}{kg}$$

Energy in unburnt Carbon per KJ of Energy input

$$\text{Carbon Calorific Value: } CV_C := 32780.32 \frac{10^3 J}{kg}$$

$$mf_{CCC} := \frac{CV_C \cdot X_C \cdot mf_C}{CV_{Coal}} = 0.0112 \cdot \frac{kg}{kg}$$

Theoretical Air Required/Stoichiometric air fuel ratio (Kg Air/Kg Fuel)

$$St := \begin{pmatrix} 1 \\ \frac{1}{4} \\ -\frac{1}{2} \\ \frac{1}{2} f_{NOX} \\ 1 \end{pmatrix} \begin{pmatrix} C \\ H \\ O \\ N \\ S \end{pmatrix} = \begin{pmatrix} 0 \\ 1 \\ 2 \\ 3 \\ 4 \end{pmatrix}$$

$$M_{air} := 28.958 \frac{10^{-3} kg}{mol}$$

$$y_{O2air} := 0.2096$$

Coal composition Molar Mass

$$M_{co} := \begin{pmatrix} 12 \\ 1 \\ 16 \\ 14 \\ 32 \end{pmatrix} \cdot 10^{-3} \frac{kg}{mol} \begin{pmatrix} C \\ H \\ O \\ N \\ S \end{pmatrix}$$

Combustion Products Molar Mass

$$M_{cp} := \begin{pmatrix} 44.01 \\ 32 \\ 28 \\ 18 \\ 64 \\ 46 \\ 28.958 \\ 39.948 \end{pmatrix} \cdot \frac{10^{-3} kg}{mol} \begin{pmatrix} CO2 \\ O2 \\ N2 \\ H2O \\ SO2 \\ NO2 \\ Air \\ Arg \end{pmatrix} = \begin{pmatrix} 0 \\ 1 \\ 2 \\ 3 \\ 4 \\ 5 \\ 6 \\ 7 \end{pmatrix}$$

$$X := \begin{pmatrix} X_C \\ X_H \\ X_O \\ X_N \\ X_S \end{pmatrix}$$

$$TAR_1 := \frac{M_{air}}{y_{O2air}} \cdot \sum_{i=0}^4 \left(St_i \cdot \frac{X_i}{M_{co_i}} \right) = 5.039 \cdot \frac{kg}{kg}$$

$$TAR_2 := [11.51 \cdot X_C + 34.29 \cdot X_H - 4.32 \cdot X_O + 4.31 \cdot X_S + (4.932 \cdot f_{NOX} \cdot X_N)] = 5.033 \cdot \frac{kg}{kg}$$

$$TAR_2 := \left[11.51 \cdot X_C + 34.29 \cdot X_H - 4.32 \cdot X_O + 4.31 \cdot X_S + (4.932 \cdot f_{NOX} \cdot X_N) \right] = 5.033 \cdot \frac{kg}{kg}$$

The highest TAR is used for further calculation

$$TAR := TAR_1 = 5.039 \cdot \frac{kg}{kg}$$

Excess Air Required

$$\%O2_{AHfginlet} := 4.08\% \quad \%mO2_{air} := 23\%$$

$$P_{ratio} := 1.032$$

$$f_{EA} := \frac{TAR + 1 - X_{Ash}}{TAR} \cdot \frac{\%O2_{AHfginlet}}{\frac{\%mO2_{air}}{P_{ratio}} - \%O2_{AHfginlet}} = 25.061\%$$

Dry Air Required (Kg air/Kg coal)

$$DAR := TAR \cdot (1 + f_{EA}) = 6.302 \cdot \frac{kg}{kg}$$

Humid Air required

$$HAR := (1 + \omega) \cdot DAR = 6.743 \cdot \frac{kg}{kg}$$

$$\omega := 7\%$$

Mass flow rate of Flue gas (Kg air/Kg coal)

$$m_{fg} := (1 - X_{Ash}) - mf_C + HAR = 7.325 \cdot \frac{kg}{kg}$$

Flue gas composition by mass:

$$m_{CO2fg} := \frac{M_{cpCO2}}{M_{coC}} \cdot (X_C - mf_C) = 1.375 \cdot \frac{kg}{kg}$$

$$y_{N2air} := 0.7812$$

$$y_{Arair} := 0.0092$$

$$m_{N2fg} := (1 - \%mO2_{air}) \cdot DAR + 0.7 \cdot \left(\frac{1}{2}\right) \cdot X_N = 4.856 \cdot \frac{kg}{kg}$$

$$M_{Arg} := 39.948 \cdot 10^{-3} \frac{kg}{mol}$$

$$f_{BA} := 30\%$$

$$m_{H2Ofg} := X_{moist} + \omega \cdot DAR + \frac{2 \cdot M_{cpH2O}}{4 \cdot M_{coC}} \cdot X_H = 0.582 \cdot \frac{kg}{kg}$$

$$Cp_{FA} := 0.73 \frac{kJ}{kg \cdot K}$$

$$m_{SO_2fg} := \frac{M_{cp_{SO_2}}}{M_{co_S}} \cdot X_S = 0.022 \cdot \frac{kg}{kg}$$

$$C_{p_{UC}} := 0.71 \frac{kJ}{kg \cdot K}$$

$$m_{NO_2fg} := \frac{0.3 M_{cp_{NO_2}}}{M_{co_N}} \cdot X_N = 9.364 \times 10^{-3} \cdot \frac{kg}{kg}$$

$$M_{NO} := 30 \cdot 10^{-3} \frac{kg}{mol}$$

$$m_{NOfg} := f_{NOX} \cdot \left(\frac{X_N}{M_{co_N}} \right) \cdot M_{NO} = 6.107 \times 10^{-3} \cdot \frac{kg}{kg}$$

$$m_{UCfg} := m_{fC}$$

$$m_{FAfg} := X_{Ash} \cdot (1 - f_{BA}) = 0.283 \cdot \frac{kg}{kg}$$

$$m_{Arfg} := DAR \cdot y_{Ar_{air}} \cdot \frac{M_{Arg}}{M_{air}} = 0.08 \cdot \frac{kg}{kg}$$

$$m_{O_2fg} := m_{fg} - m_{CO_2fg} - m_{N_2fg} - m_{H_2Ofg} - m_{SO_2fg} - m_{NO_2fg} - m_{UCfg} - m_{FAfg} - m_{Arfg}$$

$$m_{O_2fg} = 0.105 \cdot \frac{kg}{kg}$$

Flue gas constituent by mass %

$$X_{CO_2fg} := \frac{m_{CO_2fg}}{m_{fg}} = 18.773\%$$

$$X_{N_2fg} := \frac{m_{N_2fg}}{m_{fg}} = 66.285\%$$

$$X_{H_2Ofg} := \frac{m_{H_2Ofg}}{m_{fg}} = 7.945\%$$

$$X_{SO_2fg} := \frac{m_{SO_2fg}}{m_{fg}} = 0.3\%$$

$$X_{O_2fg} := \frac{m_{O_2fg}}{m_{fg}} = 1.432\%$$

$$X_{NO_2fg} := \frac{m_{NO_2fg}}{m_{fg}} = 0.128\%$$

$$X_{NOfg} := \frac{m_{NOfg}}{m_{fg}} = 0.083\%$$

$$X_{\text{Argfg}} := \frac{m_{\text{Argfg}}}{m_{\text{fg}}} = 1.092\%$$

$$X_{\text{UCfg}} := \frac{m_{\text{UCfg}}}{m_{\text{fg}}} = 0.187\%$$

$$X_{\text{FAfg}} := \frac{m_{\text{FAfg}}}{m_{\text{fg}}} = 3.858\%$$

$$FGR := HAR + 1 - X_{\text{Ash}} J_{\text{BA}} = 7.622 \quad (\text{kg fue gas/kg coal})$$

Flue gas composition by volume m³/kg coal:

$$V_{\text{CO2fg}} := \frac{m_{\text{CO2fg}}}{M_{\text{cp CO2}}} \cdot 22.4 \frac{\text{kg}}{10^3 \text{ mol}} = 0.7$$

$$V_{\text{N2fg}} := \frac{m_{\text{N2fg}}}{M_{\text{cp N2}}} \cdot 22.4 \frac{\text{kg}}{10^3 \text{ mol}} = 3.885$$

$$V_{\text{H2Ofg}} := \frac{m_{\text{H2Ofg}}}{M_{\text{cp H2O}}} \cdot 22.4 \frac{\text{kg}}{10^3 \text{ mol}} = 0.724$$

$$V_{\text{SO2fg}} := \frac{m_{\text{SO2fg}}}{M_{\text{cp SO2}}} \cdot 22.4 \frac{\text{kg}}{10^3 \text{ mol}} = 7.7 \times 10^{-3}$$

$$V_{\text{NO2fg}} := \frac{m_{\text{NO2fg}}}{M_{\text{cp NO2}}} \cdot 22.4 \frac{\text{kg}}{10^3 \text{ mol}} = 4.56 \times 10^{-3}$$

$$V_{\text{O2fg}} := \frac{m_{\text{O2fg}}}{M_{\text{cp O2}}} \cdot 22.4 \frac{\text{kg}}{10^3 \text{ mol}} = 0.073$$

$$V_{\text{fg}} := V_{\text{CO2fg}} + V_{\text{N2fg}} + V_{\text{H2Ofg}} + V_{\text{SO2fg}} + V_{\text{NO2fg}} + V_{\text{O2fg}} = 5.394$$

ENERGY BALANCE

Flue Gas Input Data

$$T_{fg,AH,inlet} := 303.614 \text{ } ^\circ\text{C}$$

$$T_{fg,AH,outlet} := 142.583 \text{ } ^\circ\text{C}$$

Flue Gas Enthalpy

$$T_{ref} := 0.01 \text{ } ^\circ\text{C}$$

$$C_{pw} := 4.183 \frac{\text{kJ}}{\text{kg}\cdot\text{K}}$$

$$C_{CO2} := \begin{pmatrix} 8.437 \cdot 10^{-1} \\ 4.258 \cdot 10^{-4} \\ -1.705 \cdot 10^{-7} \\ 2.819 \cdot 10^{-11} \end{pmatrix} \quad C_{O2} := \begin{pmatrix} 8.974 \cdot 10^{-1} \\ 1.994 \cdot 10^{-4} \\ -7.432 \cdot 10^{-8} \\ 1.255 \cdot 10^{-11} \end{pmatrix} \quad C_{N2} := \begin{pmatrix} 1.015 \cdot 10^0 \\ 1.037 \cdot 10^{-4} \\ 5.452 \cdot 10^{-9} \\ -6.693 \cdot 10^{-12} \end{pmatrix}$$

$$C_{SO2} := \begin{pmatrix} 6.426 \cdot 10^{-1} \\ 1.85 \cdot 10^{-4} \\ 0 \\ 0 \end{pmatrix} \quad C_{Arg} := \begin{pmatrix} 5.205 \cdot 10^{-1} \\ 0 \\ 0 \\ 0 \end{pmatrix} \quad C_{NO} := \begin{pmatrix} 8.861 \cdot 10^{-1} \\ 3.263 \cdot 10^{-4} \\ 0 \\ 0 \end{pmatrix}$$

$$\overset{Tx}{\Delta T} := T_{fg,AH,inlet} - T_{ref}$$

$$h_{CO2} := \left[C_{CO2_0} \frac{Tx}{K} + C_{CO2_1} \left(\frac{Tx}{K} \right)^2 + C_{CO2_2} \left(\frac{Tx}{K} \right)^3 + C_{CO2_3} \left(\frac{Tx}{K} \right)^4 \right] \cdot \frac{\text{kJ}}{\text{kg}} = 290.867 \cdot \frac{\text{kJ}}{\text{kg}}$$

$$h_{SO2} := \left[C_{SO2_0} \frac{Tx}{K} + C_{SO2_1} \left(\frac{Tx}{K} \right)^2 + C_{SO2_2} \left(\frac{Tx}{K} \right)^3 + C_{SO2_3} \left(\frac{Tx}{K} \right)^4 \right] \cdot \frac{\text{kJ}}{\text{kg}} = 212.148 \cdot \frac{\text{kJ}}{\text{kg}}$$

$$h_{NO} := \left[C_{NO_0} \frac{Tx}{K} + C_{NO_1} \left(\frac{Tx}{K} \right)^2 + C_{NO_2} \left(\frac{Tx}{K} \right)^3 + C_{NO_3} \left(\frac{Tx}{K} \right)^4 \right] \cdot \frac{\text{kJ}}{\text{kg}} = 299.1 \cdot \frac{\text{kJ}}{\text{kg}}$$

$$h_{O2} := \left[C_{O2_0} \frac{Tx}{K} + C_{O2_1} \left(\frac{Tx}{K} \right)^2 + C_{O2_2} \left(\frac{Tx}{K} \right)^3 + C_{O2_3} \left(\frac{Tx}{K} \right)^4 \right] \cdot \frac{\text{kJ}}{\text{kg}} = 288.861 \cdot \frac{\text{kJ}}{\text{kg}}$$

$$h_{N2} := \left[C_{N2_0} \frac{Tx}{K} + C_{N2_1} \left(\frac{Tx}{K} \right)^2 + C_{N2_2} \left(\frac{Tx}{K} \right)^3 + C_{N2_3} \left(\frac{Tx}{K} \right)^4 \right] \cdot \frac{\text{kJ}}{\text{kg}} = 317.812 \cdot \frac{\text{kJ}}{\text{kg}}$$

$$h_{H2O} := C_{pw} \cdot T_{fg.AH.inlet} = 2.413 \times 10^3 \cdot \frac{kJ}{kg}$$

$$h_{Arg} := \left[C_{Arg0} \frac{T_x}{K} + C_{Arg1} \left(\frac{T_x}{K} \right)^2 + C_{Arg2} \left(\frac{T_x}{K} \right)^3 + C_{Arg3} \left(\frac{T_x}{K} \right)^4 \right] \cdot \frac{kJ}{kg} = 158.026 \cdot \frac{kJ}{kg}$$

$$\begin{array}{l} \left(\begin{array}{c} h_{CO2} \\ h_{SO2} \\ h_{NO} \\ h_{O2} \\ h_{N2} \\ h_{H2O} \\ h_{Arg} \\ h_{UC} \\ h_{FA} \end{array} \right) \\ X_{fg} := \end{array} \quad \begin{array}{l} \left(\begin{array}{c} X_{CO2fg} \\ X_{SO2fg} \\ X_{NOfg} \\ X_{O2fg} \\ X_{N2fg} \\ X_{H2Ofg} \\ X_{Argfg} \\ X_{UCfg} \\ X_{FAfg} \end{array} \right) \\ H_{fg} := \end{array} \quad \begin{array}{l} h_{UC} := C_{pUC} \cdot T_{fg.AH.inlet} = 409.502 \cdot \frac{kJ}{kg} \\ h_{FA} := C_{pFA} \cdot T_{fg.AH.inlet} = 421.038 \cdot \frac{kJ}{kg} \end{array}$$

$$h_{fg} := \sum_{i=0}^8 (X_{fg_i} \cdot H_{fg_i}) = 480.704 \cdot \frac{kJ}{kg}$$

$$C_{pfg} := \frac{h_{fg}}{T_x} = 1.583 \cdot \frac{kJ}{kg \cdot K}$$

$$T_{fe} := T_{fe.AH.inlet}$$

Flue Gas enthalpy using Cp: $\int_{T_{ref}}^{T_{fg}} C_{pfg} dT_{fg}$

$$h_{fg.AH.inlet} := \left(\int_{T_{ref}}^{T_{fg}} C_{pfg} dT_{fg} \right) = 480.704 \cdot \frac{10^3 J}{kg}$$

Air Input Data & Enthalpies

Air enthalpies coefficients :

$$T_{amb} := 28 \text{ (}^\circ\text{C)}$$

$$\%Air_{ing} := 10\%$$

$$T_{air.AH.outlet} := 291.452 \text{ (}^\circ\text{C)}$$

$$RH := 7\%$$

$$T_{atm} := 25 \text{ }^\circ\text{C}$$

$$C_{air} := \begin{pmatrix} Air \\ 9.816 \cdot 10^{-1} \\ 1.245 \cdot 10^{-4} \\ -1.308 \cdot 10^{-8} \\ -2.154 \cdot 10^{-12} \end{pmatrix}$$

$$T_{ah} := T_{air.AH.outlet}$$

$$\rho_{air} := 1.225 \frac{kg}{m^3}$$

$$h_{T_{amb}} := \left(C_{air_1} \cdot T_{amb} + C_{air_2} \cdot T_{amb}^2 + C_{air_3} \cdot T_{amb}^3 + C_{air_4} \cdot T_{amb}^4 \right) \cdot \frac{10^3 J}{kg} = 27.582 \cdot \frac{kJ}{kg}$$

$$h_{T_{air.AH.outlet}} := \left(C_{air_1} \cdot T_{ah} + C_{air_2} \cdot T_{ah}^2 + C_{air_3} \cdot T_{ah}^3 + C_{air_4} \cdot T_{ah}^4 \right) \cdot \frac{10^3 J}{kg} = 296.325 \cdot \frac{kJ}{kg}$$

$$h_{air.AH.in} := \left[1.006 \cdot T_{amb} + \omega \cdot (2501 + 1.86 \cdot T_{amb}) \right] \cdot \frac{\text{kJ}}{\text{kg}} = 206.884 \cdot \frac{\text{kJ}}{\text{kg}}$$

Water and steam enthalpies

Economiser Feed water

$$P_{fw} := 18.19 \text{ MPa} \quad T_{fw.econ.in} := 226.76 \text{ }^\circ\text{C} \quad T_{fw.econ.out} := 277 \text{ }^\circ\text{C}$$

$$m_{fw.econ.in} := 414.55 \frac{\text{kg}}{\text{s}}$$

Superheater & Superheater attemperator

$$P_{sh.att} := 17.88 \text{ MPa} \quad T_{sh.att} := 249 \text{ }^\circ\text{C} \quad m_{sh.att} := 10.29 \frac{\text{kg}}{\text{s}}$$

$$P_{steam.drum} := 19.02 \text{ MPa} \quad m_{steam} := 427.73 \frac{\text{kg}}{\text{s}}$$

$$P_{steam.sh.out} := 16.37 \text{ MPa} \quad T_{steam.sh.out} := 533.2 \text{ }^\circ\text{C}$$

Re-heater & Re-heater attemperator

$$P_{rh.att} := 4.1 \text{ MPa} \quad T_{rh.att} := 165 \text{ }^\circ\text{C} \quad m_{rh.att} := 10.86 \frac{\text{kg}}{\text{s}}$$

$$P_{steam.rh.out} := 2.89 \text{ MPa} \quad T_{steam.rh.out} := 532.36 \text{ }^\circ\text{C} \quad m_{rh.steam} := 467.995 \frac{\text{kg}}{\text{s}}$$

Enthalpies of steam-water system are determined with reference to the IAPWS-IF97 worksheet

$$h_{fw.econ.in} := h_{steam}(P_{fw}, T_{fw.econ.in}, \text{""}, \text{""}, \text{""}) = 979.128 \cdot \frac{\text{kJ}}{\text{kg}}$$

$$h_{fw.econ.out} := h_{steam}(P_{fw}, T_{fw.econ.out}, \text{""}, \text{""}, \text{""}) = 1.217 \times 10^3 \cdot \frac{\text{kJ}}{\text{kg}}$$

$$h_{sh.att} := h_{steam}(P_{sh.att}, T_{sh.att}, \text{""}, \text{""}, \text{""}) = 1.082 \times 10^3 \cdot \frac{\text{kJ}}{\text{kg}}$$

$$h_{steam.drum} := h_{steam}(P_{steam.drum}, \text{""}, \text{""}, 1, \text{""}) = 2.464 \times 10^3 \cdot \frac{\text{kJ}}{\text{kg}}$$

$$h_{steam.sh.out} := h_{steam}(P_{steam.sh.out}, T_{steam.sh.out}, \text{""}, \text{""}, \text{""}) = 3.389 \times 10^3 \cdot \frac{\text{kJ}}{\text{kg}}$$

$$h_{steam.rh.out} := h_{steam}(P_{steam.rh.out}, T_{steam.rh.out}, \text{""}, \text{""}, \text{""}) = 3.531 \times 10^3 \cdot \frac{\text{kJ}}{\text{kg}}$$

$$h_{rh.att} := h_{steam}(P_{rh.att}, T_{rh.att}, \text{""}, \text{""}, \text{""}) = 699.279 \cdot \frac{\text{kJ}}{\text{kg}}$$

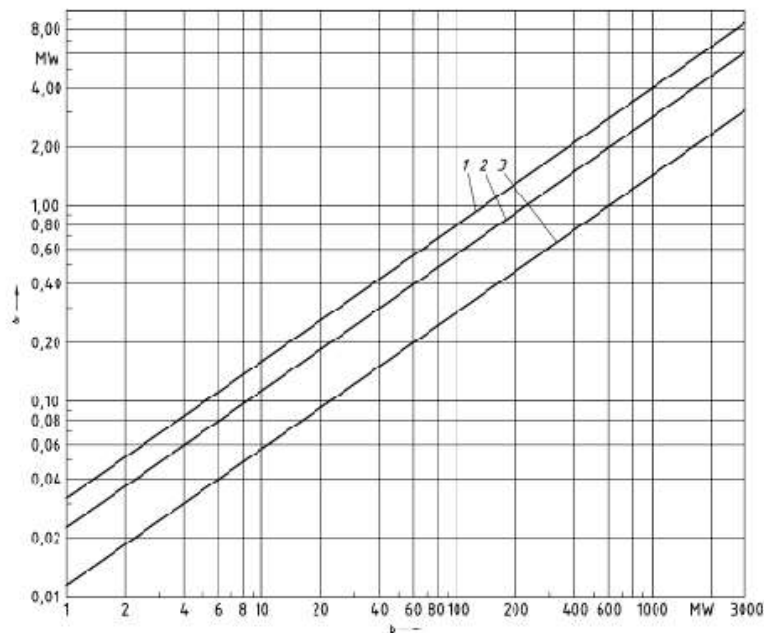
Enthalpy vapourisation at:

$$T_w := 100\text{ }^\circ\text{C} \quad C_{p_w} := 4.183 \frac{\text{kJ}}{\text{kg}\cdot\text{K}}$$

$$h_{H_2O,vap} := C_{p_w} \cdot T_w = 1.561 \times 10^3 \frac{\text{kJ}}{\text{kg}}$$

Energy losses

Using the graph provided in EN 12952, boiler convective and radiative losses to the surroundings can be estimated as follows.



Key

- a Radiation and convection losses, $\dot{Q}_{R,C}$
 - b Maximum useful heat output, \dot{Q}_U
- 1 Brown coal, blastfurnace gas and fluidized-bed boilers
 - 2 Hard coal boilers
 - 3 Fuel oil and natural gas boilers

$$\%Q_{insul.loss} := 0.8\%$$

Energy from credits

At full load, only 5 of the 6 mills are running. Using the rated power of the mills and the efficiency of 90% the total power added to the fluid stream in the mills is as follows:

Mill Load:

$$P_{mill} := \begin{pmatrix} 1459.668 \\ 1448.242 \\ 1444.629 \\ 0 \\ 1448.828 \\ 1440.527 \end{pmatrix} \cdot kW \quad \begin{pmatrix} \text{"Mill A"} \\ \text{"Mill B"} \\ \text{"Mill C"} \\ \text{"Mill D"} \\ \text{"Mill E"} \\ \text{"Mill F"} \end{pmatrix}$$

$$P_{mill.load} := \sum_{i=0}^5 P_{mill_i} = 7.242 \cdot MW$$

Primary air and forced draught fans all add energy to the air entering the boiler.

$$P_{pa.fans} := 1850kW \cdot 2 = 3.7 \times 10^6 W$$

$$P_{fd.fans} := 3148kW \cdot 2 = 6.296 \times 10^6 W$$

$$P_{others} := 75kW \cdot 5 = 3.75 \times 10^5 W$$

$$P_{fans.total} := P_{pa.fans} + P_{fd.fans} + P_{others}$$

$$V_{seal.air} := 2.65 \frac{m^3}{s}$$

$$m_{seal.air} := \rho_{air} \cdot T_{amb} \cdot V_{seal.air} = 90.895 \cdot \frac{kg}{s}$$

$$Q_{credits} := P_{mill.load} + P_{fans.total} + P_{others} = 1.799 \times 10^4 \cdot kW$$

$$C_{pFAsh} := 0.73 \frac{kJ}{kg \cdot K}$$

$$h_{coal} := C_{pcoal} \cdot T_{amb} = 38.64 \cdot \frac{kJ}{kg}$$

$$h_{ash.fg.AH.inlet} := C_{pFAsh} \cdot T_{fg.AH.inlet} = 421.038 \cdot \frac{kJ}{kg}$$

$$T_{BA} := 700^\circ C$$

$$h_{ash.BA.exit} := (1.38 \cdot T_{BA}) \cdot \frac{kJ}{kg \cdot K} = 1.343 \times 10^3 \cdot \frac{kJ}{kg}$$

Steam Energy:

$$h_{BA} := h_{FA}$$

$$Q_{sh} := [(m_{fw.econ.in} + m_{sh.att}) \cdot h_{steam.sh.out}] - (m_{fw.econ.in} \cdot h_{fw.econ.in}) - (m_{sh.att} \cdot h_{sh.att})$$

$$Q_{rh} := (m_{rh.steam} + m_{rh.att}) \cdot h_{steam.rh.out} - (m_{rh.steam} \cdot h_{steam.rh.out} + m_{rh.att} \cdot h_{rh.att})$$

$$Q_{out} := Q_{sh} + Q_{rh}$$

Mass flow rates of coal:

$$InFlows := h_{coal} + HAR \cdot \%Air_{ing} \cdot h_{Tamb} + (HAR - HAR \cdot \%Air_{ing}) \cdot h_{Tair.AH.outlet}$$

$$Flow_{Ash} := (X_{Ash} \cdot \%b_{Ash} \cdot h_{ash.BA.exit}) + (X_{Ash} \cdot \%f_{Ash} \cdot h_{ash.fg.AH.inlet})$$

$$OutFlows := -m_{fg} \cdot h_{fg.AH.inlet} - Flow_{Ash} - X_{H2O} \cdot h_{H2O.vap}$$

$$FRh_{flows} := InFlows + OutFlows$$

$$CV_{pf.coal} := HHV$$

$$m_{coal} := \frac{Q_{out} - Q_{credits}}{[CV_{pf.coal} \cdot (1 - mf_{CC} - \%Q_{insul.loss})] + FRh_{flows}}$$

$$m_{coal} = 80.254 \frac{kg}{s}$$

Mass flow rates of air:

Total air in the control volume: $m_{air.AH.total} := HAR \cdot m_{coal} = 541.145 \frac{kg}{s}$

Ingress air flow: $m_{air.ing} := m_{air.AH.total} \cdot \%Air_{ing} = 54.115 \frac{kg}{s}$

Mass Flowrate of air leaving the air heater:

$$m_{air.A/H.out} := m_{air.AH.total} - m_{air.ing} - m_{seal.air} = 396.136 \frac{kg}{s}$$

Mass flow of A/H leakage air: $m_{air.A/H.leak} := m_{coal} \cdot \%Air_{ing} \cdot HAR = 54.115 \frac{kg}{s}$

Mass flow rates of flue gas:

Mass flowrate of flue gas at A/H inlet: $mf_{fg.AH.in} := FGR \cdot m_{coal} = 611.68 \frac{kg}{s}$

$$f_{AH.leak} := 8.6\%$$

$$m_{leak} := f_{AH.leak} \cdot HAR \cdot \frac{m_{coal}}{1 - f_{AH.leak}} = 50.917 \frac{kg}{s}$$

$$m_{air.AH.in} := \frac{HAR}{1 - f_{AH.leak}} \cdot m_{coal} = 592.063 \frac{kg}{s}$$

$$m_{fg.AH.ex} := \left(FGR + \frac{f_{AH.leak}}{1 - f_{AH.leak}} \cdot HAR \right) \cdot m_{coal} = 662.597 \frac{kg}{s}$$

Heat Rate:

$$f_{aux} := 12\%$$

$$\eta_{cycle} := 42.3\%$$

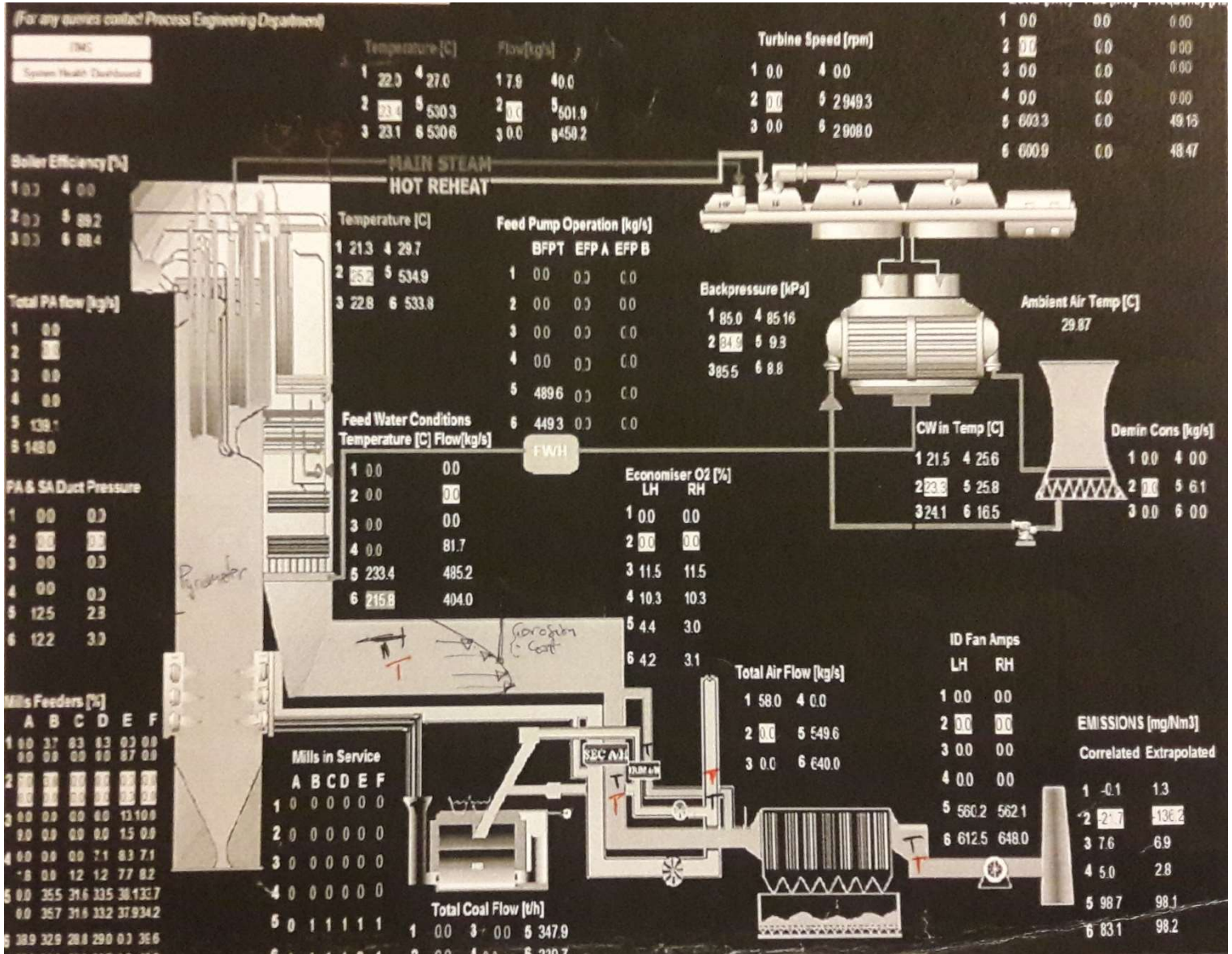
$$\eta_{boiler} := \frac{Q_{out}}{m_{coal} \cdot HHV} = 84.075\%$$

$$\eta_{gen} := 98.7\%$$

$$NHR := \left(\frac{1 + f_{aux}}{\eta_{boiler} \cdot \eta_{cycle} \cdot \eta_{gen}} \right) \cdot \frac{kJ}{kW \cdot hr} = 3.191 \cdot \frac{kJ}{kW \cdot hr}$$

```
h_steam(p, T, v, x, s) :=
  Inputs ← IsScalar(p)
  Inputs ← Inputs + 10 · IsScalar(T)
  Inputs ← Inputs + 100 · IsScalar(v)
  Inputs ← Inputs + 1000 · IsScalar(x)
  Inputs ← Inputs + 10000 · IsScalar(s)
  h_pT(p, T) if Inputs = (1 + 10)
  h_px(p, x) if Inputs = (1 + 1000)
  h_ps(p, s) if Inputs = (1 + 10000)
  h_pv(p, v) if Inputs = (1 + 100)
  h_Tx(T, x) if Inputs = (10 + 1000)
  h4_s(s) if Inputs = 10000
  h_pv(p_Tv(T, v), v) if Inputs = (10 + 100)
  if Inputs = (10 + 10000)
    pg ← plim_low · 1.001
    p ← root(T - T_ps(pg, s), pg)
    h_ps(p, s)
```

APPENDIX B: POWER STATION A-OPERATION PARAMETERS (ETAPRO CONTROL SYSTEM)



APPENDIX C: POWER STATION A- OPERATION PARAMETERS DATASHEET

Start date 2017/08/01 00:00
End date 2017/11/01 00:00

% Air ingress between 9 - 10%

	Tags		Unit
	GENERATOR LOAD	US-05SE11C210-A63	MW
Feedwater (before boiler)	TOTAL FEED WATER FLOW	US-05RL00F001-A25	kg/s
	FEED WATER TEMPERATURE	US-05RL80T002-A504	°C
	FEED WATER PRESSURE	US-05RL82P002-A507	Mpa
Main Steam (out of boiler)	MAIN STEAM FLOW	US-05RA00F001-A88	kg/s
	MAIN STEAM TEMPERATURE	US-05RA00T001-A19	°C
	MAIN STEAM PRESSURE	US-05RA00P001-A113	Mpa
Reheat steam	PRIM REHEATER STEAM INLET PRESSURE (into boiler)	US-05NE01P031-A572	Mpa
	PRIM REHEATER STEAM INLET TEMPERATURE (into boiler)	US-05NE01T060-A577	°C
	HOT REHEAT STEAM TEMPERATURE (out of boiler)	US-05RB00T001-A20	°C
	HOT REHEAT STEAM PRESSURE (out of boiler)	US-05RB01P002-A42	Mpa
Air	TOTAL FD FAN INLET AIR FLOW (total air inlet flow)	US-05NG00F600-C90	kg/s
	LH FD FAN INL AIR FLOW 1	US-05NG10F100-A172	kg/s
	RH FD FAN INL AIR FLOW 1	US-05NG20F100-A193	kg/s
	LH FD FAN INL AIR TMP 1	US-05NG11T100-A177	°C
	RH FD FAN INL AIR TMP	US-05NG21T100-A198	°C
	TOTAL PRIMARY AIR FLOW	US-05NM00U600-C8	kg/s
	MILL A PRIMARY AIR FLOW	US-05NM10C015-A129	kg/s
	MILL B PRIMARY AIR FLOW	US-05NM20C015-A130	kg/s
	MILL C PRIMARY AIR FLOW	US-05NM30C015-A131	kg/s
	MILL D PRIMARY AIR FLOW	US-05NM40C015-A132	kg/s
	MILL E PRIMARY AIR FLOW	US-05NM50C015-A133	kg/s
	MILL F PRIMARY AIR FLOW	US-05NM60C015-A134	kg/s
	LH SECONDARY AIR HEATER OUT AIR TMP 1	US-05NG11T107-A182	°C
	RH SECONDARY AIR HEATER OUT AIR TMP 1	US-05NG21T107-A203	°C
	LH PRIMARY AIR HEATER OUT AIR TMP 1	US-05NG12T118-A192	°C
	RH PRIMARY AIR HEATER OUTL AIR TMP 1	US-05NG22T118-A213	°C
Flue gas	LH ECONOMISER GAS OUT TEMP	US-05NJ10T138-A238	°C
	RH ECONOMISER GAS OUT TEMP	US-05NJ10T140-A239	°C
	LH SECONDARY AIR HEATER GAS OUT TEMP 1	US-05NR11T144-A277	°C
	RH SECONDARY AIR HEATER GAS OUT TEMP 1	US-05NR21T144-A288	°C
	LH PRIMARY AIR HEATER GAS OUT TEMP 1	US-05NR11T142-A276	°C
	RH PRIMARY AIR HEATER GAS OUT TEMP 1	US-05NR21T142-A287	°C
Fans	LH PRIMARY AIR FAN CURRENT	US-05NG12E001-A8	Amps
	RH PRIMARY AIR FAN CURRENT	US-05NG22E001-A9	Amps
	LH FD FAN CURRENT	US-05NG11E001-A7	Amps
	RH FD FAN CURRENT	US-05NG21E001-A124	Amps
Mills	MILL A LOAD	US-05NM10L601-C307	kW
	MILL B LOAD	US-05NM20L601-C308	kW
	MILL C LOAD	US-05NM30L601-C309	kW
	MILL D LOAD	US-05NM40L601-C310	kW
	MILL E LOAD	US-05NM50L601-C311	kW
	MILL F LOAD	US-05NM60L601-C312	kW
	MILL A CURRENT	US-05NM10E001-A31	Amps
	MILL B CURRENT	US-05NM20E001-A32	Amps
	MILL C CURRENT	US-05NM30E001-A33	Amps
	MILL D CURRENT	US-05NM40E001-A34	Amps
	MILL E CURRENT	US-05NM50E001-A35	Amps
	MILL F CURRENT	US-05NM60E001-A36	Amps
Coal	TOTAL COAL FLOW	IMU.C0T.A	T/H

Date and Time	GENERATOR LOAD	Feedwater (before boiler)			Main Steam (out of boiler)			Reheat steam			
		TOTAL FEED WATER FLOW	FEED WATER TEMPERATURE	FEED WATER PRESSURE	MAIN STEAM FLOW	MAIN STEAM TEMPERATURE	MAIN STEAM PRESSURE	PRIM REHEATER STEAM INLET PRESSURE (into boiler)	PRIM REHEATER STEAM INLET TEMPERATURE (into boiler)	HOT REHEAT STEAM TEMPERATURE (out of boiler)	HOT REHEAT STEAM PRESSURE (out of boiler)
17/08/01 12:00:00 AM	398.193	328.711	211.914	17.395	331.934	531.152	16.138	3.146	315.273	527.228	2.165
17/08/02 12:00:00 AM	506.885	394.922	223.828	17.920	413.086	532.617	16.235	3.820	324.234	532.647	2.777
17/08/03 12:00:00 AM	506.885	405.762	224.805	17.969	416.895	532.031	16.272	3.814	324.234	530.365	2.783
17/08/04 12:00:00 AM	613.867	479.590	233.008	18.652	501.270	531.738	16.284	4.491	329.573	533.788	3.419
17/08/05 12:00:00 AM	566.016	450.879	231.055	18.347	460.547	531.152	16.272	4.187	328.238	532.647	3.138
17/08/06 12:00:00 AM	480.225	406.055	223.438	17.908	395.801	527.930	16.260	3.674	321.946	531.507	2.637
17/08/07 12:00:00 AM	518.164	428.906	225.391	18.018	422.168	531.738	16.248	3.873	325.188	532.647	2.830
17/08/08 12:00:00 AM	547.559	423.926	228.125	18.201	444.141	531.152	16.248	4.081	325.950	533.788	3.021
17/08/09 12:00:00 AM	557.813	458.789	230.078	18.311	454.688	529.980	16.272	4.157	326.713	531.507	3.085
17/08/10 12:00:00 AM	400.586	322.852	213.477	17.480	334.570	530.273	16.235	3.190	316.608	526.942	2.194
17/08/11 12:00:00 AM	616.260	495.117	233.594	18.665	498.633	535.254	16.248	4.517	332.433	532.647	3.454
17/08/12 12:00:00 AM	520.557	414.551	226.758	18.188	427.734	533.203	16.370	3.923	326.522	532.362	2.886
17/08/13 12:00:00 AM	401.611	327.333	213.477	17.475	334.277	532.667	16.235	3.190	316.608	526.942	2.194
17/08/14 12:00:00 AM	485.352	411.621	222.461	18.091	400.195	535.254	16.431	3.683	324.044	533.503	2.651
17/08/15 12:00:00 AM	500.391	408.105	223.438	17.847	412.793	533.496	16.101	3.773	324.044	532.362	2.757
17/08/16 12:00:00 AM	401.270	328.711	177.539	17.480	323.438	528.223	16.321	3.214	318.705	526.657	2.206
17/08/17 12:00:00 AM	401.611	309.668	212.891	17.480	328.125	530.273	16.296	3.182	316.608	523.233	2.183
17/08/18 12:00:00 AM	576.611	465.234	230.664	18.408	471.094	532.031	16.248	4.201	327.667	532.362	3.164
17/08/19 12:00:00 AM	399.902	323.730	214.063	17.358	329.883	526.758	16.150	3.152	315.845	530.080	2.177
17/08/20 12:00:00 AM	507.227	411.914	223.828	17.932	413.965	533.496	16.174	3.791	324.997	532.362	2.774
17/08/21 12:00:00 AM	404.004	340.137	213.867	17.993	334.863	528.809	16.809	3.199	315.845	530.080	2.215
17/08/22 12:00:00 AM	541.406	437.129	229.797	18.140	447.383	532.374	16.174	4.040	328.738	532.647	2.941
17/08/23 12:00:00 AM	543.739	416.602	229.883	18.054	434.473	534.375	16.235	4.046	330.335	533.503	3.023
17/08/24 12:00:00 AM	507.954	387.891	224.419	17.934	413.965	533.496	16.438	3.820	324.760	533.503	2.734
17/08/25 12:00:00 AM	535.938	417.480	228.711	18.091	435.352	533.496	16.187	3.993	328.048	532.362	2.950
17/08/26 12:00:00 AM	494.922	372.070	223.633	17.932	399.902	534.375	16.357	3.741	324.997	533.503	2.713
17/08/27 12:00:00 AM	579.004	472.852	231.641	18.567	470.215	529.980	16.382	4.321	327.476	532.647	3.252
17/08/28 12:00:00 AM	501.074	377.930	223.828	17.932	406.055	532.617	16.321	3.800	324.807	534.930	2.783
17/08/29 12:00:00 AM	511.670	387.891	225.781	17.969	414.258	531.445	16.296	3.894	325.188	533.788	2.859
17/08/30 12:00:00 AM	574.561	451.465	232.813	18.237	468.457	533.789	16.113	4.295	331.289	533.788	3.217
17/08/31 12:00:00 AM	401.953	297.363	214.453	17.432	333.984	522.363	16.260	3.214	313.939	530.365	2.212
17/09/01 12:00:00 AM	495.605	377.344	223.828	17.896	405.762	532.324	16.272	3.820	324.997	533.788	2.760
17/09/02 12:00:00 AM	614.893	452.051	233.984	18.433	501.270	532.324	16.089	4.506	330.717	533.788	3.448
17/09/03 12:00:00 AM	553.027	404.883	229.492	18.213	438.574	532.617	16.382	4.122	329.001	536.070	3.091
17/09/04 12:00:00 AM	587.891	472.852	232.227	18.518	480.469	529.995	16.296	4.362	327.667	531.507	3.290
17/09/05 12:00:00 AM	451.172	364.453	219.141	17.725	375.000	527.930	16.272	3.507	318.515	532.647	2.493
17/09/06 12:00:00 AM	615.576	489.551	233.984	18.652	504.199	530.566	16.211	4.509	329.573	533.788	3.428
17/09/07 12:00:00 AM	451.514	361.816	218.945	17.700	370.313	532.031	16.260	3.521	321.184	533.788	2.505
17/09/08 12:00:00 AM	501.758	404.004	223.242	17.969	414.258	533.789	16.235	3.820	325.569	533.788	2.751
17/09/09 12:00:00 AM	613.525	472.559	233.594	18.579	505.957	532.617	16.150	4.515	331.670	532.647	3.419
17/09/10 12:00:00 AM	613.525	489.258	233.008	18.616	500.391	533.203	16.235	4.532	330.908	531.507	3.454
17/09/11 12:00:00 AM	563.623	472.266	230.469	18.372	467.285	529.395	16.235	4.225	326.141	532.647	3.152
17/09/12 12:00:00 AM	469.629	405.469	222.266	17.920	393.750	524.121	16.309	3.656	319.277	531.507	2.599
17/09/13 12:00:00 AM	487.402	403.418	223.047	17.957	407.520	526.758	16.235	3.732	320.040	532.647	2.663
17/09/14 12:00:00 AM	402.295	291.504	212.891	17.419	329.004	532.324	16.296	3.179	318.705	531.507	2.159
17/09/15 12:00:00 AM	481.934	383.496	221.094	17.834	394.922	528.809	16.211	3.650	319.277	531.507	2.607
17/09/16 12:00:00 AM	0.000	0.000	135.156	0.354	4.688	454.980	5.042	1.087	243.942	453.606	0.223
17/09/17 12:00:00 AM	0.000	0.000	71.094	0.000	0.000	309.668	0.000	0.829	86.068	339.892	0.000
17/09/18 12:00:00 AM	0.000	0.000	70.703	0.305	7.031	229.980	0.000	0.788	58.846	255.453	0.000
17/09/19 12:00:00 AM	571.826	441.797	229.883	18.262	456.738	530.273	16.223	4.213	327.667	531.507	3.158
17/09/20 12:00:00 AM	555.420	440.625	228.711	18.347	456.445	529.395	16.309	4.204	325.760	531.507	3.149
17/09/21 12:00:00 AM	581.738	461.133	230.859	18.384	483.691	529.688	16.187	4.310	325.569	530.365	3.237
17/09/22 12:00:00 AM	603.955	479.590	233.398	18.616	501.270	532.031	16.211	4.462	329.954	532.647	3.363
17/09/23 12:00:00 AM	548.584	433.887	230.273	18.286	450.500	533.496	16.260	4.110	329.191	530.365	3.041
17/09/24 12:00:00 AM	429.639	359.180	217.773	17.590	353.320	532.324	16.260	3.366	319.849	528.083	2.361
17/09/25 12:00:00 AM	423.145	351.563	218.750	17.676	350.684	527.051	16.321	3.360	317.943	526.942	2.338
17/09/26 12:00:00 AM	430.664	360.877	216.626	17.688	367.473	532.610	16.333	3.363	318.846	526.942	2.341
17/09/27 12:00:00 AM	530.127	421.289	228.125	18.127	429.199	535.840	16.296	3.937	329.001	531.507	2.909
17/09/28 12:00:00 AM	400.586	325.195	212.505	17.493	332.227	529.980	16.248	3.126	316.417	530.365	2.168
17/09/29 12:00:00 AM	0.000	24.609	114.844	3.430	0.000	411.621	2.917	0.914	221.667	454.760	0.123
17/09/30 12:00:00 AM	0.000	0.000	82.227	0.000	0.000	282.715	0.000	0.773	65.409	336.233	0.000
17/10/01 12:00:00 AM	399.902	326.367	213.672	17.468	335.449	528.809	16.211	3.164	316.799	524.949	2.209
17/10/02 12:00:00 AM	547.559	418.066	228.906	18.213	445.605	534.375	16.296	4.078	329.573	534.359	3.070
17/10/03 12:00:00 AM	489.111	390.234	221.875	17.822	404.590	533.789	16.162	3.668	323.472	531.792	2.681
17/10/04 12:00:00 AM	402.979	332.520	213.086	17.517	339.551	530.566	16.235	3.199	317.562	528.368	2.221
17/10/05 12:00:00 AM	450.146	352.148	218.555	17.737	376.758	531.445	16.260	3.472	319.849	531.792	2.470
17/10/06 12:00:00 AM	351.709	283.887	208.008	17.200	286.523	530.859	16.199	2.804	315.273	530.650	1.869
17/10/07 12:00:00 AM	400.586	322.559	213.086	17.432	336.328	530.566	16.211	3.158	316.799	528.368	2.191
17/10/08 12:00:00 AM	470.996	380.566	221.094	17.822	386.133	530.273	16.248	3.557	321.375	531.792	2.581
17/10/09 12:00:00 AM	427.246	345.117	215.430	17.615	352.441	530.273	16.260	3.302	318.324	531.792	2.329
17/10/10 12:00:00 AM	617.969	482.227	232.813	18.640	508.301	530.273	16.223	4.453	329.191	530.650	3.437
17/10/11 12:00:00 AM	493.213	405.469	223.828	17.871	406.934	528.809	16.199	3.680	320.040	530.650	2.707
17/10/12 12:00:00 AM	602.588	460.547	232.227	18.396	497.168	531.445	16.040	4.359	329.191	531.792	3.328
17/10/13 12:00:00 AM	611.133	483.691	232.617	18.640	498.633	532.031	16.272	4.433	328.620	532.933	3.387
17/10/14 12:00:00 AM	544.482	423.926	228.516	18.140	454.102	529.688	16.125	4.025	325.950	528.368	3.012
17/10/15 12:00:00 AM	548.584	446.777	228.516	18.335	450.293	533.496	16.357	4.069	327.285	531.792	3.038
17/10/16 12:00:00 AM	548.926	444.434	229.688	18.213	449.414	530.566	16.211	4.055	327.094	531.792	3.026
17/10/17 12:00:00 AM	613.184	495.703	233.203	18.604	504.492	529.980	16.138	4.438	329.191	535.215	3.413
17/10/18 12:00:00 AM	507.910	401.074	224.023	17.969	407.227	534.375	16.272	3.788	326.332	535.215	2.810

Date and Time	Air															
	TOTAL FD FAN INLET AIR FLOW (total air inlet flow)	LH FD FAN INLET AIR FLOW 1	RH FD FAN INLET AIR FLOW 1	LH FD FAN INLET AIR TEMP 1	RH FD FAN INLET AIR TEMP 1	TOTAL PRIMARY AIR FLOW	MILL A PRIMARY AIR FLOW	MILL B PRIMARY AIR FLOW	MILL C PRIMARY AIR FLOW	MILL D PRIMARY AIR FLOW	MILL E PRIMARY AIR FLOW	MILL F PRIMARY AIR FLOW	LH SECONDARY AIR HEATER OUT AIR	RH SECONDARY AIR HEATER OUT AIR	LH PRIMARY AIR HEATER OUT AIR	RH PRIMARY AIR HEATER OUT AIR
17/08/01 12:00:00 AM	439.063	227.539	211.328	27.943	27.920	113.323	25.549	26.421	26.729	0.000	24.644	9.758	270.508	261.341	257.248	244.773
17/08/02 12:00:00 AM	437.070	260.156	231.695	29.530	29.385	125.833	24.729	25.635	25.934	0.000	24.045	25.276	288.167	281.020	267.384	259.587
17/08/03 12:00:00 AM	501.367	260.156	240.430	27.510	27.744	126.772	24.797	25.959	26.079	0.000	24.780	25.396	295.849	274.011	268.164	258.028
17/08/04 12:00:00 AM	558.384	290.820	267.969	29.326	29.385	133.198	26.335	27.087	27.344	0.000	25.959	26.660	295.122	286.429	277.520	269.138
17/08/05 12:00:00 AM	530.273	275.195	251.712	27.943	28.301	127.952	25.396	26.250	26.421	0.000	24.114	25.754	293.577	284.110	276.740	268.343
17/08/06 12:00:00 AM	466.406	244.531	221.484	28.623	28.564	103.667	25.959	26.797	26.917	0.000	24.370	0.000	293.577	283.145	276.545	268.359
17/08/07 12:00:00 AM	492.383	258.398	236.314	27.451	27.539	126.636	23.755	25.173	25.344	0.000	27.258	24.661	294.350	289.317	273.427	263.875
17/08/08 12:00:00 AM	510.156	257.422	245.508	27.422	27.691	130.618	24.968	25.840	26.230	0.000	28.335	25.464	296.996	283.145	280.440	268.554
17/08/09 12:00:00 AM	525.586	261.523	257.227	31.434	31.289	127.917	23.704	24.626	28.130	0.000	26.797	24.421	302.077	287.781	283.531	273.816
17/08/10 12:00:00 AM	407.031	204.102	202.930	30.820	30.820	93.702	23.934	25.259	25.447	0.000	24.814	0.000	276.545	262.121	260.172	246.138
17/08/11 12:00:00 AM	564.453	246.044	248.384	31.058	30.890	138.898	27.173	27.894	28.079	0.000	28.181	27.494	301.498	287.781	279.374	268.090
17/08/12 12:00:00 AM	436.438	260.547	237.891	30.438	30.146	136.565	24.632	25.754	26.165	5.315	29.087	25.583	291.452	282.758	269.333	260.562
17/08/14 12:00:00 AM	462.109	240.234	221.875	30.463	30.367	111.135	26.028	26.780	26.917	5.042	25.925	0.000	288.361	277.325	271.130	268.359
17/08/15 12:00:00 AM	483.984	254.102	229.883	30.703	30.732	117.866	27.839	28.232	28.335	5.024	28.574	0.000	284.497	273.427	270.893	261.341
17/08/16 12:00:00 AM	421.034	225.000	203.906	32.607	32.988	103.394	23.806	25.105	25.413	5.042	24.661	0.000	272.842	264.070	260.757	251.791
17/08/17 12:00:00 AM	422.070	222.852	198.242	26.104	26.191	104.812	23.789	24.575	25.054	5.007	24.729	0.000	275.376	265.630	265.630	257.638
17/08/18 12:00:00 AM	523.047	275.391	243.219	19.014	19.169	133.113	24.866	26.028	26.233	5.223	25.156	25.601	296.281	288.340	278.884	271.672
17/08/19 12:00:00 AM	412.500	213.867	197.266	21.709	22.500	104.846	23.977	25.020	25.344	0.000	27.480	0.000	280.826	271.087	267.369	257.638
17/08/20 12:00:00 AM	487.109	243.414	229.297	22.207	22.969	127.593	24.336	25.155	25.857	25.823	26.489	0.000	292.417	281.213	267.774	254.519
17/08/21 12:00:00 AM	408.384	208.384	194.727	26.191	26.367	98.762	23.806	23.926	23.909	0.000	26.746	0.000	283.327	273.427	274.791	259.977
17/08/23 12:00:00 AM	531.445	271.034	252.344	21.475	20.859	136.975	25.088	25.906	26.284	26.216	6.426	25.737	294.736	289.713	276.351	268.749
17/08/25 12:00:00 AM	537.500	276.563	259.961	26.324	26.836	137.197	0.521	26.797	27.207	26.814	26.267	26.250	289.327	284.497	272.452	263.875
17/08/26 12:00:00 AM	487.695	253.516	232.617	24.053	24.844	110.349	26.558	0.000	0.000	27.734	27.634	26.353	277.520	271.283	270.893	261.791
17/08/27 12:00:00 AM	557.422	287.305	260.742	29.180	28.945	131.301	24.951	25.959	26.182	25.327	0.000	296.088	286.815	282.565	271.867	
17/08/28 12:00:00 AM	485.352	252.344	230.664	27.022	27.656	124.688	24.114	25.413	25.310	25.549	0.000	25.088	289.193	284.497	277.130	270.113
17/08/29 12:00:00 AM	502.539	250.391	258.008	31.729	31.406	126.038	24.421	25.310	25.669	25.413	0.000	25.122	292.225	282.179	275.571	268.554
17/08/30 12:00:00 AM	590.039	300.195	280.469	33.369	32.813	138.206	27.122	27.634	27.925	27.549	0.000	27.378	296.088	292.397	279.469	271.672
17/08/31 12:00:00 AM	424.609	216.211	203.320	30.088	30.117	103.018	1.521	25.936	25.652	25.737	0.000	25.595	285.077	279.859	278.689	268.749
17/09/01 12:00:00 AM	508.203	262.500	241.992	35.596	35.156	126.710	24.678	25.942	25.925	25.430	0.000	25.583	286.429	282.179	273.232	263.875
17/09/02 12:00:00 AM	589.063	315.039	289.453	24.434	25.020	147.947	23.226	23.446	30.010	29.395	0.000	29.258	292.397	289.906	276.351	270.113
17/09/03 12:00:00 AM	550.586	274.609	261.328	27.510	27.480	136.907	26.162	27.070	27.463	27.310	0.000	26.631	296.088	291.452	281.020	273.816
17/09/04 12:00:00 AM	563.672	296.800	269.141	29.063	29.154	133.574	0.000	26.421	26.831	26.934	26.162	26.163	293.306	288.042	275.571	267.774
17/09/05 12:00:00 AM	458.789	240.039	223.438	31.729	31.025	104.573	0.000	26.250	0.000	26.284	25.635	25.874	278.105	271.478	263.333	260.757
17/09/06 12:00:00 AM	577.734	301.953	285.156	31.641	31.025	141.743	0.000	28.639	28.779	28.662	28.813	28.164	294.350	291.065	277.130	270.187
17/09/07 12:00:00 AM	494.141	252.930	243.750	33.281	33.018	109.717	0.000	26.831	3.350	26.899	26.617	26.592	275.766	270.503	268.554	259.782
17/09/08 12:00:00 AM	493.023	262.695	241.992	35.332	35.127	128.635	0.000	25.635	26.182	26.301	24.900	25.874	284.304	279.080	267.774	257.833
17/09/09 12:00:00 AM	631.445	326.758	302.734	37.705	37.236	147.417	0.000	29.258	29.736	29.360	30.129	29.087	291.258	286.815	275.571	269.333
17/09/10 12:00:00 AM	613.672	314.844	293.945	35.566	35.479	143.179	0.000	28.967	29.309	28.796	27.874	28.950	293.770	289.906	277.130	271.672
17/09/11 12:00:00 AM	568.555	289.844	266.797	35.977	35.479	136.514	0.000	27.122	27.617	27.292	26.968	26.899	292.225	289.103	274.791	268.359
17/09/12 12:00:00 AM	490.625	250.391	231.641	36.211	36.094	110.042	0.000	27.130	0.000	27.258	26.848	26.934	286.815	286.042	277.310	273.622
17/09/13 12:00:00 AM	456.836	237.109	219.141	37.178	36.563	119.595	1.812	28.574	3.896	28.130	28.885	28.044	282.179	276.740	265.435	254.129
17/09/14 12:00:00 AM	390.625	205.664	195.352	37.764	36.914	104.521	23.840	0.273	0.000	27.686	23.823	24.165	269.138	261.146	252.960	240.485
17/09/15 12:00:00 AM	482.422	249.805	234.766	35.947	35.508	119.492	3.315	27.771	5.417	27.874	27.891	27.686	280.054	274.011	269.333	259.332
17/09/16 12:00:00 AM	390.586	187.500	160.938	36.533	36.211	0.000	0.000	0.000	0.000	0.000	0.000	0.000	234.500	231.02	242.884	236.899
17/09/17 12:00:00 AM	0.000	0.000	0.000	24.229	23.672	0.000	0.000	0.000	0.000	0.000	0.000	0.000	45.626	38.168	120.119	131.578
17/09/18 12:00:00 AM	126.758	60.547	64.063	17.930	18.047	0.000	0.000	0.000	0.000	0.000	0.000	0.000	44.816	34.987	78.432	74.584
17/09/19 12:00:00 AM	561.719	289.063	268.359	32.754	32.578	132.976	26.045	26.814	0.000	26.865	26.335	26.634	292.417	286.235	277.325	275.571
17/09/20 12:00:00 AM	546.094	281.055	262.109	35.566	34.688	130.601	25.669	26.387	0.000	26.609	25.857	26.250	290.872	282.758	277.325	273.622
17/09/21 12:00:00 AM	575.596	298.438	271.034	35.918	35.625	141.367	2.273	27.925	28.198	27.651	27.423	27.634	286.235	279.080	265.630	262.511
17/09/22 12:00:00 AM	585.742	303.906	287.891	35.684	35.859	139.197	27.036	27.634	27.959	28.010	0.000	293.366	287.202	276.545	271.283	
17/09/23 12:00:00 AM	523.242	267.773	251.367	38.115	37.969	132.805	25.190	26.165	26.472	3.435	25.840	25.994	289.327	284.883	271.867	269.528
17/09/24 12:00:00 AM	433.008	223.242	204.102	29.180	29.678	107.596	24.729	25.703	25.942	3.657	27.310	0.000	277.115	267.969	264.070	257.053
17/09/25 12:00:00 AM	430.664	224.023	204.102	34.834	34.834	107.666	25.686	23.909	24.063	3.435	30.249	0.000	282.372	274.207	268.749	262.511
17/09/26 12:00:00 AM	463.086	237.891	217.188	30.234	30.537	106.111	24.866	25.874	26.190	3.686	25.197	0.000	279.287	265.045	264.070	257.833
17/09/27 12:00:00 AM	496.633	252.734	238.867	25.254	25.371	132.224	25.020	25.857	26.028	5.178	24.268	25.635	293.190	289.327	270.308	268.359
17/09/29 12:00:00 AM	258.534	135.742	122.266	29.707	30.176	0.000	0.000	0.000	0.000	0.000	0.000	0.000	167.647	160.031	194.303	174.261
17/09/30 12:00:00 AM	0.000	0.000	0.000	23.027	22.793	0.000	0.000	0.000	0.000	0.000	0.000	0.000	30.017	24.650	39.758	39.361
17/10/01 12:00:00 AM	412.500	214.258	198.242	31.436	31.729	103.240	24.336	26.660	27.019	0.000	25.601	0				

Date and Time	Flue gas						Fans			
	LH ECONOMI SER GAS OUT TEMP	RH ECONOMI SER GAS OUT TEMP	LH SECONDARY AIR HEATER GAS OUT	RH SECONDARY AIR HEATER GAS OUT	LH PRIMARY AIR HEATER GAS OUT	RH PRIMARY AIR HEATER GAS OUT	LH PRIMARY AIR FAN CURRENT	RH PRIMARY AIR FAN CURRENT	LH FD FAN CURRENT	RH FD FAN CURRENT
17/08/01 12:00:00 AM	284.368	284.084	123.905	118.645	114.584	103.978	242.676	248.779	239.746	242.188
17/08/02 12:00:00 AM	304.528	305.053	136.014	130.643	118.258	111.973	252.930	258.057	253.662	257.324
17/08/03 12:00:00 AM	302.089	301.175	134.549	123.221	118.549	108.895	255.127	260.254	255.127	259.277
17/08/04 12:00:00 AM	314.284	315.808	139.823	132.791	126.346	118.741	262.207	266.113	268.066	273.193
17/08/05 12:00:00 AM	311.845	314.589	136.698	129.178	125.955	117.775	253.662	259.033	259.766	264.404
17/08/06 12:00:00 AM	303.309	304.833	138.455	125.858	123.905	114.294	236.328	243.408	241.455	245.361
17/08/07 12:00:00 AM	305.748	308.492	137.772	126.737	120.780	110.426	254.150	259.521	250.488	253.662
17/08/08 12:00:00 AM	309.406	309.711	145.345	127.127	124.295	114.681	258.057	261.475	250.000	261.719
17/08/09 12:00:00 AM	314.284	317.027	146.529	129.959	130.545	121.268	253.662	260.010	251.465	264.648
17/08/10 12:00:00 AM	283.801	286.352	137.088	119.515	121.561	105.325	234.619	240.723	224.609	235.840
17/08/11 12:00:00 AM	284.368	284.368	123.905	118.645	114.584	103.978	242.676	248.779	239.746	242.188
17/08/12 12:00:00 AM	303.614	304.833	142.583	133.865	118.451	110.813	260.010	265.869	242.432	246.582
17/08/13 12:00:00 AM	285.620	290.887	130.336	119.128	120.780	107.349	234.863	241.211	228.027	231.201
17/08/14 12:00:00 AM	302.395	304.833	133.280	122.733	130.936	121.366	243.896	248.291	239.746	243.164
17/08/15 12:00:00 AM	297.691	298.825	135.526	123.905	123.514	114.004	246.826	252.197	249.023	253.906
17/08/16 12:00:00 AM	282.950	282.950	127.323	118.741	120.780	111.790	237.061	244.385	232.910	236.572
17/08/17 12:00:00 AM	285.218	285.218	123.709	114.294	117.291	108.981	235.352	241.455	235.107	238.037
17/08/18 12:00:00 AM	315.808	318.247	129.959	127.811	118.451	114.971	258.301	264.160	263.428	269.531
17/08/19 12:00:00 AM	292.021	292.021	124.100	116.808	114.971	106.479	238.525	244.141	231.689	236.328
17/08/20 12:00:00 AM	306.053	306.053	132.889	125.662	110.813	104.476	258.057	262.939	249.023	253.174
17/08/21 12:00:00 AM	295.423	294.289	134.354	114.100	122.537	106.672	236.107	242.432	228.760	232.178
17/08/22 12:00:00 AM	312.150	313.369	138.260	136.209	124.491	119.128	267.324	264.160	265.371	260.010
17/08/23 12:00:00 AM	318.247	318.247	134.158	131.619	116.711	112.940	261.963	268.555	259.277	266.357
17/08/24 12:00:00 AM	303.309	306.053	126.993	126.993	116.324	112.940	258.057	264.160	258.057	262.207
17/08/25 12:00:00 AM	310.016	312.150	133.963	132.498	117.484	113.617	263.428	268.799	262.695	269.043
17/08/26 12:00:00 AM	297.744	299.958	122.440	118.548	120.194	113.907	246.338	250.732	258.545	262.695
17/08/27 12:00:00 AM	314.894	318.247	140.215	130.448	129.569	120.096	259.033	263.916	268.066	274.658
17/08/28 12:00:00 AM	305.138	306.053	132.401	129.178	118.548	114.487	253.174	259.277	249.023	254.395
17/08/29 12:00:00 AM	305.138	310.930	141.103	128.299	121.268	117.291	252.441	258.301	244.385	262.939
17/08/30 12:00:00 AM	319.771	321.905	141.498	140.906	127.909	123.221	262.207	269.531	273.926	280.518
17/08/31 12:00:00 AM	294.573	294.289	132.498	127.323	121.659	114.874	233.887	242.188	229.736	233.643
17/09/01 12:00:00 AM	306.357	306.053	136.698	133.670	123.221	117.775	252.930	258.789	253.906	258.057
17/09/02 12:00:00 AM	317.333	320.686	136.307	136.405	119.031	115.841	273.438	278.564	284.180	290.039
17/09/03 12:00:00 AM	314.894	318.247	138.162	136.014	123.709	119.322	264.648	269.287	264.648	271.240
17/09/04 12:00:00 AM	312.455	317.027	135.037	133.573	120.194	116.808	260.254	268.799	273.926	279.541
17/09/05 12:00:00 AM	294.573	295.423	129.276	122.049	119.031	112.843	236.328	247.070	245.361	250.977
17/09/06 12:00:00 AM	317.333	321.905	139.920	138.944	122.928	119.225	269.043	277.832	274.902	283.936
17/09/07 12:00:00 AM	295.707	298.825	127.323	123.709	124.491	118.451	241.943	249.268	250.488	257.080
17/09/08 12:00:00 AM	302.699	303.614	137.283	133.280	119.031	113.133	255.615	262.695	248.779	253.174
17/09/09 12:00:00 AM	316.113	319.466	142.780	141.695	127.225	124.393	277.588	283.691	291.016	300.537
17/09/10 12:00:00 AM	317.333	319.466	142.681	141.991	126.444	123.905	274.170	278.809	279.785	288.086
17/09/11 12:00:00 AM	313.674	319.466	141.202	140.314	125.272	122.049	264.404	271.973	267.334	274.414
17/09/12 12:00:00 AM	303.918	307.272	138.065	135.428	128.006	125.077	240.234	249.756	252.441	258.301
17/09/13 12:00:00 AM	297.974	299.958	137.772	132.401	122.635	113.520	243.164	251.953	240.479	245.361
17/09/14 12:00:00 AM	282.100	284.651	132.987	122.147	116.421	104.459	232.910	242.676	223.145	226.074
17/09/15 12:00:00 AM	297.974	299.392	133.670	129.080	126.932	118.355	248.535	255.371	248.779	254.395
17/09/16 12:00:00 AM	232.981	235.609	148.205	121.073	167.118	152.842	0.000	0.000	207.764	210.205
17/09/17 12:00:00 AM	52.123	53.621	41.982	37.809	31.772	24.725	0.000	0.000	0.000	0.000
17/09/18 12:00:00 AM	56.916	57.216	28.745	23.745	67.092	59.801	0.000	0.000	172.363	177.002
17/09/19 12:00:00 AM	308.796	315.198	137.381	134.940	127.323	130.838	259.277	266.846	271.484	278.564
17/09/20 12:00:00 AM	305.138	310.321	137.772	133.963	128.104	128.494	258.057	262.695	265.869	270.020
17/09/21 12:00:00 AM	306.357	307.882	139.725	137.381	119.902	121.854	268.311	275.146	269.043	273.926
17/09/22 12:00:00 AM	312.455	313.979	141.892	141.498	128.885	130.155	264.893	272.217	276.123	282.471
17/09/23 12:00:00 AM	307.577	310.321	141.103	139.334	126.541	128.957	258.545	263.916	251.953	257.568
17/09/24 12:00:00 AM	291.717	291.455	127.420	120.194	119.128	114.197	237.793	244.873	235.107	238.770
17/09/25 12:00:00 AM	295.707	297.124	131.619	126.053	125.370	122.342	234.619	240.723	230.225	233.398
17/09/26 12:00:00 AM	288.801	289.688	122.942	119.902	121.854	118.268	234.191	240.479	244.181	248.898
17/09/27 12:00:00 AM	310.016	313.979	133.280	132.498	115.357	115.647	258.789	264.404	250.977	254.883
17/09/28 12:00:00 AM	286.820	289.319	126.993	119.319	117.309	110.716	233.019	244.385	231.394	233.943
17/09/29 12:00:00 AM	135.807	142.140	125.370	110.426	192.898	168.214	0.000	0.000	184.082	186.035
17/09/30 12:00:00 AM	26.462	24.564	28.157	21.882	35.570	23.058	0.000	0.000	0.000	0.000
17/10/01 12:00:00 AM	284.084	283.234	134.940	117.775	122.733	117.508	237.061	242.432	228.271	232.178
17/10/02 12:00:00 AM	310.625	315.198	137.772	135.428	124.393	124.491	257.080	262.207	260.254	265.137
17/10/03 12:00:00 AM	291.738	297.124	131.815	123.318	123.577	120.487	240.967	246.826	241.943	245.361
17/10/04 12:00:00 AM	284.368	288.053	132.987	126.541	120.194	117.001	232.178	239.258	214.844	218.018
17/10/05 12:00:00 AM	289.753	292.588	133.377	134.061	122.342	119.225	239.502	245.605	231.445	227.783
17/10/06 12:00:00 AM	288.620	289.187	130.350	121.659	114.487	110.329	234.863	243.604	219.238	223.389
17/10/07 12:00:00 AM	286.352	289.187	143.964	120.975	117.775	102.919	236.572	242.920	219.971	227.539
17/10/08 12:00:00 AM	302.395	303.004	137.088	126.248	126.932	120.389	244.141	248.291	243.164	245.361
17/10/09 12:00:00 AM	293.155	293.722	131.912	120.780	116.228	108.404	237.793	245.605	232.178	235.107
17/10/10 12:00:00 AM	310.930	309.101	135.526	135.623	120.487	121.659	261.230	269.043	262.695	269.287
17/10/11 12:00:00 AM	295.423	300.565	121.073	120.780	119.708	119.515	240.234	247.070	256.104	262.207
17/10/12 12:00:00 AM	309.711	312.759	137.186	138.260	119.515	121.073	262.939	270.508	261.475	266.357
17/10/13 12:00:00 AM	309.711	312.759	141.103	141.991	123.807	125.760	260.498	267.334	254.639	259.766
17/10/14 12:00:00 AM	306.053	307.882	138.162	135.916	124.881	124.393	255.859	263.916	259.277	264.160
17/10/15 12:00:00 AM	303.614	305.443	142.484	138.944	122.830	121.659	257.568	265.137	249.268	255.615
17/10/16 12:00:00 AM	312.150	313.979	142.583	139.237	125.662	124.588	254.883	262.939	247.314	252.930
17/10/17 12:00:00 AM	310.930	310.321	142.681	141.103	124.491	122.537	268.311	275.635	266.602	271.973
17/10/18 12:00:00 AM	305.138	304.224	136.600	131.313	121.756	117.871	255.371	259.277	245.361	250.244
17/10/19 12:00:00 AM	297.974	297.124	136.209	131.522	124.981	122.245	246.582	253.906	253.174	257.080
17/10/20 12:00:00 AM	315.808	318.856	145.937	143.668	126.737	125.272	260.742	269.287	258.301	264.893
17/10/21 12:00:00 AM	309.711	310.321	135.428	138.748	129.959	126.834	257.324	262.451	266.357	264.648
17/10/22 12:00:00 AM	309.711	310.321	139.823	140.511						

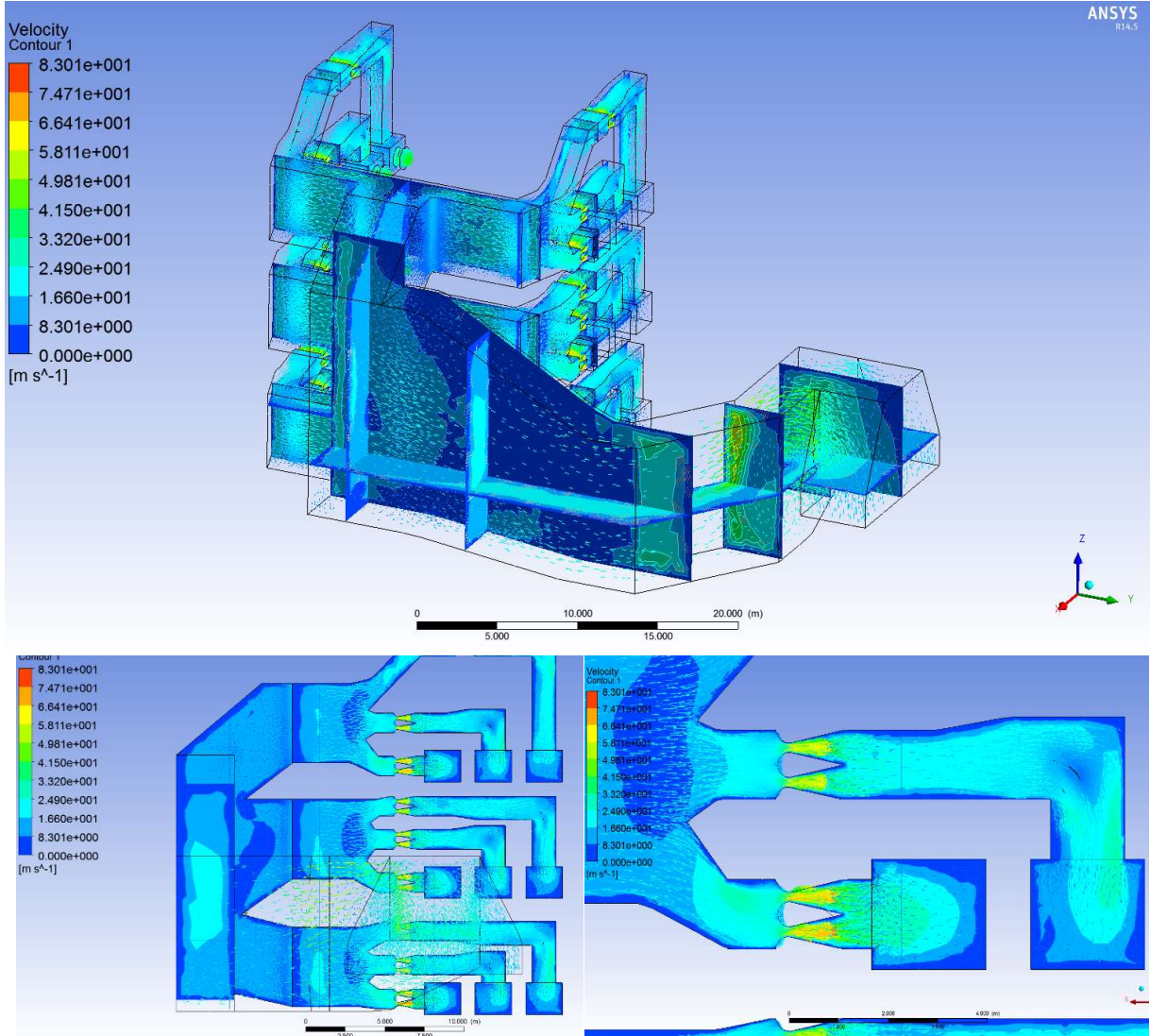
Date and Time	Mills											Coal	
	MILL A LOAD	MILL B LOAD	MILL C LOAD	MILL D LOAD	MILL E LOAD	MILL F LOAD	MILL A CURRENT	MILL B CURRENT	MILL C CURRENT	MILL D CURRENT	MILL E CURRENT	MILL F CURRENT	TOTAL COAL FLOW
17/08/01 12:00:00 AM	1456.641	1448.828	1446.973	0.000	1454.395	0.000	307.031	317.188	295.313	0.000	296.875	0.000	254.260
17/08/02 12:00:00 AM	1439.063	1443.946	1438.574	0.000	1450.781	1439.551	302.344	316.406	301.563	0.000	299.219	313.281	276.254
17/08/03 12:00:00 AM	1460.449	1459.375	1451.953	0.000	1458.887	1448.777	300.000	318.750	298.438	0.000	306.250	312.500	330.726
17/08/04 12:00:00 AM	1457.129	1458.301	1449.316	0.000	1455.762	1472.754	303.906	315.625	300.000	0.000	310.156	310.156	385.965
17/08/05 12:00:00 AM	1452.441	1452.637	1447.168	0.000	1451.855	1443.848	301.563	317.188	295.313	0.000	303.125	309.375	301.438
17/08/06 12:00:00 AM	1459.473	1460.742	1452.051	0.000	1455.176	0.000	303.906	316.406	298.438	0.000	304.688	0.000	299.616
17/08/07 12:00:00 AM	1454.237	1455.566	1447.852	0.000	1453.223	1443.652	303.125	318.750	296.094	0.000	300.000	311.719	282.263
17/08/08 12:00:00 AM	1449.609	1450.586	1445.801	0.000	1443.652	1441.309	300.781	313.281	298.438	0.000	299.219	310.938	291.912
17/08/09 12:00:00 AM	1458.008	1447.363	1449.121	0.000	1448.535	1443.066	302.344	315.625	298.438	0.000	301.563	0.000	309.090
17/08/10 12:00:00 AM	1464.951	1454.004	1443.805	0.000	1451.172	0.000	306.250	307.813	301.563	0.000	302.344	0.000	295.453
17/08/11 12:00:00 AM	1463.680	1461.173	1449.023	0.000	1450.000	1447.420	304.688	313.281	296.094	0.000	297.656	314.063	273.430
17/08/12 12:00:00 AM	1459.688	1448.242	1444.629	0.000	1448.828	1440.527	303.906	314.063	296.094	0.000	296.875	312.500	328.460
17/08/13 12:00:00 AM	1459.620	1453.111	1450.000	0.000	1453.125	0.000	303.125	312.500	300.000	0.000	296.875	0.000	273.739
17/08/14 12:00:00 AM	1461.523	1449.219	1446.973	0.000	1452.344	0.000	299.219	313.281	296.875	0.000	299.219	0.000	273.017
17/08/15 12:00:00 AM	1461.133	1442.189	1446.592	0.000	1456.934	0.000	300.000	316.406	296.094	0.000	300.781	0.000	309.340
17/08/16 12:00:00 AM	1461.914	1442.773	1447.363	0.000	1455.273	0.000	298.438	314.844	305.469	0.000	304.688	0.000	248.026
17/08/17 12:00:00 AM	1462.695	1442.188	1447.949	0.000	1456.152	0.000	304.688	314.844	301.563	0.000	299.219	0.000	245.206
17/08/18 12:00:00 AM	1449.805	1458.789	1422.363	0.000	1451.465	1449.219	295.313	315.625	296.875	0.000	300.000	314.844	306.555
17/08/19 12:00:00 AM	1448.242	1457.227	1429.395	0.000	1452.930	0.000	301.563	321.094	297.656	0.000	296.094	0.000	246.292
17/08/20 12:00:00 AM	1451.465	1458.398	1431.348	1446.592	1453.516	0.000	298.438	317.188	296.094	297.656	303.125	0.000	271.272
17/08/21 12:00:00 AM	1453.711	1460.742	1431.836	0.000	1454.237	0.000	302.344	321.875	297.656	0.000	306.250	0.000	233.250
17/08/22 12:00:00 AM	1458.301	1444.629	1447.168	0.000	1453.805	0.000	303.125	316.406	300.000	0.000	303.125	0.000	303.500
17/08/23 12:00:00 AM	1451.465	1451.270	1427.637	1437.207	0.000	1455.371	302.344	319.531	301.563	300.781	0.000	313.281	267.881
17/08/24 12:00:00 AM	0.000	1455.762	1428.809	1430.809	1452.539	1456.738	0.000	313.281	296.875	291.406	298.438	315.625	303.414
17/08/25 12:00:00 AM	0.000	1455.469	1426.074	1458.762	1454.893	1458.105	0.000	314.063	292.369	299.219	310.156	312.500	334.814
17/08/26 12:00:00 AM	1453.906	0.000	1427.246	1451.563	1456.543	0.000	297.656	0.000	289.844	306.250	303.125	0.000	321.602
17/08/27 12:00:00 AM	1443.164	1459.398	1446.387	1441.797	1449.926	0.000	301.563	317.188	300.000	302.344	299.219	0.000	314.419
17/08/28 12:00:00 AM	1444.727	1459.863	1447.754	1443.652	0.000	1462.109	294.531	317.188	296.875	293.750	0.000	314.844	301.535
17/08/29 12:00:00 AM	1449.512	1457.031	1444.824	1442.383	0.000	1458.887	296.094	310.938	298.438	301.563	0.000	314.844	303.173
17/08/30 12:00:00 AM	1447.754	1455.367	1443.955	1441.719	0.000	1457.129	301.563	317.969	298.438	306.250	0.000	311.719	346.105
17/08/31 12:00:00 AM	0.000	1450.195	1432.520	1427.266	0.000	1445.215	0.000	314.844	294.531	303.906	0.000	317.969	264.529
17/09/01 12:00:00 AM	1457.617	1460.352	1434.082	1469.531	0.000	1463.965	300.781	320.313	295.313	304.688	0.000	314.063	300.455
17/09/02 12:00:00 AM	1457.813	1457.820	1429.395	1470.396	0.000	1457.617	301.563	314.844	294.531	304.688	0.000	316.406	386.186
17/09/03 12:00:00 AM	1457.813	1460.449	1434.766	1471.582	0.000	1463.965	303.125	314.844	297.656	313.281	0.000	314.844	348.458
17/09/04 12:00:00 AM	0.000	1458.789	1433.203	1471.875	1452.246	1461.133	0.000	320.313	293.750	308.594	299.219	310.156	344.152
17/09/05 12:00:00 AM	0.000	1445.410	0.000	1465.820	1446.875	1434.375	0.000	311.719	0.000	303.125	301.563	314.844	290.867
17/09/06 12:00:00 AM	0.000	1447.168	1423.730	1470.117	1446.680	1440.039	0.000	317.969	297.656	310.156	303.125	311.719	403.219
17/09/07 12:00:00 AM	0.000	1444.322	0.000	1457.520	1451.758	1446.191	0.000	315.625	0.000	307.813	306.250	314.844	267.989
17/09/08 12:00:00 AM	0.000	1446.973	1436.621	1458.887	1452.734	1449.340	0.000	316.406	300.000	309.375	307.031	314.844	303.453
17/09/09 12:00:00 AM	0.000	1450.684	1441.018	1461.328	1456.152	1450.977	0.000	315.625	296.094	306.250	305.469	314.844	427.585
17/09/10 12:00:00 AM	0.000	1448.242	1439.258	1461.035	1457.422	1448.438	0.000	318.750	297.656	307.813	302.344	313.281	433.804
17/09/11 12:00:00 AM	0.000	1447.952	1438.867	1452.637	1443.945	1441.016	0.000	317.188	295.313	306.250	300.000	310.156	335.557
17/09/12 12:00:00 AM	0.000	1444.141	0.000	1457.422	1467.383	1442.578	0.000	316.406	0.000	305.469	307.031	310.156	305.836
17/09/13 12:00:00 AM	0.000	1456.055	0.000	1449.805	1465.625	1441.602	0.000	315.313	0.000	295.313	309.375	312.500	276.547
17/09/14 12:00:00 AM	1460.398	0.000	0.000	1459.570	1468.639	1453.613	302.344	0.000	0.000	317.188	309.375	318.750	237.799
17/09/15 12:00:00 AM	0.000	1455.371	0.000	1458.496	1462.207	1453.906	0.000	320.313	0.000	307.813	307.031	314.063	289.694
17/09/16 12:00:00 AM	0.000	0.000	0.000	0.000	0.000	0.000	0.000	0.000	0.000	0.000	0.000	0.000	0.000
17/09/17 12:00:00 AM	0.000	0.000	0.000	0.000	0.000	0.000	0.000	0.000	0.000	0.000	0.000	0.000	0.000
17/09/18 12:00:00 AM	0.000	0.000	0.000	0.000	0.000	0.000	0.000	0.000	0.000	0.000	0.000	0.000	0.000
17/09/19 12:00:00 AM	1459.766	1455.371	0.000	1456.055	1461.816	1450.176	300.781	319.531	0.000	310.938	315.625	310.938	327.606
17/09/20 12:00:00 AM	1462.793	1458.789	0.000	1456.934	1464.063	1475.098	301.563	314.844	0.000	300.000	310.156	315.625	321.551
17/09/21 12:00:00 AM	0.000	1451.074	1443.848	1422.559	1449.023	1449.707	0.000	316.406	293.750	306.250	304.688	312.500	358.208
17/09/22 12:00:00 AM	1468.895	1450.391	1441.639	1421.875	1449.902	0.000	307.813	314.844	295.313	295.313	303.125	0.000	384.544
17/09/23 12:00:00 AM	1450.977	1458.008	1457.910	0.000	1461.914	1446.484	290.625	312.500	296.875	0.000	304.688	308.594	297.550
17/09/24 12:00:00 AM	1454.698	1464.551	1462.402	0.000	1466.016	0.000	298.438	318.750	303.125	0.000	300.781	0.000	262.710
17/09/25 12:00:00 AM	1452.734	1457.422	1459.473	0.000	1462.500	0.000	307.813	313.281	305.469	0.000	300.781	0.000	250.404
17/09/26 12:00:00 AM	1464.883	1463.888	1463.179	0.000	1463.887	0.000	303.125	316.406	303.125	0.000	309.219	0.000	343.181
17/09/27 12:00:00 AM	1453.613	1460.645	1459.961	0.000	1463.184	1457.520	304.688	317.969	303.125	0.000	299.219	314.844	322.185
17/09/28 12:00:00 AM	0.000	0.000	0.000	0.000	0.000	0.000	0.000	0.000	0.000	0.000	0.000	0.000	0.000
17/09/29 12:00:00 AM	0.000	0.000	0.000	0.000	0.000	0.000	0.000	0.000	0.000	0.000	0.000	0.000	0.000
17/09/30 12:00:00 AM	0.000	0.000	0.000	0.000	0.000	0.000	0.000	0.000	0.000	0.000	0.000	0.000	0.000
17/10/01 12:00:00 AM	1453.125	1457.422	1461.914	0.000	1463.477	0.000	306.250	316.406	298.438	0.000	303.125	0.000	238.133
17/10/02 12:00:00 AM	1453.809	1460.254	1462.598	0.000	1460.840	1456.055	304.688	319.531	297.656	0.000	307.031	313.281	298.762
17/10/03 12:00:00 AM	1455.273	1459.473	1452.441	0.000	1459.688	0.000	304.688	317.969	301.563	0.000	298.438	0.000	266.659
17/10/04 12:00:00 AM	1456.348	1458.984	1451.074	0.000	1461.230	0.000	300.000	321.875	296.094	0.000	300.781	0.000	243.498
17/10/05 12:00:00 AM	1443.262	1448.535	1450.391	0.000	1451.465	0.000	297.656	315.625	300.000	0.000	305.469	0.000	265.207
17/10/06 12:00:00 AM	0.000	1457.422	1456.445	1463.281	1451.563	0.000	0.000	314.063	300.781	307.031	302.344	0.000	226.602
17/10/07 12:00:00 AM	1456.543	1458.984	1456.250	0.000	145								

APPENDIX D: COAL ANALYSIS REPORT

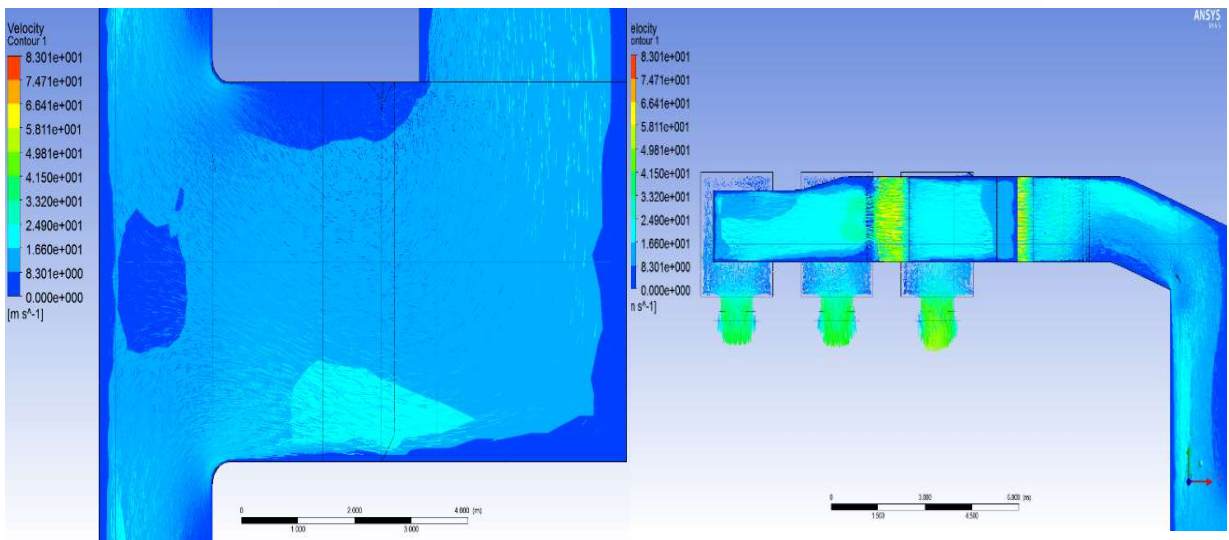
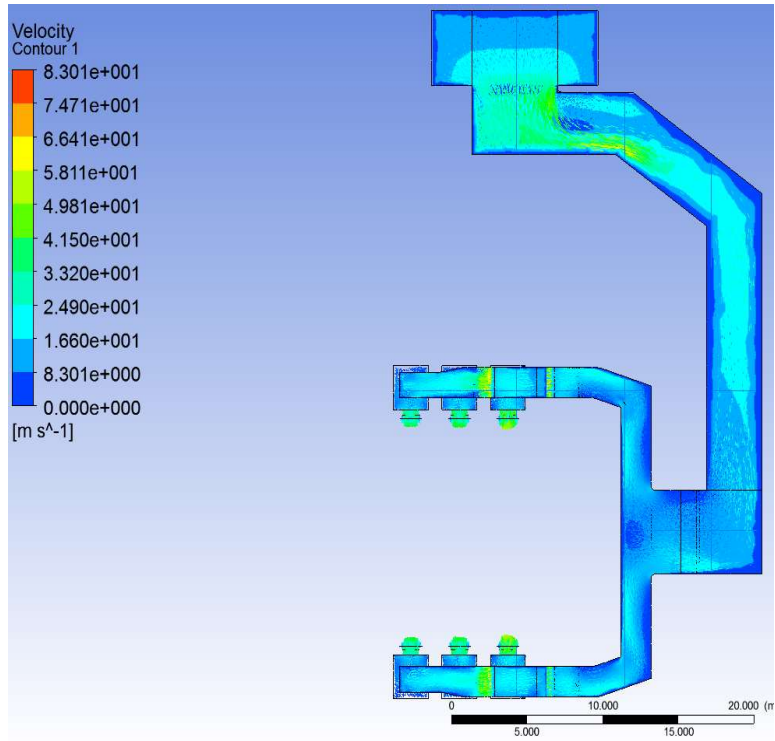
Date	Report Ref	Sample ID	%										(MJ/Kg)
			Analytical Moisture	Ash	Volatile Matter	Fixed Carbon(by difference)	Carbon	Hydrogen	Nitrogen	Total Sulphur	Carbonate	Oxygen(by Difference)	Gross Calorific Value
21-Jun-17	COA2017-010195	7991973	5,5	41,2	19,6	34	39,77	2,13	0,95	0,9	1,99	7,56	15,07
27-Sep-17	COA2017-010332	8215883	4,6	40,6	20,3	34,5	40,48	2,06	1	0,76	2,06	8,44	15,44
31-Aug-17	COA2017-010279	8141855	5,1	40,4	19,9	34,6	40,11	1,97	0,95	1,1	2,01	8,36	15,64
31-Jul-17	COA2017-010233	8060671	5,7	39,8	19,2	35,3	42,07	1,97	1	0,78	2,1	6,01	15,64
01-Nov-17	COA2017-010417	8311094	5,2	39,9	20,1	34,8	41,72	2,64	1,01	0,83	2,09	6,61	15,65
01-Nov-17	COA2017-010418	8311094	5,5	41,2	19,6	34	39,77	2,13	0,95	0,9	1,99	7,56	15,07
			5,27	40,52	19,78	34,53	40,65	2,15	0,98	0,88	2,04	7,42	15,42

Component	Unit	Value
Analytical Moisture	%	5.2
Ash	%	39.9
Volatile Matter	%	20.1
Fixed Carbon (by difference)	%	34.8
Carbon	%	41.72
Hydrogen	%	2.64
Nitrogen	%	1.01
Total Sulphur	%	0.83
Carbonate	%	2.09
Oxygen (by difference)	%	6.61
Gross Calorific Value	MJ/kg	15.65
Elemental Analysis		
SiO ₂	%	54.8
Al ₂ O ₃	%	29.3
Fe ₂ O ₃	%	3.9
TiO ₂	%	1.5
P ₂ O ₅	%	0.37
CaO	%	4.4
MgO	%	1.0
Na ₂ O	%	0.3
K ₂ O	%	0.7
SO ₃	%	3.3
MnO	%	0.01
Ash Fusion Temperature		
Deformation Temperature	°C	1400
Softening Temperature	°C	1430
Hemisphere Temperature	°C	1450
Flow Temperature	°C	1500

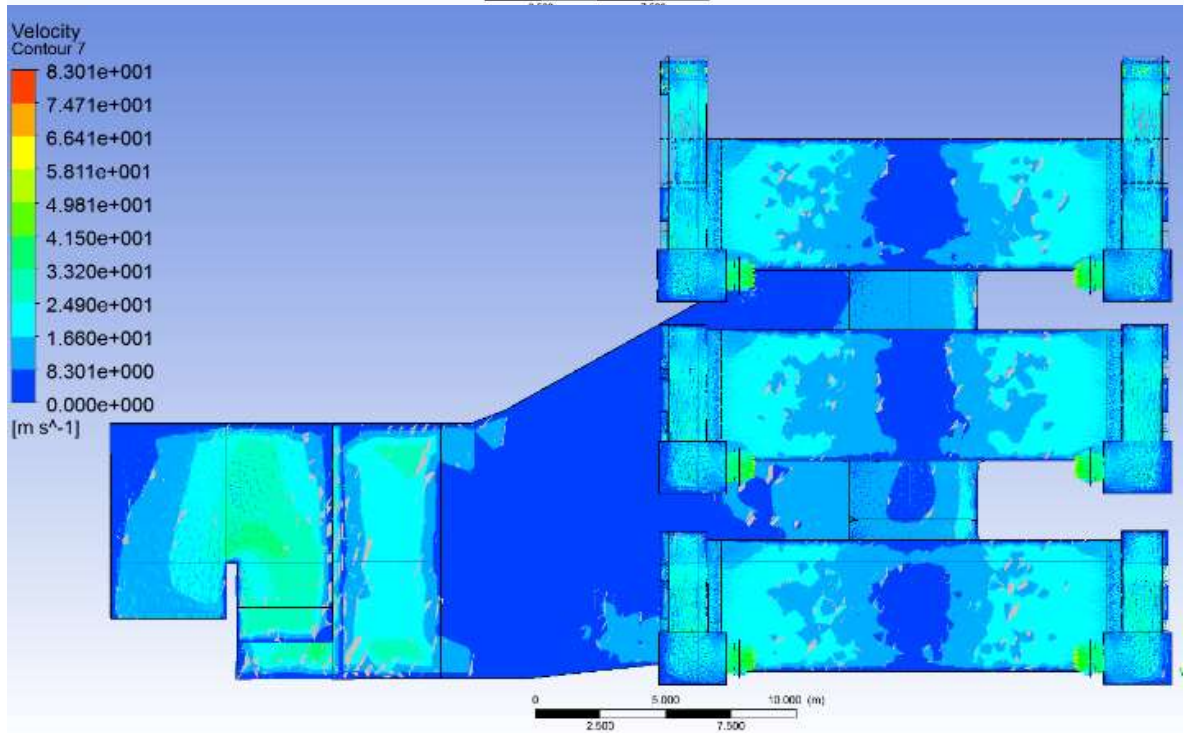
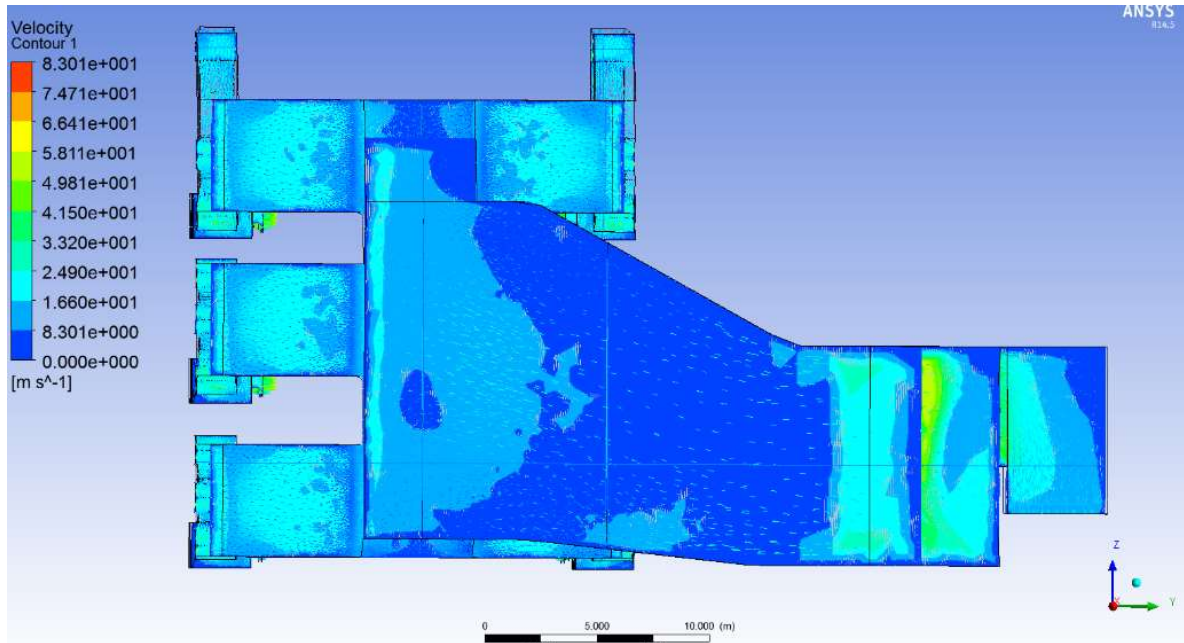
APPENDIX E: ANSYS CFD SIMULATION



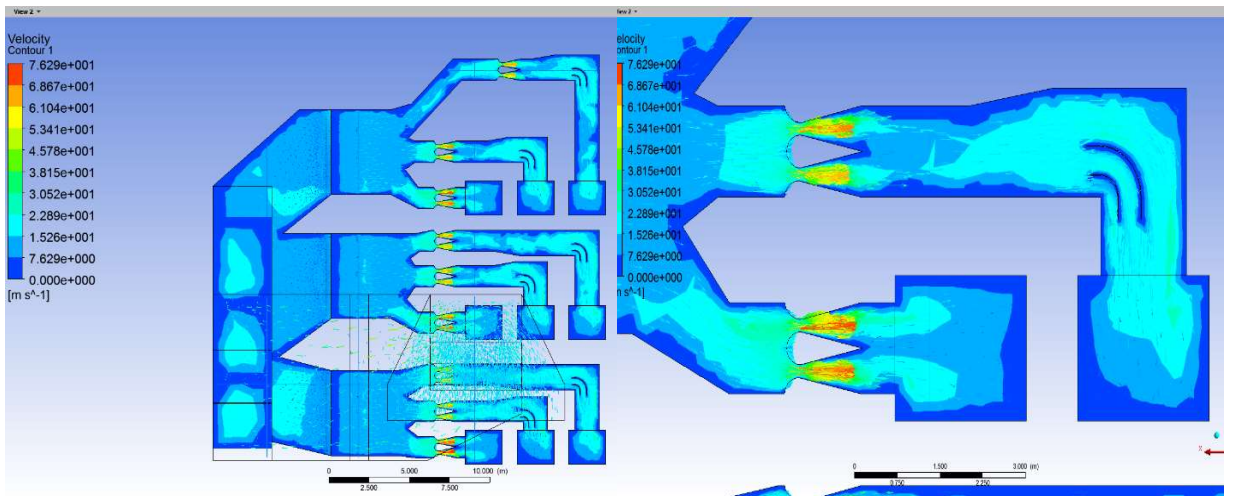
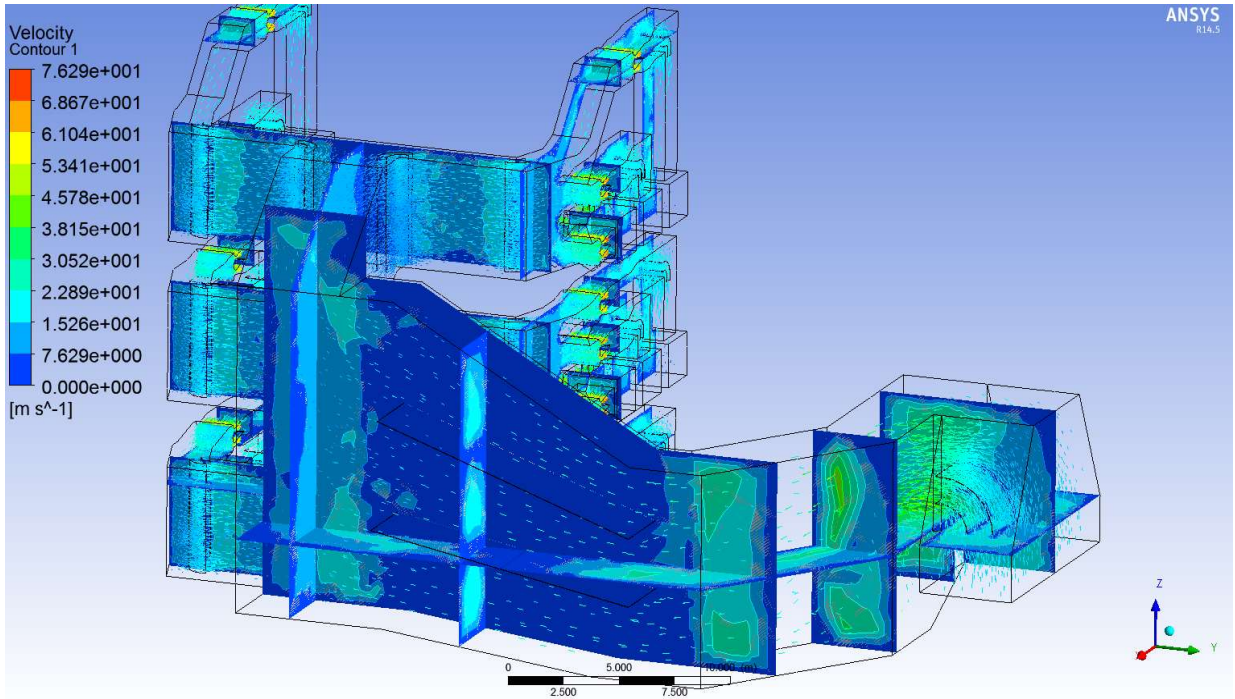
Air flow simulation overview using coarse mesh



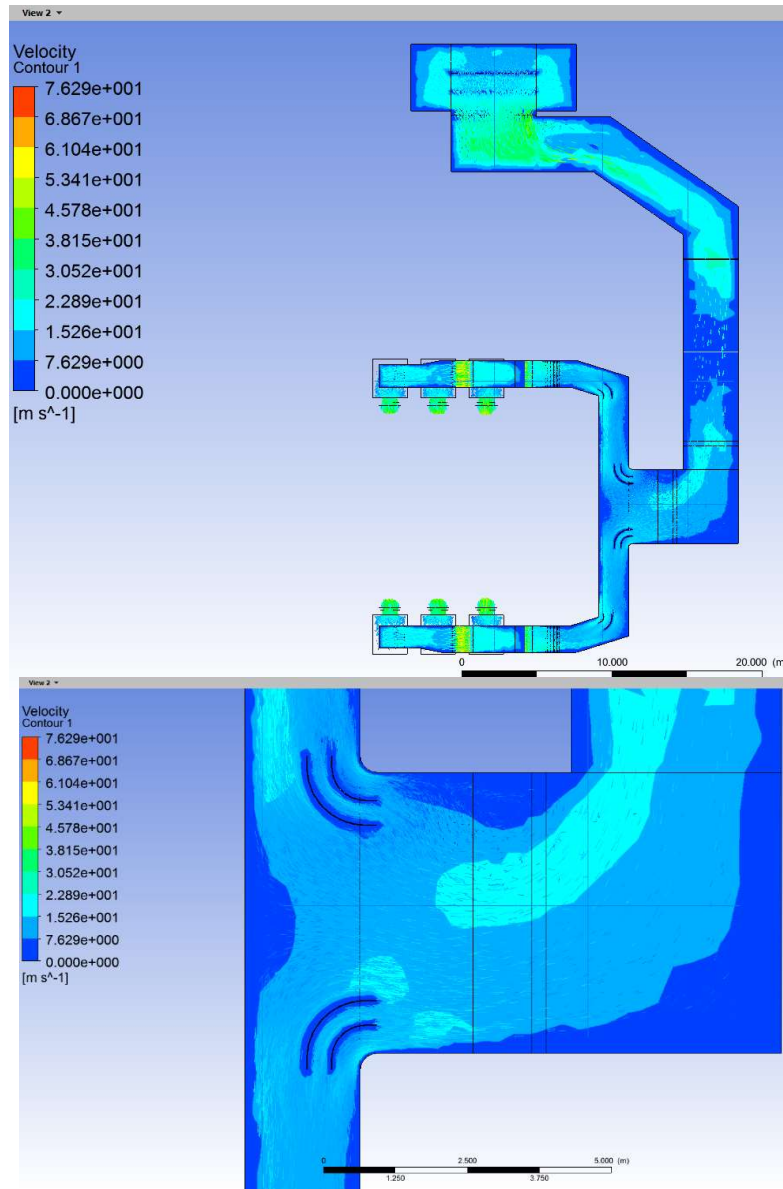
Air flow in main and distribution ducting using coarse mesh (top view)



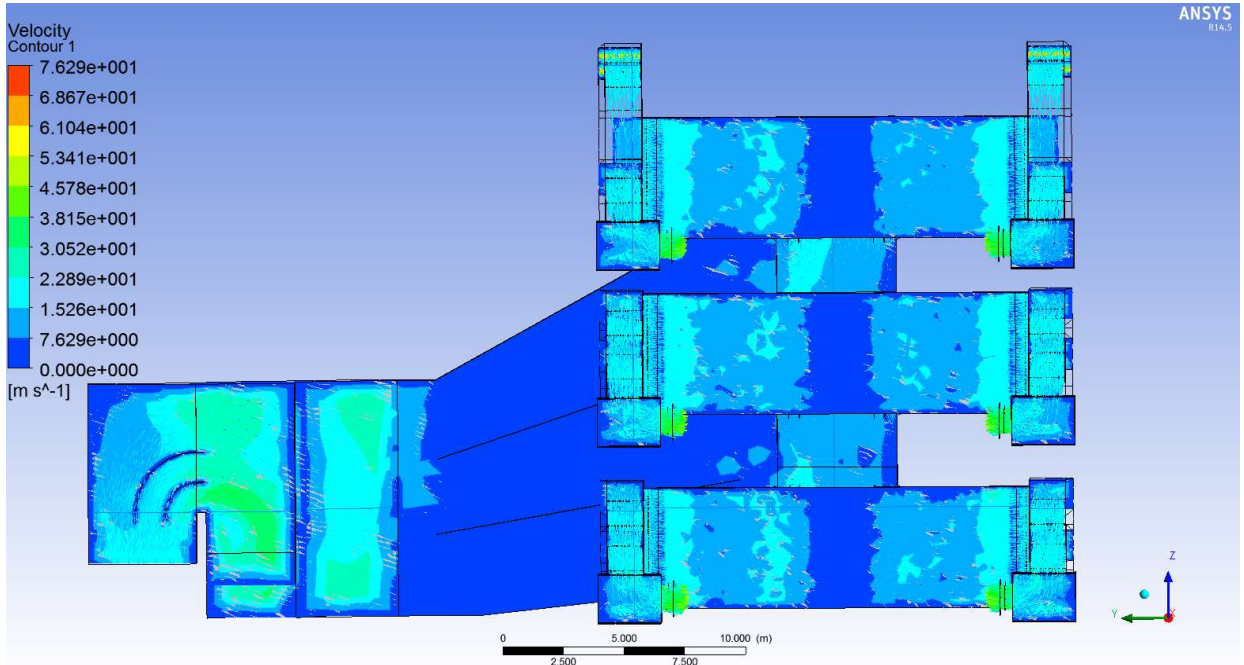
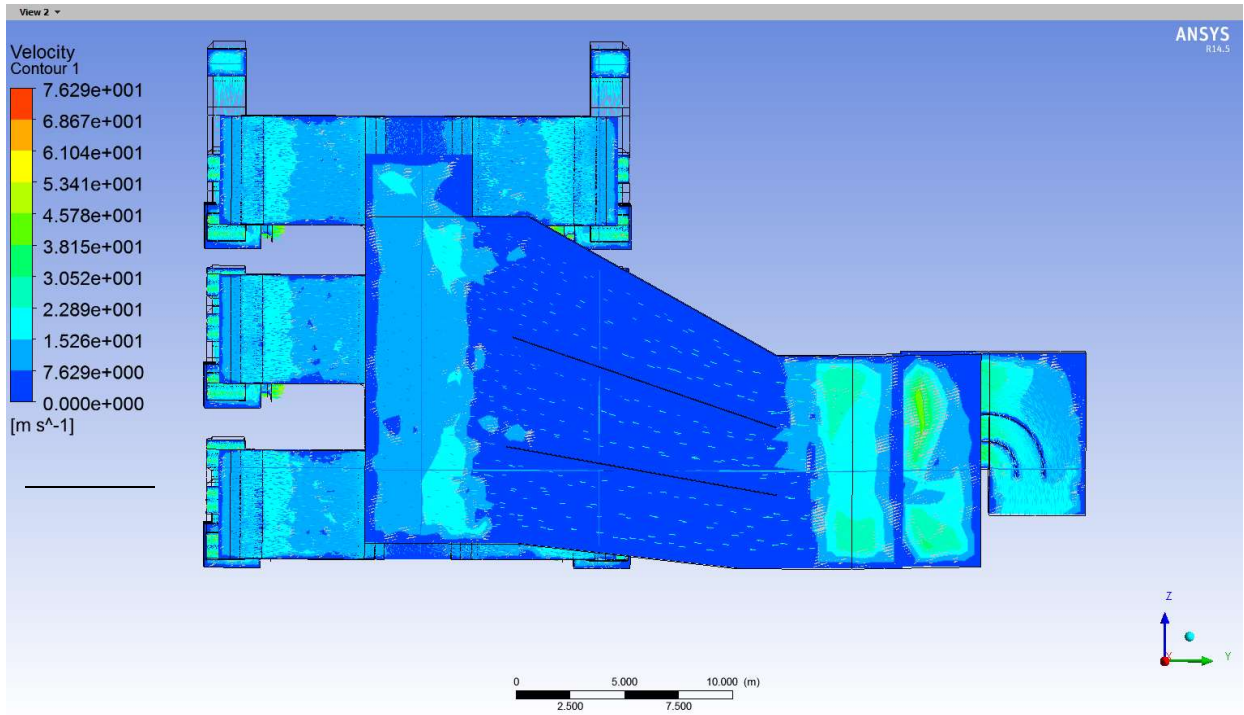
Air flow in main and distribution ducting using coarse mesh (front view)



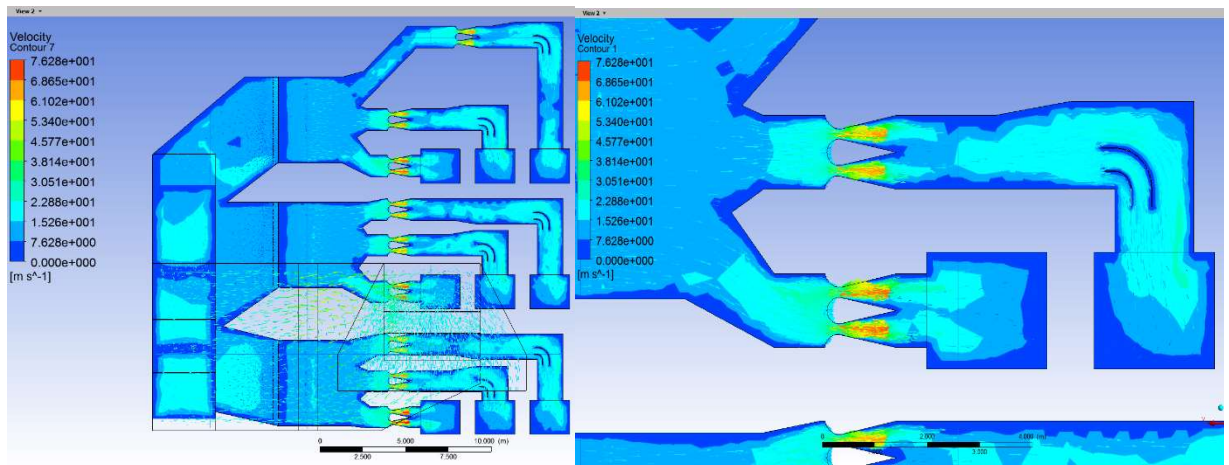
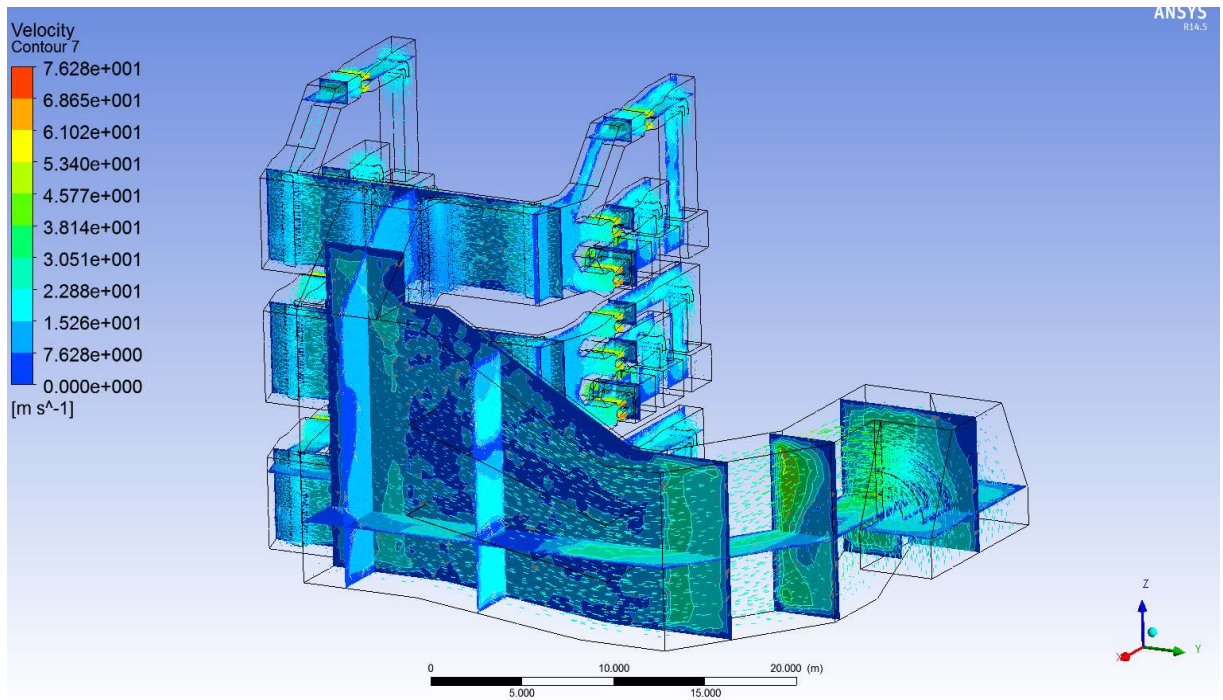
Air flow simulation overview using medium mesh



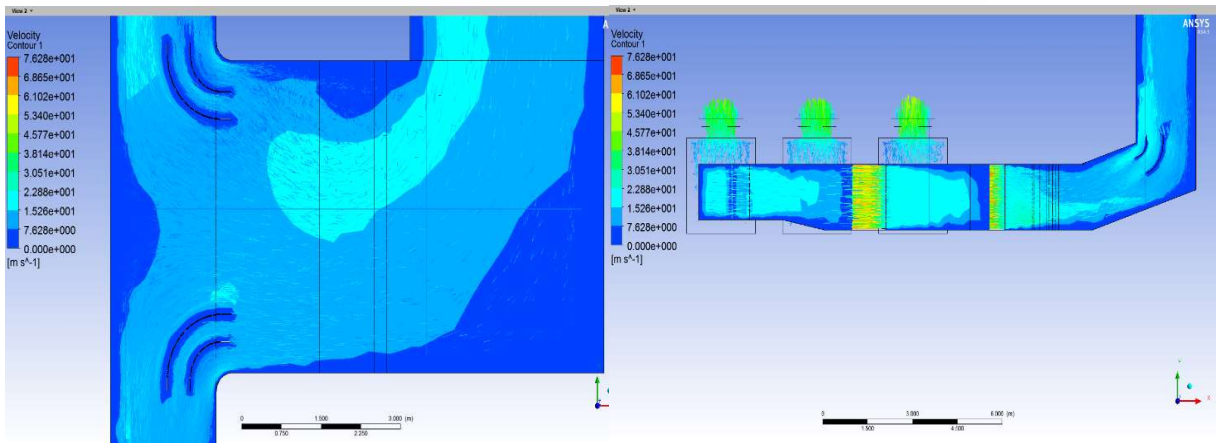
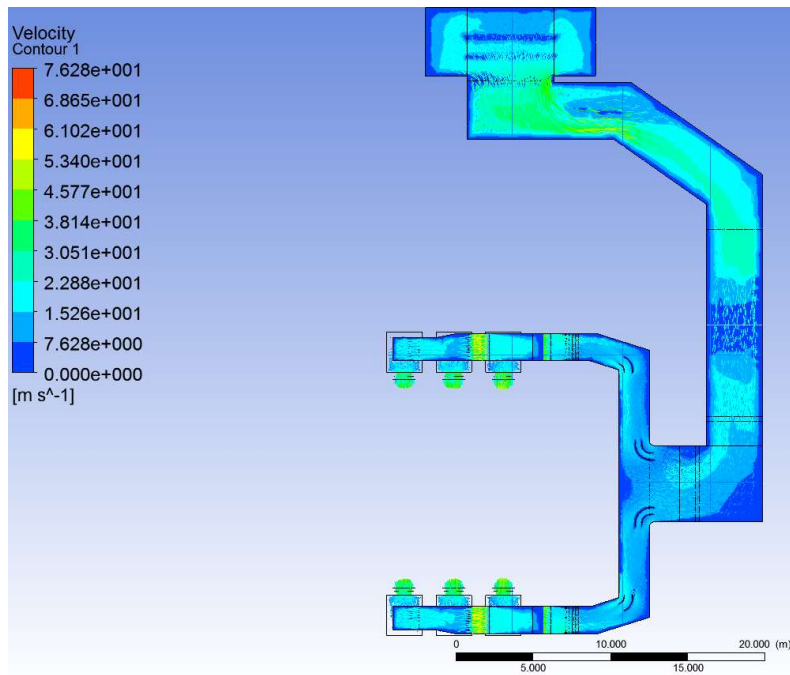
Air flow in main and distribution ducting using medium mesh (top view)



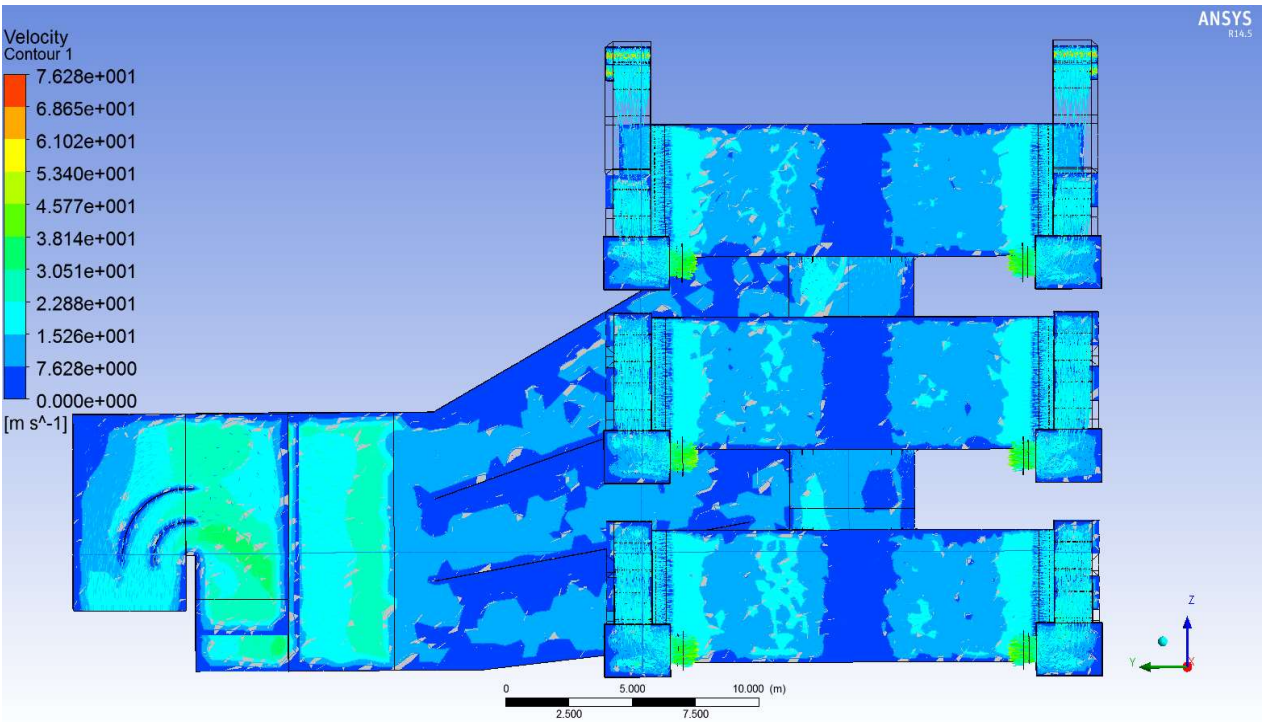
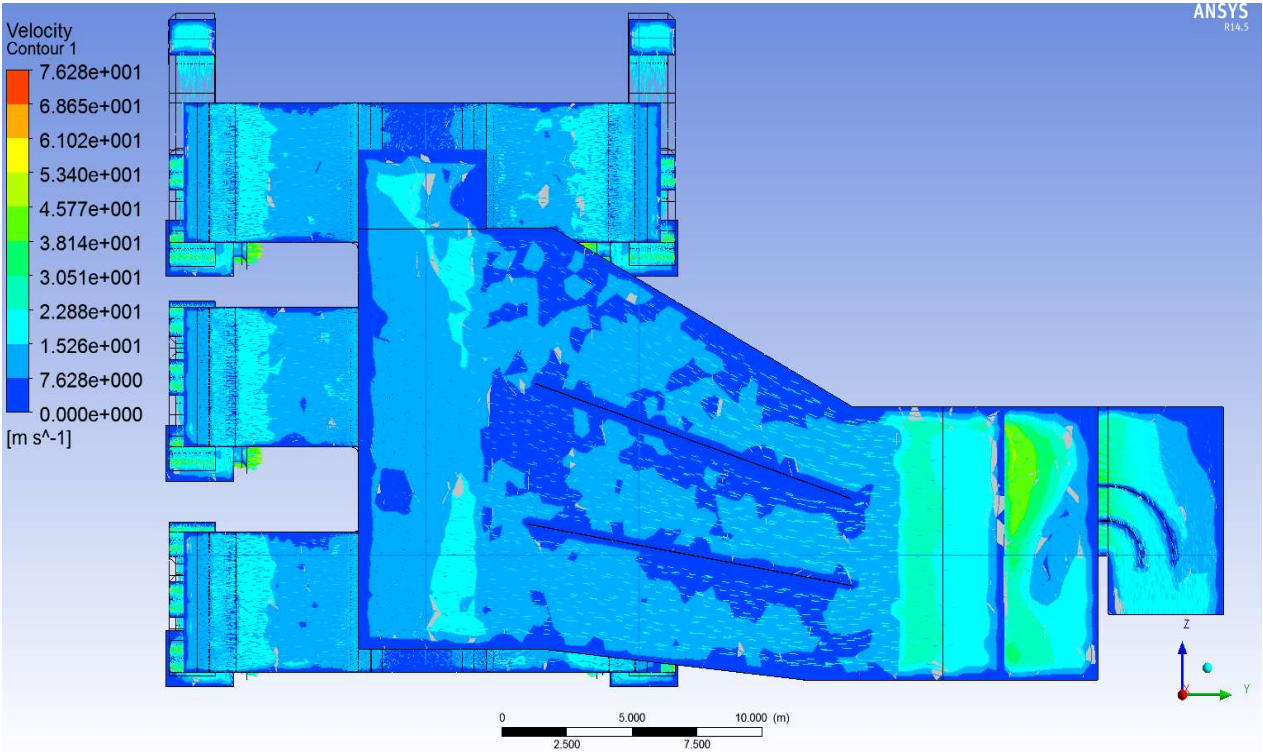
Air flow in main and distribution ducting using medium mesh (front view)



Air flow simulation overview using fine mesh



Air flow in main and distribution ducting using fine mesh (top view)



Air flow in main and distribution ducting using fine mesh (front view)

**Loading "C:\PROGRA~1\ANSYSI~1\v145\fluent\fluent14.5.7\lib\fl114-64.dmp"
Done.**

Welcome to ANSYS Fluent 14.5.7

Copyright 2013 ANSYS, Inc.. All Rights Reserved.
Unauthorized use, distribution or duplication is prohibited.
This product is subject to U.S. laws governing export and re-export.
For full Legal Notice, see documentation.

Build Time: Mar 25 2013 17:12:51 Build Id: 10514
Loading "C:\PROGRA~1\ANSYSI~1\v145\fluent\fluent14.5.7\lib\flprim1119-64.dmp"
Done.

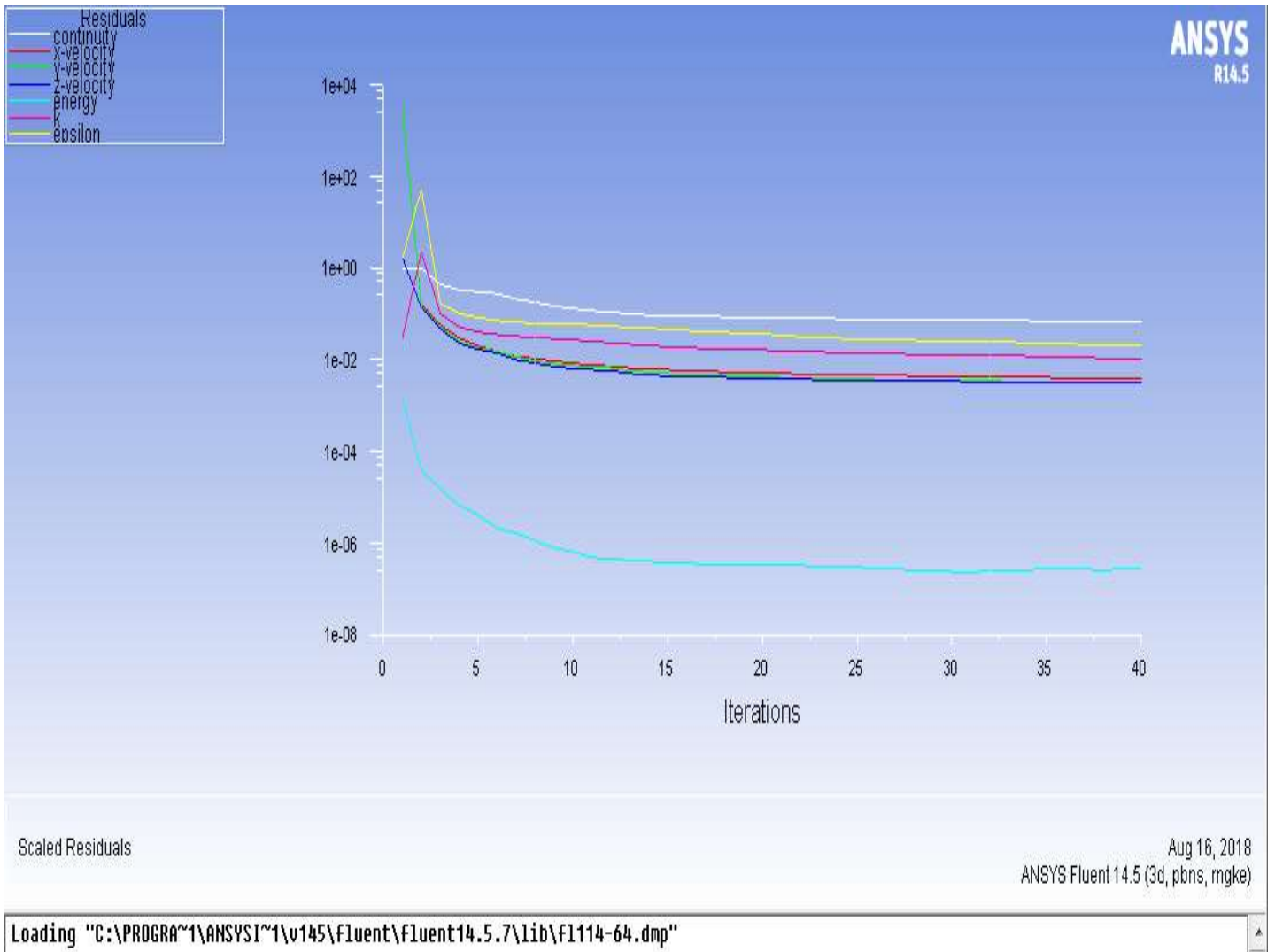
Host spawning Node 0 on machine "PLMCC_TEST" (win64).
WARNING: No cached password or password provided.
 use '-pass' or '-cache' to provide password
Platform-MPI licensed for FLUENT.
Host 0 -- ip 10.27.23.165 -- ranks 0

```
host | 0  
=====|=====  
0 : SHM
```

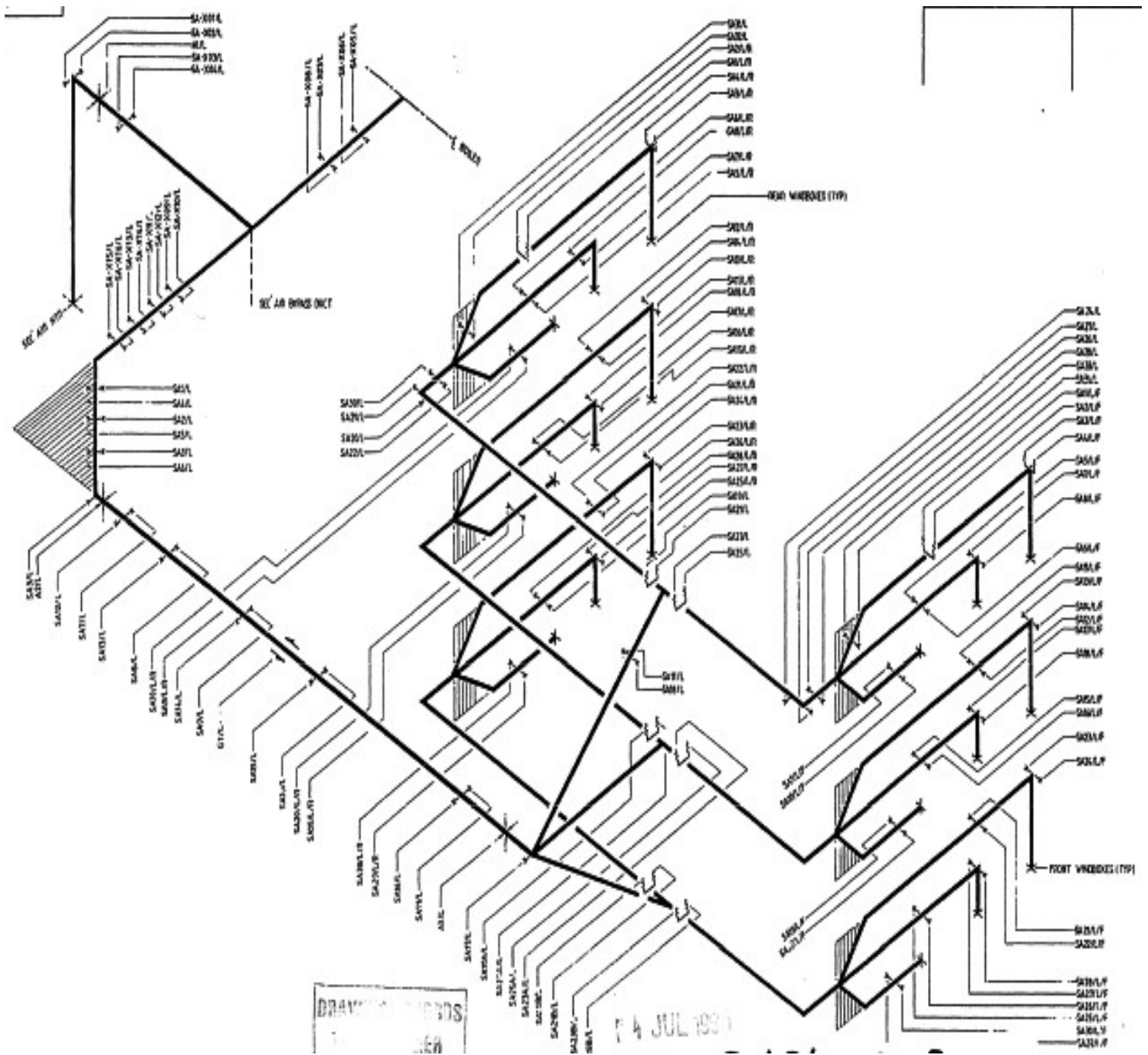
Prot - All Intra-node communication is: SHM

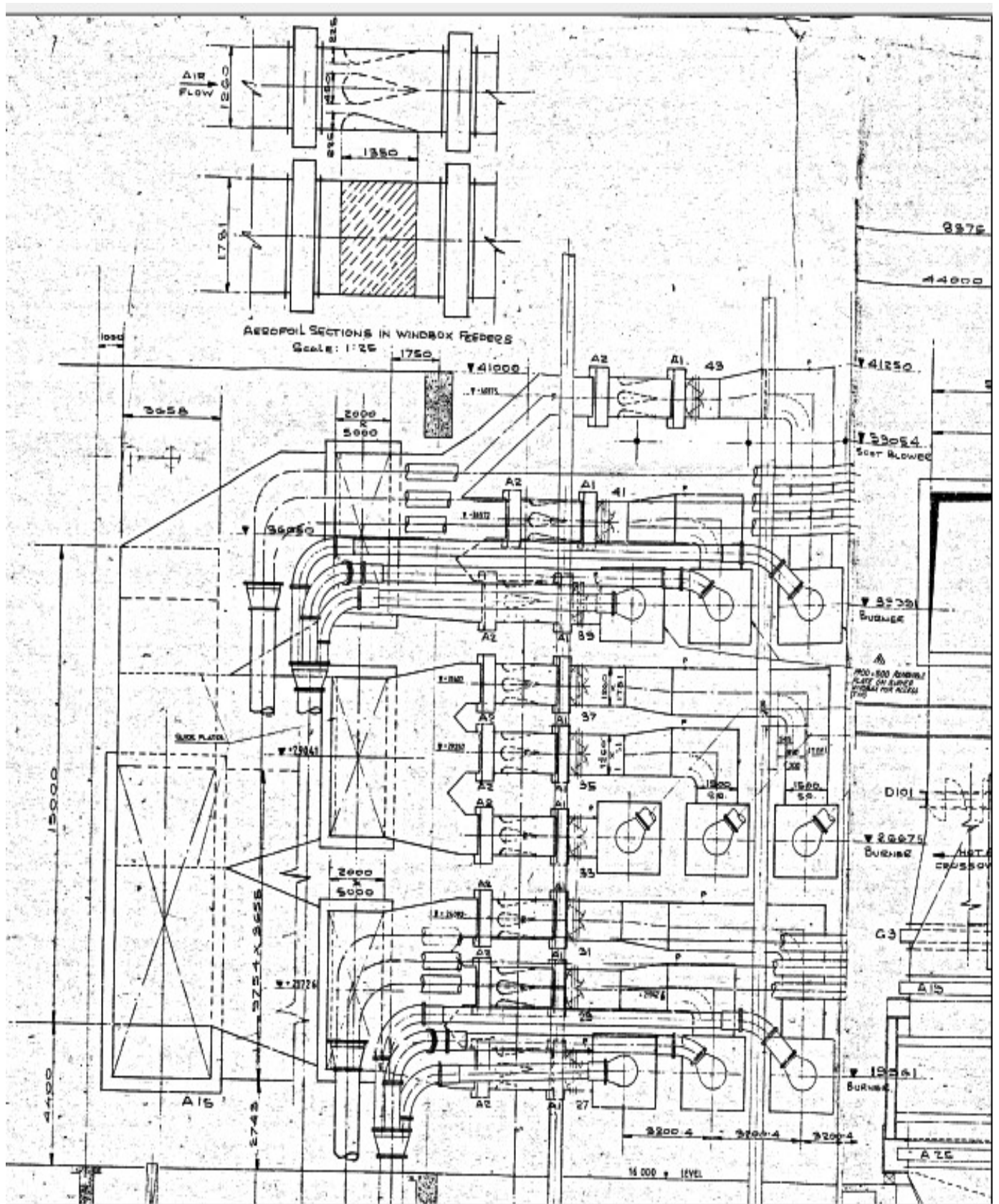
```
-----  
ID   Comm.  Hostname    O.S.    PID   Mach ID HW ID  Name  
-----  
host* net   PLMCC_TEST  Windows-x64 8748   0     -1    Fluent Host  
n0   pcmpi   PLMCC_TEST  Windows-x64 6116   0     404   Fluent Node  
-----
```

Cleanup script file is C:\Users\Student\Desktop\Fine Mesh CFD - Complete\cleanup-fluent-PLMCC_TEST-8748.bat



Loading "C:\PROGRA~1\ANSYSI~1\v145\fluent\fluent14.5.7\lib\fl114-64.dmp"
Done.





APPENDIX G: COAL-FIRED BOILER 3D PLANT LAYOUT

